Sophie Littke

Investigating the role of frequency-dependent pre-conditioning to low oxygen and pH in building coral stress tolerance

UNIVERSIDADE DO ALGARVE

Faculdade de Ciências e Tecnologia

2025

Sophie Littke

Investigating the role of frequency-dependent pre-conditioning to low oxygen and pH in building coral stress tolerance

Mestrado em Biologia Marinha

Supervisors:

Dr. Verena Schoepf (University of Amsterdam)

Dr. Aschwin Engelen (University of Algarve)

UNIVERSIDADE DO ALGARVE

Faculdade de Ciências e Tecnologia

2025

UNIVERSITEIT VAN AMSTERDAM

Smithsonian *Tropical Research Institute*

Declaração de autoria de trabalho

Investigating the role of frequency-dependent pre-conditioning to low oxygen and pH in building coral stress tolerance

Declaro ser a autora deste trabalho, que é original e inédito. Autores e trabalhos consultados estão devidamente citados no texto e constam da listagem de referências incluída.

Assinatura

Assinatura

Abstract

Severe hypoxia, often coupled with low pH, is an emerging threat to coral reefs, yet their combined effects, and the potential for environmental priming to modulate coral responses under such stress, remain understudied. In particular, the frequency and timing of prior sublethal exposure to combined low oxygen and pH are largely unexplored as drivers of coral stress tolerance. We conducted a controlled laboratory experiment to test how the frequency of nightly low dissolved oxygen (DO) and pH exposure shapes physiological responses of two Caribbean coral species, *Agaricia tenuifolia* and *Siderastrea siderea*, during subsequent, acute combined stress. Corals received six (high frequency, HF), three (low frequency, LF), or no (control) priming pulses, each lasting two consecutive nights, over four weeks, mimicking natural diel DO and pH cycles in shallow reefs, followed by 4–7 days of acute stress or ambient conditions. Results revealed contrasting species-specific outcomes. In *A. tenuifolia,* HF priming reduced baseline photosynthetic efficiency by 32% by the end of the priming period, with no further change during acute stress. HF primed *A. tenuifolia* also exhibited a ~42% reduction in symbiont densities, and a nearly tenfold increased risk of tissue loss compared to controls, regardless of acute stress treatment, while biomass and calcification remained unchanged. In contrast, *S. siderea* showed physiological stability across treatments, with LF priming supporting tissue biomass maintenance under acute stress. By the experimental end, biomass declined 28% and 22% in unprimed and HF-primed corals under acute stress*,* respectively, whereas LF primed corals maintained biomass. These findings highlight stress frequency as a critical yet understudied dimension of environmental priming and a direct modulator of baseline coral physiology. HF priming impaired the hypoxia-sensitive *A. tenuifolia*, while LF priming was neutral. The more hypoxia-tolerant *S. siderea* showed subtle LF priming benefits and no HF effects. As climate change and coastal eutrophication intensify diel variability and acute low DO and pH events, understanding frequency-dependent stress responses will improve predictions of reef community trajectories and help identify resilient coral populations.

Key words: Environmental priming, coral resilience, diel hypoxia and acidification, physiological plasticity, *Agaricia tenuifolia, Siderastrea siderea*

Resumo

Investigação do papel do pré-condicionamento dependente da frequência a baixos níveis de oxigénio e pH na construção da resiliência dos corais ao stress

A hipóxia severa, ou períodos de baixos níveis de oxigénio dissolvido (OD) na água, tem emergido recentemente como uma ameaça crescente aos ecossistemas de recifes de coral, a nível global. Quando combinada com condições de baixo pH (acidificação dos oceanos), esta dupla ocorrência de fatores de stress impõe desafios fisiológicos complexos aos corais, embora que os seus efeitos combinados ainda sejam pouco compreendidos. A hipóxia e a acidificação são frequentemente observadas em ambientes costeiros e recifes rasos, especialmente devido à eutrofização, proliferações de algas e circulação de água limitada — fatores todos intensificados pelas alterações climáticas e atividades humanas locais. Apesar da evidência crescente de que estes fatores de stress reduzem a saúde, crescimento e sobrevivência dos corais, poucos estudos abordaram como exposições repetidas e subletais influenciam a tolerância e resiliência dos corais a eventos agudos de OD baixo e pH reduzido.

O priming ambiental, um conceito originado da fisiologia vegetal e animal, sugere que exposições prévias a stress subletal podem induzir plasticidade fenotípica ou aclimatização, aumentando a tolerância a eventos de stress subsequentes. Este fenómeno tem sido documentado em corais expostos a stress térmico e de acidificação, com evidências crescentes de que o historial ambiental pode moldar trajetórias fisiológicas. No entanto, o papel do priming ambiental sob condições de stress compostas — como a ocorrência simultânea de baixo oxigénio e pH — permanece mal compreendido. Em particular, os efeitos de priming envolvendo hipóxia, isoladamente ou em combinação com outros fatores de stress, têm recebido pouca atenção. Além disso, a frequência e o tempo de exposição subletal — nomeadamente com que frequência e durante quanto tempo os corais experienciam stress moderado antes de um evento agudo — podem determinar criticamente a direção e intensidade dos efeitos de priming. Compreender o papel da frequência de stress é fundamental para prever as respostas dos corais em ambientes costeiros cada vez mais variáveis e extremos, sendo esta uma lacuna importante no conhecimento atual.

Para abordar esta questão, realizámos uma experiência controlada em laboratório para testar como a frequência da exposição noturna a baixos níveis de OD e pH influencia o desempenho fisiológico de duas espécies de corais das Caraíbas, *Agaricia tenuifolia* e *Siderastrea siderea*,

durante um evento subsequente de stress agudo combinado. Estas espécies representam diferentes estratégias ecológicas e fisiológicas: *A. tenuifolia* é geralmente mais sensível à hipóxia, enquanto *S. siderea* é considerada mais tolerante. Ao comparar as suas respostas, procurámos compreender a suscetibilidade específica de cada espécie e os mecanismos subjacentes ao priming sob stress composto.

Os corais foram submetidos a três regimes de priming ao longo de um período de quatro semanas: priming de alta frequência (HF), com um total de seis pulsos noturnos de OD (~2.6 mg L^{-1}) e pH (~7.75) reduzidos durante seis horas cada; priming de baixa frequência (LF), com um total de três pulsos; e um grupo controlo mantido em condições ambientais estáveis. Estes pulsos simularam flutuações naturais diárias observadas em recifes rasos das Caraíbas, como os da Baía de Almirante, no Panamá, onde hipóxia e acidificação noturnas ocorrem regularmente. Após o priming, os corais foram expostos durante 4–7 dias a um evento agudo de stress combinado, simulando hipóxia e acidificação severas, ou mantidos em condições ambientais, para avaliar a sua capacidade de tolerar stress mais intenso e prolongado.

Os nossos resultados revelaram diferenças marcantes entre espécies nas respostas ao priming e nos resultados fisiológicos. Em *A. tenuifolia*, o priming HF provocou uma redução significativa de 32% na eficiência fotossintética basal (F_v/F_m) até ao final do período de priming, indicando um comprometimento da fotofisiologia dos simbiontes antes mesmo da exposição ao stress agudo. Curiosamente, esta deterioração não se agravou durante a exposição subsequente ao stress agudo, sugerindo que o priming frequente foi mais prejudicial do que o próprio evento agudo. Além disso, *A. tenuifolia* sob priming HF apresentou uma redução de aproximadamente 42% na densidade de simbiontes em comparação com os controlos, sugerindo perda ou disfunção de simbiose. De forma alarmante, o priming HF levou a um aumento de quase dez vezes no risco de perda de tecido — um indicador de stress severo e potencial mortalidade — independentemente da exposição ao stress agudo. Estes resultados sugerem que impulsos noturnos frequentes de hipóxia e acidificação podem ultrapassar a capacidade de plasticidade fisiológica desta espécie sensível à hipóxia, comprometendo a saúde basal e aumentando a vulnerabilidade a stress adicional.

Em contraste, *S. siderea* demonstrou uma notável estabilidade fisiológica entre tratamentos. A eficiência fotossintética, densidade de simbiontes e calcificação mantiveram-se relativamente estáveis, sem perda de tecido significativa em qualquer grupo. Notavelmente, o priming LF apoiou a manutenção da biomassa tecidular durante o stress agudo. Enquanto a biomassa decresceu 28% e 22% nos corais controlo e com priming HF, respetivamente, os corais com

priming LF mantiveram níveis de biomassa semelhantes aos de pré-stress. Isto sugere que exposições subletais moderadas e pouco frequentes à combinação de baixo OD e pH podem induzir mecanismos de aclimatização benéficos que protegem a integridade dos tecidos do hospedeiro, possivelmente através de maior capacidade metabólica ou antioxidante.

Estes resultados realçam a frequência de stress como uma dimensão crítica, embora pouco explorada, do priming ambiental em corais, atuando como modulador direto da fisiologia basal e da resiliência ao stress. O efeito prejudicial do priming HF em *A. tenuifolia* evidencia a importância dos limites de tolerância específicos da espécie e o potencial de stress ambiental frequente induzir declínio fisiológico em vez de aclimatização. Por outro lado, os benefícios subtis do priming LF em *S. siderea* destacam o potencial de ciclos de stress naturais** e pouco frequentes para promover a resiliência dos corais.

O nosso estudo fornece informações cruciais sobre como a variabilidade ambiental diária, especificamente a frequência de eventos noturnos de hipóxia e acidificação, pode moldar trajetórias fisiológicas dos corais num contexto de alterações climáticas e eutrofização costeira crescentes. À medida que as águas costeiras enfrentam flutuações diárias mais intensas e episódios agudos mais frequentes de baixo OD e pH, compreender os mecanismos e limites do priming entre espécies será essencial para prever mudanças comunitárias e a resiliência dos ecossistemas recifais. Estes resultados sugerem que populações de corais expostas a diferentes frequências de stress subletal podem divergir na sua capacidade de persistir no futuro, com implicações para estratégias de conservação e restauro.

Investigações futuras devem explorar as vias moleculares e bioquímicas subjacentes ao priming dependente da frequência, a duração e os intervalos de recuperação entre pulsos de stress, e como as múltiplas dimensões de stress (frequência, intensidade, duração) interagem na indução de aclimatização versus maladaptação. Além disso, são necessários estudos *in situ* para validar os resultados laboratoriais e avaliar a relevância ecológica em diferentes habitats recifais. O nosso trabalho contribui para um conjunto crescente de evidências que destacam a complexidade das respostas dos corais a fatores de stress ambientais simultâneos e a necessidade de integrar a frequência do stress em modelos de futuro dos recifes de coral.

Palavras-chave: Pré-condicionamento ambiental, resiliência dos corais, hipóxia e acidificação diárias, plasticidade fisiológica*, Agaricia tenuifolia; Siderastrea siderea*

Thesis acknowledgements

First and foremost, I would like to express my deepest gratitude to Kelly Wong Johnson for her continuous guidance and support throughout this project. From the very beginning to the final stages, your supervision, valuable insights, and engaging discussion have helped me so much to grow as a researcher. I am especially thankful for our time together in the field in Panama, where I learned an incredible amount from you while feeling immense joy and excitement about our projects.

I would also like to sincerely thank Dr. Verena Schoepf for welcoming me into her group and for providing exceptional guidance and feedback. Your encouragement and expertise have been instrumental in shaping both my thesis and my growth as a scientist.

Additionally, I am also thankful to Dr. Rene van der Zande for his invaluable help during fieldwork and offering important insights and feedback. Your support was deeply appreciated.

Thank you to Antonie Kooymans for helping with the analyses of the environmental data, it was very much appreciated.

To the entire Schoepf lab group at the University of Amsterdam, thank you for always providing constructive feedback, thought-provoking discussions, and a fun and supportive atmosphere during our lab meetings. Working with you has been truly inspiring and enjoyable.

I am also grateful to Dr. Aschwin Engelen for their guidance and constructive feedback in his role as internal supervisor at UAlg.

Last but not least, this work would have not been possible without the generous support of the staff at the Smithsonian Tropical Research Institute in Bocas del Toro, Panama. Thank you for your assistance throughout fieldwork, and in particular to Plinio Gondola for helping with all logistics and solving the countless day-to-day challenges that come with field research.

Finally, I would like to extend my appreciation to everyone who, in one way or another, contributed to the completion of this thesis. Especially to all my family and friends, who always managed to put a smile on my face when my work got stressful.

Table of Contents

List of abbreviations

AS	Air saturation
A. tenuifolia	*Agaricia tenuifolia*
DO	Dissolved oxygen
HF	High frequency
LF	Low frequency
OA	Ocean acidification
PAR	Photosynthetically active radiation
P_{crit}	Critical oxygen partial pressure / Critical oxygen tension
pH_T	pH (total scale)
PS II	Photosystem II
ROS	Reactive oxygen species
RTE	Reciprocal transplant experiment
S. siderea	*Siderastrea siderea*

1. General introduction

Coral reefs: Distribution, Diversity, and Importance

Coral reefs represent some of the most ecologically important and diverse marine ecosystems on Earth (Bellwood et al., 2019; Fisher et al., 2015). These biogenic structures are primarily constructed by reef-building, scleractinian corals, which produce aragonitic skeletons, and serve as foundational species by creating complex habitat structures (Allemand et al., 2004; Putnam et al., 2017). Coral reefs occur in several morphologically distinct forms that were already described by Darwin: (1) fringing reefs, which develop adjacent to shorelines, (2) barrier reefs, which are separated from land by deeper lagoons, and (3) atolls, ring-shaped reefs surrounding lagoons that often arise from subsiding volcanic islands (Darwin, 1842). While this classification still accommodates most reefs globally, the distinguishment between reef types is not always unequivocal (Kennedy, 2002). Beyond shallow-water systems, cold-water coral reefs also occur along continental margins and seamounts at tropical to polar latitudes, where they provide vital habitat and contribute to carbon cycling (Cordes et al., 2023). Nevertheless, this work will focus on shallow tropical coral reef systems.

The distribution of reef-building corals is primarily constrained by temperature and light availability. Shallow reefs are restricted to tropical and subtropical latitudes (~34° N-32° S) where minimum annual sea surface temperatures remain above ~18 °C (Johannes et al., 1983; Jones et al., 2022). Although shallow coral reef hotspots (i.e., shallow tropical areas where corals might be found, even if sparse) are distributed globally, most coral habitat hotspots (areas that are likely or able to support significant coral coverage) are centered in the Central Indo-Pacific, where benthic complexity and biodiversity are among the highest worldwide (Li and Asner, 2023; Lyons et al., 2024)

Coral reefs have long been portrayed as “oases in marine deserts” for their ability to thrive in nutrient-poor tropical and subtropical waters, but they in fact span a wide range of nutrient regimes, with the majority occurring in mesotrophic to eutrophic conditions (Morais et al., 2025). Across these diverse environments, coral reefs sustain exceptionally high productivity levels (Hatcher, 1990; Putnam et al., 2017) and support remarkable biodiversity and endemism (Fisher et al., 2015; Hughes et al., 2002). At the basis of these ecosystems are reef-building, scleractinian corals, which provide shelter, substrate, and feeding grounds for a wide array of marine organisms (Putnam et al., 2017). Coral reefs are also critical drivers of

nutrient cycling and contribute to biogeochemical processes through transformation and retention of organic and inorganic matter (Moberg and Folke, 1999; Wild et al., 2011).

Beyond their ecological functions, they also provide an array of vital ecosystem services with great socioeconomic importance for human societies. These include coastal protection from wave and storm surges (Beck et al., 2018), food provision from fisheries that support food security in many tropical nations (Golden et al., 2016), and revenue from reef-based tourism, which was estimated to contribute approximately US$ 35.8 billion annually to the global economy (Spalding et al., 2017). The well-being of hundreds of millions of people is thus directly or indirectly linked to the health of coral reefs (Moberg and Folke, 1999; Woodhead et al., 2019). However, coral reefs are under increasing pressure in the Anthropocene, as global environmental changes alter their ecological function and diminish their capacity to deliver ecosystem services. A suite of anthropogenic stressors, including climate change, pollution, and overfishing, can disrupt coral physiology, destabilize intricate symbiotic networks, and degrade reef community structure, habitat complexity, and ecosystem functioning (Hughes et al., 2017a; Woodhead et al., 2019).

Coral morphology and life-history traits

Coral biology is shaped by key life-history traits such as morphology, growth rate, longevity, and reproductive mode, which mediate ecological strategies and stress sensitivity (e.g., Darling et al., 2012; Hughes and Tanner, 2000). Trait-based frameworks (e.g., Darling et al., 2012) classify reef-building corals into four general strategies: (I) competitive species, such as *Acropora* and *Montipora*, which are fast-growing branching or plating corals that dominate under favorable conditions but are highly disturbance sensitive; (II) weedy species, including *Agaricia* and some *Porites*, which are small, brooding taxa with opportunistic colonization ability and high persistence in disturbed habitats; (III) stress-tolerant genera, such as *Siderastrea*, *Montastraea*, and massive *Porites*, which grow slowly but invest in long lifespans, large corallites, and high fecundity, enabling persistence under chronically harsh conditions; and (IV) generalist species, which combine intermediate traits and occupy environments where neither competition nor disturbance strongly dominates. These strategies reflect trade-offs between growth, reproduction, and survival, and help explain why coral assemblages often shift toward stress-tolerant or weedy taxa as disturbances increase.

In the context of this study, the contrasting life-history traits of *Agaricia tenuifolia* (weedy, opportunistic) and *Siderastrea siderea* (stress-tolerant) provide an interesting comparison regarding their priming potential under diel low pH and dissolved oxygen conditions. The

weedy strategy of *A. tenuifolia* may enable rapid colonization but confer limited capacity to withstand repeated stress exposure, while the stress-tolerant strategy of *S. siderea* may support persistence through physiological buffering, albeit at the cost of slower growth. While such colony-level traits determine how corals interact with their environment and compete within reef communities, the foundation of these strategies ultimately lies in the physiology of the coral holobiont, the integrated partnership between the coral host and its associated symbiotic partners.

The coral holobiont

Scleractinian corals are colonial marine invertebrates within the phylum Cnidaria, composed of clonal polyps connected by a shared gastrovascular system (Hughes et al., 1992; Putnam et al., 2017). Each polyp exhibits a diploblastic tissue organization, with an outer epidermis and inner gastrodermis, which each contain a variety of specialized cell types. Dedicated host cells within the gastrodermis known as symbiocytes, house endosymbiotic algae of the family Symbiodiniaceae (LaJeunesse et al., 2018).

This intimate partnership forms the basis of the coral holobiont, which encompasses not only the coral host and algal symbionts, but also an array of associated microorganisms including bacteria, archaea, fungi, and viruses (Bourne et al., 2009). Each component of the holobiont contributes to the organism's overall fitness and resilience. Disruption to any member through environmental or biological stressors can undermine the stability of the entire system (Bourne et al., 2009; Lesser, 2021).

The success of corals in oligotrophic environments is largely attributed to this symbiosis, with Symbiodiniaceae providing up to 100% of the coral host's energy demands via photosynthesis (Muscatine et al., 1981). These symbionts not only supply photosynthetically fixed carbon but also facilitate the recycling of essential inorganic nutrients (Lesser, 2021). In return, the coral host provides a protected intracellular habitat and access to nutrients from heterotrophic feeding (Ferrier-Pagès et al., 2010). Importantly, corals are not strictly autotrophic. They are mixotrophs, capable of deriving energy from both photosynthesis and prey capture. The relative contribution of these sources varies with environmental conditions, depth, and species identity (Sturaro et al., 2021). For example, corals inhabiting variable or deeper environments often exhibit greater trophic plasticity and thus a greater capacity to switch between autotrophy and heterotrophy, than conspecifics from more stable, shallow habitats (Solomon et al., 2025; Sturaro et al., 2021). Such trophic flexibility can help buffer corals against stress

events by providing alternative energy pathways, but its effectiveness is highly species-specific and depends on the magnitude and duration of disturbance (Grottoli et al., 2006).

Despite this flexibility, the holobiont remains highly sensitive to environmental perturbations such as warming, acidification, and deoxygenation. Warming and deoxygenation can impair photosynthetic efficiency, leading to photodamage of photosystem II (PS II) and excessive production of reactive oxygen species (ROS), which compromise host-symbiont stability (Jones and Hoegh-Guldberg, 2001; Wooldridge, 2013). The resulting oxidative stress can trigger symbiont expulsion known as coral bleaching and potentially lead to mortality if symbiosis is not restored (Wooldridge, 2013). In contrast, ocean acidification (OA) has comparatively less direct impact on photosynthetic processes, but can impair the coral host by reducing calcification, survival, and recruitment success (Kroeker et al., 2013; Putnam et al., 2017).

Importantly, the physiological performance of the coral holobiont is shaped by the traits of the coral host, algal symbionts, and associated microbial communities, as well as the degree of functional integration and flexibility in their association under changing conditions. Moreover, the diverse cellular architecture within corals generates steep intra- and extracellular gradients of pH, oxygen, and ions such as calcium, bicarbonate, and hydrogen, which are highly responsive to environmental cues (Hohn and Merico, 2015; Putnam et al., 2017). Understanding these fine-scale physiological interactions is crucial to predicting how holobionts will respond to global change.

Anthropogenic threats to coral reefs

The global cover of live coral has declined by approximately 50% since the 1950s (Eddy et al., 2021). This decline is driven by a combination of global and local anthropogenic stressors that often act simultaneously and synergistically (Knowlton and Jackson, 2008). Historically, ocean warming, overfishing, and pollution have been principal drivers of coral reef degradation (Wear, 2016), with OA and coastal deoxygenation exacerbating stress on coral reef ecosystems (Altieri et al., 2017; Camp et al., 2018; Hoegh-Guldberg et al., 2007). While warming is widely recognized as the primary driver of mass coral bleaching and mortality events (Hoegh-Guldberg et al., 2007), OA has been studied extensively over the past three decades (Anthony et al., 2011; Hoegh-Guldberg et al., 2007; Kroeker et al., 2013) for its projected impacts on coral calcification and recruitment. In contrast, coastal deoxygenation has only been recognized as a significant threat to coral reefs more recently, posing dangers

both on its own and through compounding effects with other stressors (Altieri et al., 2017; Hughes et al., 2022).

Ocean acidification

OA is a direct consequence of increasing atmospheric CO_2 levels and the ocean's role as a carbon sink. The absorption of excess CO_2 lowers seawater pH and alters carbonate chemistry, reducing the saturation state of calcium carbonate minerals like aragonite, of which coral skeletons are made (Hill and Hoogenboom, 2022; Hsiao et al., 2025; Orr et al., 2005). A lower aragonite saturation state (Ω_{arag}) reduces the thermodynamic potential for skeleton formation, directly compromising calcification rates and skeletal integrity, as well as fecundity, coral metabolism, and growth (Hill and Hoogenboom, 2022; Hsiao et al., 2025).

Research in naturally low-pH environments has shown that chronic acidification can lead to compromised reef structure and biodiversity (Camp et al., 2018; Kroeker et al., 2013), underscoring the vulnerability of marine calcifiers and especially reef-building corals to future OA scenarios. Even if carbon emissions were stabilized today, the ocean's thermal and chemical inertia would drive continued OA for decades to come (Lee et al., 2023). However, mitigation efforts can substantially alter the trajectory: surface ocean pH is projected to decline by ~0.29 pH units by 2081-2100 under high emission scenarios (RCP8.5), compared to just 0.04 pH units under strong mitigation (RCP2.6; IPCC, 2022).

Ocean deoxygenation

In parallel with OA, dissolved oxygen (DO) levels are declining globally due to warming-induced reductions in oxygen solubility and increased biological oxygen demand driven by nutrient enrichment and organic matter loading (Oschlies et al., 2018). This phenomenon, known as ocean deoxygenation, encompasses large-scale declines in DO across the global ocean, including both open-ocean and coastal regions (Oschlies et al., 2018). Much of the early research on ocean deoxygenation focused on oxygen minimum zones (OMZs), which develop in deeper waters of tropical and temperate oceans (typically 100-1000 m depth) due to combined effects of nutrient-driven productivity, microbial respiration, and strong thermal stratification (Gobler and Baumann, 2016). These OMZs, already extensive, are projected to expand further under ocean warming, with significant implications for midwater and pelagic ecosystems (Gobler and Baumann, 2016; Oschlies et al., 2018). Future projections suggest that global oxygen content is projected to decrease by 3.2-3.7% by 2100 under RCP8.5, versus 1.6-2.0% under RCP2.6, with expansion of oxygen minimum zones affecting 79-91%

of the ocean area by century's end (IPCC, 2022). In contrast, the occurrence and ecological importance of deoxygenation in shallow tropical reef habitats have only gained attention more recently, yet mounting evidence indicates that hypoxia represents a major emerging threat to tropical coral reefs (Altieri et al., 2021).

In coastal waters, oxygen variability is often further amplified by eutrophication, microbial respiration, lack of circulation, and processes like upwelling (Fusi et al., 2025). Hypoxia, typically defined as DO concentrations below 2 mg L^{-1} (e.g., Vaquer-Sunyer and Duarte, 2008), can severely impair coral metabolism, suppress calcification, and increase susceptibility to bleaching and mortality (Altieri et al., 2017; Hughes et al., 2022). Although this threshold is commonly used to define hypoxic conditions, true DO tolerance limits can vary by species, exposure duration, and environmental contexts (Haas et al., 2014; Johnson et al., 2021; Pezner et al., 2023). Contrary to the traditional attribution of coral bleaching solely to elevated temperatures, recent studies suggest that low DO levels may be a primary trigger of bleaching under certain conditions (e.g., Alderdice et al., 2021, 2022; Lucey et al., 2025), emphasizing the need to consider DO dynamics in coral reef vulnerability assessments and climate adaptation strategies.

The extent of compound hypoxia-acidification

OA and hypoxia are not independent stressors but tightly coupled through respiration and biogeochemical cycling (Gobler and Baumann, 2016; Melzner et al., 2013). In coastal and upwelling-influenced systems, microbial degradation of organic matter simultaneously consumes oxygen and produces CO_2, creating water masses that are both hypoxic and acidified. As a result, pCO_2 levels during hypoxia can reach extreme values (1700-3200 µatm under current conditions, and up to 4500 µatm in the future, Melzner et al., 2013), far exceeding the ranges predicted for the open ocean under OA alone. Geographically, shallow reef-systems in semi-enclosed coastal bays are especially vulnerable. As a result, the frequency and severity of hypoxic events, often coupled with low pH, on shallow coral reefs have increased notably over the past two decades (Altieri et al., 2017; Johnson et al., 2018; Kealoha et al., 2020; Raj et al., 2020). A global survey of reef oxygen dynamics (Pezner et al., 2023) revealed that hypoxia is already pervasive, with 84% of coral reefs experiencing weak to moderate, and 13% severe events, and projections indicate that more than 90% of coral reefs could face such conditions by 2100 under high emission scenarios.

Natural environmental variability on coral reefs

Coral reefs, particularly those located in nearshore, lagoonal, and semi-enclosed systems, often experience pronounced natural fluctuation in key environmental parameters, including pH and DO. Diel variation in pH and DO is primarily driven by benthic photosynthesis and respiration cycles, which elevate DO and pH during the day and deplete them at night (Camp et al., 2018; Pezner et al., 2023; Price et al., 2012). In contrast, seasonal oscillations are more strongly influenced by external climatic factors such as light availability, rainfall, and temperature, which in turn modulate biological activity and water chemistry (Camp et al., 2018; Guadayol et al., 2014). These dynamics are amplified in shallow habitats with limited water exchange, where DO levels can range from hypoxic (< 20% air saturation) at night to hyperoxic (> 200% air saturation) during the day (Lucey et al., 2024; Nelson and Altieri, 2019). In photosynthesizing organisms such as corals, such fluctuations occur not only at reef-wide scales but also at cellular levels, including the diffusive boundary layers surrounding coral tissues (Fusi et al., 2025; Hughes et al., 2020; Shashar et al., 1993).

The spatial and temporal heterogeneity of these fluctuations is shaped by many factors such as reef geomorphology, benthic community composition, and hydrodynamics (Altieri et al., 2021; Guadayol et al., 2014). For example, abrupt depth gradients and restricted water flow in coastal reef flats can amplify metabolic-driven variation, sometimes exposing organisms to environmental extremes that exceed projected future ocean conditions (Altieri et al., 2021). In the Caribbean, Almirante Bay, Bocas del Toro, Panama, exemplifies such a system. This semi-enclosed bay at the Caribbean coast of Panama exhibits strong spatial and temporal variability in environmental conditions, particularly temperature, DO, and pH (Lucey et al., 2020). More pronounced diel fluctuations and lower DO minima are found at inner bay reefs compared to outer bay sites, where the proximity to oceanic flow creates more stable conditions (Adelson et al., 2022; Lucey et al., 2020). Notably, severe hypoxic events have been recorded within the bay in 2010 (Altieri et al., 2017) and 2017 (Johnson et al., 2018). The well-documented history of such events in Almirante Bay provides a valuable natural laboratory for understanding coral tolerance under compound stressors. Yet, while natural observations provide critical insights, controlled laboratory studies remain necessary to disentangle physiological thresholds and mechanisms of stress resistance.

Coral stress tolerance

Coral tolerance to environmental stress arises from both long-term genetic adaptation and shorter-term acclimatization, or phenotypic plasticity (Hackerott et al., 2021). Adaptation

involves changes in allele frequencies across generations, enabling populations to survive under recurrent or long-term stress conditions (Hackerott et al., 2021). In contrast, acclimatization allows individual corals to adjust rapidly to variable conditions within their lifetime through mechanisms such as energy reallocation, upregulation of antioxidant defenses, restructuring of symbiont and microbial communities, and epigenetic modifications (Hackerott et al., 2021; Palumbi et al., 2014; Putnam et al., 2017).

Thermal tolerance is the most extensively studied form of stress resistance in corals, with numerous populations thriving in extreme thermal environments (see review by Camp et al., 2018), demonstrating their capacity to acquire enhanced heat tolerance. The ability of corals to persist in such environments (e.g., Persian-Arabian Gulf and Red Sea) was found to be linked to metabolic trade-offs (Howells et al., 2016) or through associations with heat-specialist Symbiodiniaceae (Smith et al., 2017), illustrating multiple routes to elevated tolerance. A growing body of studies has also investigated coral tolerance to OA, which has been linked to the ability to regulate internal pH as shown in both field (Wall et al., 2016) and laboratory settings (McCulloch et al., 2012; Venn et al., 2011). Complementary work points to epigenetic changes such as shifts in DNA methylation as a potential mechanism for acclimatization to OA (Liew et al., 2018; Putnam et al., 2016).

Much of our mechanistic understanding of acquired stress tolerance stems from single-stressor studies as they allow a more precise attribution of responses. However, many reef habitats like mangrove systems and macrotidal reefs, that are particularly characterized by extreme or highly variable multi-stressor regimes, can still support coral communities with substantial species richness and cover (Camp et al., 2018, 2019), making it inevitable to further our understanding of tolerance acquisition to compound stress conditions. Together, studies of corals in extreme habitats and experimental evidence from controlled stress exposures highlight that repeated exposure to sublethal stress can enhance coral stress tolerance through environmental memory, a retained alteration of physiological or molecular responses linked to prior exposure (Hackerott et al., 2021).

The concept of environmental priming

A growing body of research supports the idea that a coral's environmental history, particularly prior exposure to sublethal stress, can shape its future performance. This process, often referred to as environmental memory, pre-conditioning, or priming, occurs when an initial, sublethal stress exposure improves the organism's tolerance to subsequent stress (Hackerott et al., 2021; Hilker et al., 2016). While well established in terrestrial plants (Hilker and

Schmülling, 2019) and increasingly studied in marine plants and invertebrates (Klein et al., 2017; Li et al., 2020; Nguyen et al., 2020), the concept is gaining recognition in coral reef research more recently (Hackerott et al., 2021).

The mechanisms underlying coral priming are likely multifaceted, involving antioxidant production, shifts in energy allocation, epigenetic regulation of gene expression, and reconfiguration of symbiont or microbiome communities (Baumann et al., 2021; Nelson and Altieri, 2019; Pezner et al., 2023). In reef environments, naturally occurring diel variability in conditions such as temperature, pH, and DO can act as a form of physiological pre-conditioning, enhancing tolerance if exposure remains within sublethal limits, but causing damage if thresholds are exceeded (e.g., Altieri et al., 2021; Safaie et al., 2018).

The dose and temporal pattern of priming are also critical determinants of the corals' priming response to more extreme or prolonged stress exposures that exceed the typical amplitudes of natural diel variation. Insufficient magnitude or duration of priming may not induce detectable memory (e.g., Bellantuono et al., 2012), whereas excessive priming can weaken organisms and negate benefits (e.g., Ainsworth et al., 2016). Most evidence for these temporal nuances comes from thermal bleaching studies: corals exposed to annual bleaching pulses sometimes show reduced severity during a second, consecutive year (Fisch et al., 2019; Hughes et al., 2019), but protective effects can be lost when intervals between events span multiple years (Hughes et al., 2017b). However, such patterns are highly species-specific, reflecting differences in baseline tolerance, energy reserves, and Symbiodiniaceae plasticity (Grottoli et al., 2014; Schoepf et al., 2015).

While most priming research in corals has focused on thermal stress (Hughes et al., 2019; Middlebrook et al., 2012; Puisay et al., 2023), and, to a lesser extent on ocean acidification (Putnam et al., 2020), multi-stressor priming studies remain rare (e.g., warming x OA; Putnam and Gates, 2015). For low DO, natural tolerance acquisition has been documented through reciprocal exposure experiments (Lucey et al., 2025), but these patterns likely reflect long-term adaptation rather than short-term priming.

Understanding whether and how priming can operate under emerging threats like hypoxia, especially in combination with OA, will provide important insight into coral persistence under climate change. This requires defining the dimension and limits of priming (including frequency, duration, magnitude, and recovery windows) and determining whether the benefits observed in single-stressor contexts extend to ecologically relevant compound stress events.

Research gaps and relevance

While the concept of environmental priming has been increasingly studied in corals, the majority of experimental work has focused on single pre-exposure events or chronic conditioning regimes. The latter includes reciprocal transplant experiments where corals experience altered environments over much of their lifetime, providing more insight into longer-term adaptation than into short-term acclimatization/priming (Baumann et al., 2021; Lucey et al., 2025; Palumbi et al., 2014). Few studies have explicitly examined the role of exposure frequency, even though it is likely a critical determinant of priming outcomes, shaping whether corals acclimate, become sensitized, or experience cumulative physiological damage (Hughes et al., 2019; Lucey et al., 2023). To date, frequency effects have been investigated almost exclusively under thermal stress regimes (Safaie et al., 2018), leaving a major gap in understanding for other stressors, which often exhibit different and less predictable temporal dynamics than temperature.

Furthermore, most priming studies have focused on warming and OA (Middlebrook et al., 2012; Puisay et al., 2023; Putnam et al., 2020), whereas hypoxia, and especially its co-occurrence with low pH, remains severely underexplored. This gap is critical, as projections indicate that future reef conditions will increasingly involve simultaneous declines in DO and pH rather than isolated stressors (Melzner et al., 2013). It also remains unclear whether different physiological traits, such as host metabolism, calcification, or symbiont photophysiology, respond in parallel or diverge in their hypoxia-acidification priming response. Thus, it is still poorly resolved under which conditions priming under repeated low DO and pH exposure becomes beneficial or detrimental to coral performance

Filling these gaps is not only of scientific interest but also of practical relevance. From a predictive standpoint, the frequency of stress exposure is likely to determine whether corals exhibit acclimatization or cumulative damage. These outcomes can directly affect population persistence models under future climate scenarios. From a management perspective, understanding frequency effects, specific thresholds, and trait-specific responses can inform coral reef conservation strategies, such as selecting naturally resistant coral populations, optimizing the timing of outplanting, and setting realistic expectations for recovery following hypoxia-acidification events.

1.1. References- General introduction

Adelson, A.E., Altieri, A.H., Boza, X., Collin, R., Davis, K.A., Gaul, A., Giddings, S.N., Reed, V., Pawlak, G., 2022. Seasonal hypoxia and temperature inversions in a tropical bay. Limnology & Oceanography 67, 2174–2189. https://doi.org/10.1002/lno.12196

Ainsworth, T.D., Heron, S.F., Ortiz, J.C., Mumby, P.J., Grech, A., Ogawa, D., Eakin, C.M., Leggat, W., 2016. Climate change disables coral bleaching protection on the Great Barrier Reef. Science 352, 338–342. https://doi.org/10.1126/science.aac7125

Allemand, D., Ferrier-Pagès, C., Furla, P., Houlbrèque, F., Puverel, S., Reynaud, S., Tambutté, É., Tambutté, S., Zoccola, D., 2004. Biomineralisation in reef-building corals: from molecular mechanisms to environmental control. Comptes Rendus Palevol 3, 453–467. https://doi.org/10.1016/j.crpv.2004.07.011

Altieri, A.H., Harrison, S.B., Seemann, J., Collin, R., Diaz, R.J., Knowlton, N., 2017. Tropical dead zones and mass mortalities on coral reefs. Proc. Natl. Acad. Sci. U.S.A. 114, 3660–3665. https://doi.org/10.1073/pnas.1621517114

Altieri, A.H., Johnson, M.D., Swaminathan, S.D., Nelson, H.R., Gedan, K.B., 2021. Resilience of Tropical Ecosystems to Ocean Deoxygenation. Trends in Ecology and Evolution 36, 227–238. https://doi.org/10.1016/j.tree.2020.11.003

Anthony, K.R.N., Maynard, J.A., Diaz-Pulido, G., Mumby, P.J., Marshall, P.A., Cao, L., Hoegh-Guldberg, O., 2011. Ocean acidification and warming will lower coral reef resilience: CO2 AND CORAL REEF RESILIENCE. Global Change Biology 17, 1798–1808. https://doi.org/10.1111/j.1365-2486.2010.02364.x

Baumann, J.H., Bove, C.B., Carne, L., Gutierrez, I., Castillo, K.D., 2021. Two offshore coral species show greater acclimatization capacity to environmental variation than nearshore counterparts in southern Belize. Coral Reefs 40, 1181–1194. https://doi.org/10.1007/s00338-021-02124-8

Beck, M.W., Losada, I.J., Menéndez, P., Reguero, B.G., Díaz-Simal, P., Fernández, F., 2018. The global flood protection savings provided by coral reefs. Nat Commun 9, 2186. https://doi.org/10.1038/s41467-018-04568-z

Bellantuono, A.J., Granados-Cifuentes, C., Miller, D.J., Hoegh-Guldberg, O., Rodriguez-Lanetty, M., 2012. Coral Thermal Tolerance: Tuning Gene Expression to Resist Thermal Stress. PLoS ONE 7, e50685. https://doi.org/10.1371/journal.pone.0050685

Bellwood, D.R., Streit, R.P., Brandl, S.J., Tebbett, S.B., 2019. The meaning of the term 'function' in ecology: A coral reef perspective. Functional Ecology 33, 948–961. https://doi.org/10.1111/1365-2435.13265

Bourne, D.G., Garren, M., Work, T.M., Rosenberg, E., Smith, G.W., Harvell, C.D., 2009. Microbial disease and the coral holobiont. Trends in Microbiology 17, 554–562. https://doi.org/10.1016/j.tim.2009.09.004

Camp, E., Edmondson, J., Doheny, A., Rumney, J., Grima, A., Huete, A., Suggett, D., 2019. Mangrove lagoons of the Great Barrier Reef support coral populations persisting under extreme environmental conditions. Mar. Ecol. Prog. Ser. 625, 1–14. https://doi.org/10.3354/meps13073

Camp, E.F., Schoepf, V., Mumby, P.J., Hardtke, L.A., Rodolfo-Metalpa, R., Smith, D.J., Suggett, D.J., 2018. The Future of Coral Reefs Subject to Rapid Climate Change: Lessons from Natural Extreme Environments. Front. Mar. Sci. 5, 4. https://doi.org/10.3389/fmars.2018.00004

Cordes, E.E., Mienis, F., Gasbarro, R., Davies, A., Baco, A.R., Bernardino, A.F., Clark, M.R., Freiwald, A., Hennige, S.J., Huvenne, V.A.I., Buhl-Mortensen, P., Orejas, C., Quattrini, A.M., Tracey, D.M., Wheeler, A.J., Wienberg, C., 2023. A Global View of the Cold-Water Coral Reefs of the World, in: Cordes, E., Mienis, F. (Eds.), Cold-Water

Coral Reefs of the World, Coral Reefs of the World. Springer International Publishing, Cham, pp. 1–30. https://doi.org/10.1007/978-3-031-40897-7_1
Darling, E.S., Alvarez-Filip, L., Oliver, T.A., McClanahan, T.R., Côté, I.M., 2012. Evaluating life-history strategies of reef corals from species traits. Ecology Letters 15, 1378–1386. https://doi.org/10.1111/j.1461-0248.2012.01861.x
Darwin, C., 1842. The Structure and Distribution of Coral Reefs: Being the First Part of the Geology of the Voyage of the Beagle, under the Command of Capt. Fitzroy, R.N. during the Years 1832 to 1836, 1st ed. Cambridge University Press. https://doi.org/10.1017/CBO9781107325098
Eddy, T.D., Lam, V.W.Y., Reygondeau, G., Cisneros-Montemayor, A.M., Greer, K., Palomares, M.L.D., Bruno, J.F., Ota, Y., Cheung, W.W.L., 2021. Global decline in capacity of coral reefs to provide ecosystem services. One Earth 4, 1278–1285. https://doi.org/10.1016/j.oneear.2021.08.016
Ferrier-Pagès, C., Rottier, C., Beraud, E., Levy, O., 2010. Experimental assessment of the feeding effort of three scleractinian coral species during a thermal stress: Effect on the rates of photosynthesis. Journal of Experimental Marine Biology and Ecology 390, 118–124. https://doi.org/10.1016/j.jembe.2010.05.007
Fisch, J., Drury, C., Towle, E.K., Winter, R.N., Miller, M.W., 2019. Physiological and reproductive repercussions of consecutive summer bleaching events of the threatened Caribbean coral Orbicella faveolata. Coral Reefs 38, 863–876. https://doi.org/10.1007/s00338-019-01817-5
Fisher, R., O'Leary, R.A., Low-Choy, S., Mengersen, K., Knowlton, N., Brainard, R.E., Caley, M.J., 2015. Species Richness on Coral Reefs and the Pursuit of Convergent Global Estimates. Current Biology 25, 500–505. https://doi.org/10.1016/j.cub.2014.12.022
Fusi, M., Stephenson, F., Navarrete, S.A., Tapia, F.J., Largier, J.L., Marasco, R., Rueger, T., MacDonald, C., Daffonchio, D., Fernandez, M., Wieters, E.A., Booth, J., Daghio, M., Sugden, H., Scaife, K., Evans, D.M., Moore, P., Baldanzi, S., 2025. The ecology of the oxyscape in coastal ecosystems. Trends in Ecology & Evolution S0169534725001636. https://doi.org/10.1016/j.tree.2025.06.008
Gobler, C.J., Baumann, H., 2016. Hypoxia and acidification in ocean ecosystems: coupled dynamics and effects on marine life. Biol. Lett. 12, 20150976. https://doi.org/10.1098/rsbl.2015.0976
Golden, C.D., Allison, E.H., Cheung, W.W.L., Dey, M.M., Halpern, B.S., McCauley, D.J., Smith, M., Vaitla, B., Zeller, D., Myers, S.S., 2016. Nutrition: Fall in fish catch threatens human health. Nature 534, 317–320. https://doi.org/10.1038/534317a
Grottoli, A.G., Rodrigues, L.J., Palardy, J.E., 2006. Heterotrophic plasticity and resilience in bleached corals. Nature 440, 1186–1189. https://doi.org/10.1038/nature04565
Grottoli, A.G., Warner, M.E., Levas, S.J., Aschaffenburg, M.D., Schoepf, V., McGinley, M., Baumann, J., Matsui, Y., 2014. The cumulative impact of annual coral bleaching can turn some coral species winners into losers. Global Change Biology 20, 3823–3833. https://doi.org/10.1111/gcb.12658
Guadayol, Ò., Silbiger, N.J., Donahue, M.J., Thomas, F.I.M., 2014. Patterns in Temporal Variability of Temperature, Oxygen and pH along an Environmental Gradient in a Coral Reef. PLoS ONE 9, e85213. https://doi.org/10.1371/journal.pone.0085213
Haas, A.F., Smith, J.E., Thompson, M., Deheyn, D.D., 2014. Effects of reduced dissolved oxygen concentrations on physiology and fluorescence of hermatypic corals and benthic algae. PeerJ 2, e235. https://doi.org/10.7717/peerj.235
Hackerott, S., Martell, H.A., Eirin-Lopez, J.M., 2021. Coral environmental memory: causes, mechanisms, and consequences for future reefs. Trends in Ecology & Evolution 36, 1011–1023. https://doi.org/10.1016/j.tree.2021.06.014

Hatcher, B.G., 1990. Coral reef primary productivity. A hierarchy of pattern and process. Trends in Ecology & Evolution 5, 149–155. https://doi.org/10.1016/0169-5347(90)90221-X
Hilker, M., Schmülling, T., 2019. Stress priming, memory, and signalling in plants. Plant Cell & Environment 42, 753–761. https://doi.org/10.1111/pce.13526
Hilker, M., Schwachtje, J., Baier, M., Balazadeh, S., Bäurle, I., Geiselhardt, S., Hincha, D.K., Kunze, R., Mueller-Roeber, B., Rillig, M.C., Rolff, J., Romeis, T., Schmülling, T., Steppuhn, A., Van Dongen, J., Whitcomb, S.J., Wurst, S., Zuther, E., Kopka, J., 2016. Priming and memory of stress responses in organisms lacking a nervous system. Biological Reviews 91, 1118–1133. https://doi.org/10.1111/brv.12215
Hill, T.S., Hoogenboom, M.O., 2022. The indirect effects of ocean acidification on corals and coral communities. Coral Reefs 41, 1557–1583. https://doi.org/10.1007/s00338-022-02286-z
Hoegh-Guldberg, O., Mumby, P.J., Hooten, A.J., Steneck, R.S., Greenfield, P., Gomez, E., Harvell, C.D., Sale, P.F., Edwards, A.J., Caldeira, K., Knowlton, N., Eakin, C.M., Iglesias-Prieto, R., Muthiga, N., Bradbury, R.H., Dubi, A., Hatziolos, M.E., 2007. Coral Reefs Under Rapid Climate Change and Ocean Acidification. Science 318, 1737–1742. https://doi.org/10.1126/science.1152509
Hohn, S., Merico, A., 2015. Quantifying the relative importance of transcellular and paracellular ion transports to coral polyp calcification. Front. Earth Sci. 2. https://doi.org/10.3389/feart.2014.00037
Howells, E.J., Ketchum, R.N., Bauman, A.G., Mustafa, Y., Watkins, K.D., Burt, J.A., 2016. Species-specific trends in the reproductive output of corals across environmental gradients and bleaching histories. Marine Pollution Bulletin 105, 532–539. https://doi.org/10.1016/j.marpolbul.2015.11.034
Hsiao, S.-C., Wu, H.-L., Fu, H.-S., Chen, W.-B., 2025. Accelerated Ocean acidification (1985–2022) threatens tropical coral reefs and highlights biogeochemical refugia for marine conservation. Journal of Sea Research 207, 102612. https://doi.org/10.1016/j.seares.2025.102612
Hughes, D.J., Alderdice, R., Cooney, C., Kühl, M., Pernice, M., Voolstra, C.R., Suggett, D.J., 2020. Coral reef survival under accelerating ocean deoxygenation. Nat. Clim. Chang. 10, 296–307. https://doi.org/10.1038/s41558-020-0737-9
Hughes, D.J., Alexander, J., Cobbs, G., Kühl, M., Cooney, C., Pernice, M., Varkey, D., Voolstra, C.R., Suggett, D.J., 2022. Widespread oxyregulation in tropical corals under hypoxia. Marine Pollution Bulletin 179, 113722. https://doi.org/10.1016/j.marpolbul.2022.113722
Hughes, T.P., Ayre, D., Connell, J.H., 1992. The evolutionary ecology of corals. Trends in Ecology & Evolution 7, 292–295. https://doi.org/10.1016/0169-5347(92)90225-z
Hughes, T.P., Barnes, M.L., Bellwood, D.R., Cinner, J.E., Cumming, G.S., Jackson, J.B.C., Kleypas, J., Van De Leemput, I.A., Lough, J.M., Morrison, T.H., Palumbi, S.R., Van Nes, E.H., Scheffer, M., 2017a. Coral reefs in the Anthropocene. Nature 546, 82–90. https://doi.org/10.1038/nature22901
Hughes, T.P., Bellwood, D.R., Connolly, S.R., 2002. Biodiversity hotspots, centres of endemicity, and the conservation of coral reefs. Ecology Letters 5, 775–784. https://doi.org/10.1046/j.1461-0248.2002.00383.x
Hughes, T.P., Kerry, J.T., Álvarez-Noriega, M., Álvarez-Romero, J.G., Anderson, K.D., Baird, A.H., Babcock, R.C., Beger, M., Bellwood, D.R., Berkelmans, R., Bridge, T.C., Butler, I.R., Byrne, M., Cantin, N.E., Comeau, S., Connolly, S.R., Cumming, G.S., Dalton, S.J., Diaz-Pulido, G., Eakin, C.M., Figueira, W.F., Gilmour, J.P., Harrison, H.B., Heron, S.F., Hoey, A.S., Hobbs, J.-P.A., Hoogenboom, M.O., Kennedy, E.V., Kuo, C., Lough, J.M., Lowe, R.J., Liu, G., McCulloch, M.T., Malcolm, H.A.,

McWilliam, M.J., Pandolfi, J.M., Pears, R.J., Pratchett, M.S., Schoepf, V., Simpson, T., Skirving, W.J., Sommer, B., Torda, G., Wachenfeld, D.R., Willis, B.L., Wilson, S.K., 2017b. Global warming and recurrent mass bleaching of corals. Nature 543, 373–377. https://doi.org/10.1038/nature21707

Hughes, T.P., Kerry, J.T., Connolly, S.R., Baird, A.H., Eakin, C.M., Heron, S.F., Hoey, A.S., Hoogenboom, M.O., Jacobson, M., Liu, G., Pratchett, M.S., Skirving, W., Torda, G., 2019. Ecological memory modifies the cumulative impact of recurrent climate extremes. Nature Clim Change 9, 40–43. https://doi.org/10.1038/s41558-018-0351-2

Hughes, T.P., Tanner, J.E., 2000. RECRUITMENT FAILURE, LIFE HISTORIES, AND LONG-TERM DECLINE OF CARIBBEAN CORALS. Ecology 81, 2250–2263. https://doi.org/10.1890/0012-9658(2000)081%255B2250:RFLHAL%255D2.0.CO;2

IPCC, 2022. The Ocean and Cryosphere in a Changing Climate: Special Report of the Intergovernmental Panel on Climate Change, 1st ed. Cambridge University Press. https://doi.org/10.1017/9781009157964

Johannes, R., Wiebe, W., Crossland, C., Rimmer, D., Smith, S., 1983. Latitudinal limits of coral reef growth. Mar. Ecol. Prog. Ser. 11, 105–111. https://doi.org/10.3354/meps011105

Johnson, M.D., Rodriguez, L.M., Altieri, A.H., 2018. Shallow-water hypoxia and mass mortality on a Caribbean coral reef. bms 94, 143–144. https://doi.org/10.5343/bms.2017.1163

Johnson, M.D., Swaminathan, S.D., Nixon, E.N., Paul, V.J., Altieri, A.H., 2021. Differential susceptibility of reef-building corals to deoxygenation reveals remarkable hypoxia tolerance. Sci Rep 11, 23168. https://doi.org/10.1038/s41598-021-01078-9

Jones, L.A., Mannion, P.D., Farnsworth, A., Bragg, F., Lunt, D.J., 2022. Climatic and tectonic drivers shaped the tropical distribution of coral reefs. Nat Commun 13, 3120. https://doi.org/10.1038/s41467-022-30793-8

Jones, R.J., Hoegh-Guldberg, O., 2001. Diurnal changes in the photochemical efficiency of the symbiotic dinoflagellates (Dinophyceae) of corals: photoprotection, photoinactivation and the relationship to coral bleaching. Plant Cell & Environment 24, 89–99. https://doi.org/10.1046/j.1365-3040.2001.00648.x

Kealoha, A.K., Doyle, S.M., Shamberger, K.E.F., Sylvan, J.B., Hetland, R.D., DiMarco, S.F., 2020. Localized hypoxia may have caused coral reef mortality at the Flower Garden Banks. Coral Reefs 39, 119–132. https://doi.org/10.1007/s00338-019-01883-9

Kennedy, D., 2002. Fringing reef growth and morphology: a review. Earth-Science Reviews 57, 255–277. https://doi.org/10.1016/S0012-8252(01)00077-0

Klein, S.G., Pitt, K.A., Carroll, A.R., 2017. Pre-exposure to simultaneous, but not individual, climate change stressors limits acclimation capacity of Irukandji jellyfish polyps to predicted climate scenarios. Coral Reefs 36, 987–1000. https://doi.org/10.1007/s00338-017-1590-9

Knowlton, N., Jackson, J.B.C., 2008. Shifting Baselines, Local Impacts, and Global Change on Coral Reefs. PLoS Biol 6, e54. https://doi.org/10.1371/journal.pbio.0060054

Kroeker, K.J., Kordas, R.L., Crim, R., Hendriks, I.E., Ramajo, L., Singh, G.S., Duarte, C.M., Gattuso, J., 2013. Impacts of ocean acidification on marine organisms: quantifying sensitivities and interaction with warming. Global Change Biology 19, 1884–1896. https://doi.org/10.1111/gcb.12179

LaJeunesse, T.C., Parkinson, J.E., Gabrielson, P.W., Jeong, H.J., Reimer, J.D., Voolstra, C.R., Santos, S.R., 2018. Systematic Revision of Symbiodiniaceae Highlights the Antiquity and Diversity of Coral Endosymbionts. Current Biology 28, 2570-2580.e6. https://doi.org/10.1016/j.cub.2018.07.008

Lee, H., Calvin, K., Dasgupta, D., Krinner, G., Mukherji, A., Thorne, P.W., Trisos, C., Romero, J., Aldunce, P., Barrett, K., Blanco, G., Cheung, W.W.L., Connors, S.,

Denton, F., Diongue-Niang, A., Dodman, D., Garschagen, M., Geden, O., Hayward, B., Jones, C., Jotzo, F., Krug, T., Lasco, R., Lee, Y.-Y., Masson-Delmotte, V., Meinshausen, M., Mintenbeck, K., Mokssit, A., Otto, F.E.L., Pathak, M., Pirani, A., Poloczanska, E., Pörtner, H.-O., Revi, A., Roberts, D.C., Roy, J., Ruane, A.C., Skea, J., Shukla, P.R., Slade, R., Slangen, A., Sokona, Y., Sörensson, A.A., Tignor, M., Van Vuuren, D., Wei, Y.-M., Winkler, H., Zhai, P., Zommers, Z., Hourcade, J.-C., Johnson, F.X., Pachauri, S., Simpson, N.P., Singh, C., Thomas, A., Totin, E., Arias, P., Bustamante, M., Elgizouli, I., Flato, G., Howden, M., Méndez-Vallejo, C., Pereira, J.J., Pichs-Madruga, R., Rose, S.K., Saheb, Y., Sánchez Rodríguez, R., Ürge-Vorsatz, D., Xiao, C., Yassaa, N., Alegría, A., Armour, K., Bednar-Friedl, B., Blok, K., Cissé, G., Dentener, F., Eriksen, S., Fischer, E., Garner, G., Guivarch, C., Haasnoot, M., Hansen, G., Hauser, M., Hawkins, E., Hermans, T., Kopp, R., Leprince-Ringuet, N., Lewis, J., Ley, D., Ludden, C., Niamir, L., Nicholls, Z., Some, S., Szopa, S., Trewin, B., Van Der Wijst, K.-I., Winter, G., Witting, M., Birt, A., Ha, M., Romero, J., Kim, J., Haites, E.F., Jung, Y., Stavins, R., Birt, A., Ha, M., Orendain, D.J.A., Ignon, L., Park, S., Park, Y., Reisinger, A., Cammaramo, D., Fischlin, A., Fuglestvedt, J.S., Hansen, G., Ludden, C., Masson-Delmotte, V., Matthews, J.B.R., Mintenbeck, K., Pirani, A., Poloczanska, E., Leprince-Ringuet, N., Péan, C., 2023. IPCC, 2023: Climate Change 2023: Synthesis Report. Contribution of Working Groups I, II and III to the Sixth Assessment Report of the Intergovernmental Panel on Climate Change [Core Writing Team, H. Lee and J. Romero (eds.)]. IPCC, Geneva, Switzerland. Intergovernmental Panel on Climate Change (IPCC). https://doi.org/10.59327/IPCC/AR6-9789291691647

Lesser, M.P., 2021. Eutrophication on Coral Reefs: What Is the Evidence for Phase Shifts, Nutrient Limitation and Coral Bleaching. BioScience 71, 1216–1233. https://doi.org/10.1093/biosci/biab101

Li, H., Huang, X., Zhan, A., 2020. Stress Memory of Recurrent Environmental Challenges in Marine Invasive Species: Ciona robusta as a Case Study. Front. Physiol. 11, 94. https://doi.org/10.3389/fphys.2020.00094

Li, J., Asner, G.P., 2023. Global analysis of benthic complexity in shallow coral reefs. Environ. Res. Lett. 18, 024038. https://doi.org/10.1088/1748-9326/acb3e6

Liew, Y.J., Zoccola, D., Li, Y., Tambutté, E., Venn, A.A., Michell, C.T., Cui, G., Deutekom, E.S., Kaandorp, J.A., Voolstra, C.R., Forêt, S., Allemand, D., Tambutté, S., Aranda, M., 2018. Epigenome-associated phenotypic acclimatization to ocean acidification in a reef-building coral. Sci. Adv. 4, eaar8028. https://doi.org/10.1126/sciadv.aar8028

Lucey, N., César-Ávila, C., Eckert, A., Veintimilla, P., Collin, R., 2025. Locally Adapted Coral Species Withstand a 2-Week Hypoxic Event. Oceans 6, 5. https://doi.org/10.3390/oceans6010005

Lucey, N., Haskett, E., Collin, R., 2020. Multi-stressor Extremes Found on a Tropical Coral Reef Impair Performance. Front. Mar. Sci. 7, 588764. https://doi.org/10.3389/fmars.2020.588764

Lucey, N.M., César-Ávila, C., Eckert, A., Rajagopalan, A., Brister, W.C., Kline, E., Altieri, A.H., Deutsch, C.A., Collin, R., 2024. Coral Community Composition Linked to Hypoxia Exposure. Global Change Biology 30. https://doi.org/10.1111/gcb.17545

Lucey, N.M., Deutsch, C.A., Carignan, M.-H., Vermandele, F., Collins, M., Johnson, M.D., Collin, R., Calosi, P., 2023. Climate warming erodes tropical reef habitat through frequency and intensity of episodic hypoxia. PLOS Clim 2, e0000095. https://doi.org/10.1371/journal.pclm.0000095

Lyons, M.B., Murray, N.J., Kennedy, E.V., Kovacs, E.M., Castro-Sanguino, C., Phinn, S.R., Acevedo, R.B., Alvarez, A.O., Say, C., Tudman, P., Markey, K., Roe, M., Canto, R.F., Fox, H.E., Bambic, B., Lieb, Z., Asner, G.P., Martin, P.M., Knapp, D.E., Li, J., Skone,

M., Goldenberg, E., Larsen, K., Roelfsema, C.M., 2024. New global area estimates for coral reefs from high-resolution mapping. Cell Reports Sustainability 1, 100015. https://doi.org/10.1016/j.crsus.2024.100015
McCulloch, M., Falter, J., Trotter, J., Montagna, P., 2012. Coral resilience to ocean acidification and global warming through pH up-regulation. Nature Clim Change 2, 623–627. https://doi.org/10.1038/nclimate1473
Melzner, F., Thomsen, J., Koeve, W., Oschlies, A., Gutowska, M.A., Bange, H.W., Hansen, H.P., Körtzinger, A., 2013. Future ocean acidification will be amplified by hypoxia in coastal habitats. Mar Biol 160, 1875–1888. https://doi.org/10.1007/s00227-012-1954-1
Middlebrook, R., Anthony, K.R.N., Hoegh-Guldberg, O., Dove, S., 2012. Thermal priming affects symbiont photosynthesis but does not alter bleaching susceptibility in Acropora millepora. Journal of Experimental Marine Biology and Ecology 432–433, 64–72. https://doi.org/10.1016/j.jembe.2012.07.005
Moberg, F., Folke, C., 1999. Ecological goods and services of coral reef ecosystems. Ecological Economics 29, 215–233. https://doi.org/10.1016/s0921-8009(99)00009-9
Morais, R.A., Patricio-Valerio, L., Narvaez, P., Parravicini, V., Brandl, S.J., 2025. Rethinking Darwin's coral reef paradox and the ubiquity of "marine oases." Current Biology 35, 3241-3250.e6. https://doi.org/10.1016/j.cub.2025.05.033
Muscatine, L., R. McCloskey, L., E. Marian, R., 1981. Estimating the daily contribution of carbon from zooxanthellae to coral animal respiration1. Limnology & Oceanography 26, 601–611. https://doi.org/10.4319/lo.1981.26.4.0601
Nelson, H.R., Altieri, A.H., 2019. Oxygen: the universal currency on coral reefs. Coral Reefs 38, 177–198. https://doi.org/10.1007/s00338-019-01765-0
Nguyen, H.M., Kim, M., Ralph, P.J., Marín-Guirao, L., Pernice, M., Procaccini, G., 2020. Stress Memory in Seagrasses: First Insight Into the Effects of Thermal Priming and the Role of Epigenetic Modifications. Front. Plant Sci. 11, 494. https://doi.org/10.3389/fpls.2020.00494
Orr, J.C., Fabry, V.J., Aumont, O., Bopp, L., Doney, S.C., Feely, R.A., Gnanadesikan, A., Gruber, N., Ishida, A., Joos, F., Key, R.M., Lindsay, K., Maier-Reimer, E., Matear, R., Monfray, P., Mouchet, A., Najjar, R.G., Plattner, G.-K., Rodgers, K.B., Sabine, C.L., Sarmiento, J.L., Schlitzer, R., Slater, R.D., Totterdell, I.J., Weirig, M.-F., Yamanaka, Y., Yool, A., 2005. Anthropogenic ocean acidification over the twenty-first century and its impact on calcifying organisms. Nature 437, 681–686. https://doi.org/10.1038/nature04095
Oschlies, A., Brandt, P., Stramma, L., Schmidtko, S., 2018. Drivers and mechanisms of ocean deoxygenation. Nature Geosci 11, 467–473. https://doi.org/10.1038/s41561-018-0152-2
Palumbi, S.R., Barshis, D.J., Traylor-Knowles, N., Bay, R.A., 2014. Mechanisms of reef coral resistance to future climate change. Science 344, 895–898. https://doi.org/10.1126/science.1251336
Pezner, A.K., Courtney, T.A., Barkley, H.C., Chou, W.-C., Chu, H.-C., Clements, S.M., Cyronak, T., DeGrandpre, M.D., Kekuewa, S.A.H., Kline, D.I., Liang, Y.-B., Martz, T.R., Mitarai, S., Page, H.N., Rintoul, M.S., Smith, J.E., Soong, K., Takeshita, Y., Tresguerres, M., Wei, Y., Yates, K.K., Andersson, A.J., 2023. Increasing hypoxia on global coral reefs under ocean warming. Nat. Clim. Chang. 13, 403–409. https://doi.org/10.1038/s41558-023-01619-2
Price, N.N., Martz, T.R., Brainard, R.E., Smith, J.E., 2012. Diel Variability in Seawater pH Relates to Calcification and Benthic Community Structure on Coral Reefs. PLoS ONE 7, e43843. https://doi.org/10.1371/journal.pone.0043843

Puisay, A., Hédouin, L., Pilon, R., Goiran, C., Pujol, B., 2023. How thermal priming of coral gametes shapes fertilization success. Journal of Experimental Marine Biology and Ecology 566, 151920. https://doi.org/10.1016/j.jembe.2023.151920

Putnam, H.M., Barott, K.L., Ainsworth, T.D., Gates, R.D., 2017. The Vulnerability and Resilience of Reef-Building Corals. Current Biology 27, R528–R540. https://doi.org/10.1016/j.cub.2017.04.047

Putnam, H.M., Davidson, J.M., Gates, R.D., 2016. Ocean acidification influences host DNA methylation and phenotypic plasticity in environmentally susceptible corals. Evolutionary Applications 9, 1165–1178. https://doi.org/10.1111/eva.12408

Putnam, H.M., Gates, R.D., 2015. Preconditioning in the reef-building coral *Pocillopora damicornis* and the potential for trans-generational acclimatization in coral larvae under future climate change conditions. Journal of Experimental Biology 218, 2365–2372. https://doi.org/10.1242/jeb.123018

Raj, K.D., Mathews, G., Obura, D.O., Laju, R.L., Bharath, M.S., Kumar, P.D., Arasamuthu, A., Kumar, T.K.A., Edward, J.K.P., 2020. Low oxygen levels caused by Noctiluca scintillans bloom kills corals in Gulf of Mannar, India. Sci Rep 10, 22133. https://doi.org/10.1038/s41598-020-79152-x

Safaie, A., Silbiger, N.J., McClanahan, T.R., Pawlak, G., Barshis, D.J., Hench, J.L., Rogers, J.S., Williams, G.J., Davis, K.A., 2018. High frequency temperature variability reduces the risk of coral bleaching. Nat Commun 9, 1671. https://doi.org/10.1038/s41467-018-04074-2

Schoepf, V., Stat, M., Falter, J.L., McCulloch, M.T., 2015. Limits to the thermal tolerance of corals adapted to a highly fluctuating, naturally extreme temperature environment. Sci Rep 5, 17639. https://doi.org/10.1038/srep17639

Shashar, N., Cohen, Y., Loya, Y., 1993. Extreme Diel Fluctuations of Oxygen in Diffusive Boundary Layers Surrounding Stony Corals. The Biological Bulletin 185, 455–461. https://doi.org/10.2307/1542485

Smith, E.G., Hume, B.C.C., Delaney, P., Wiedenmann, J., Burt, J.A., 2017. Genetic structure of coral-Symbiodinium symbioses on the world's warmest reefs. PLoS ONE 12, e0180169. https://doi.org/10.1371/journal.pone.0180169

Spalding, M., Burke, L., Wood, S.A., Ashpole, J., Hutchison, J., Zu Ermgassen, P., 2017. Mapping the global value and distribution of coral reef tourism. Marine Policy 82, 104–113. https://doi.org/10.1016/j.marpol.2017.05.014

Sturaro, N., Hsieh, Y.E., Chen, Q., Wang, P., Denis, V., 2021. Trophic plasticity of mixotrophic corals under contrasting environments. Functional Ecology 35, 2841–2855. https://doi.org/10.1111/1365-2435.13924

Vaquer-Sunyer, R., Duarte, C.M., 2008. Thresholds of hypoxia for marine biodiversity. Proc. Natl. Acad. Sci. U.S.A. 105, 15452–15457. https://doi.org/10.1073/pnas.0803833105

Venn, A., Tambutté, E., Holcomb, M., Allemand, D., Tambutté, S., 2011. Live Tissue Imaging Shows Reef Corals Elevate pH under Their Calcifying Tissue Relative to Seawater. PLoS ONE 6, e20013. https://doi.org/10.1371/journal.pone.0020013

Wall, M., Fietzke, J., Schmidt, G.M., Fink, A., Hofmann, L.C., De Beer, D., Fabricius, K.E., 2016. Internal pH regulation facilitates in situ long-term acclimation of massive corals to end-of-century carbon dioxide conditions. Sci Rep 6, 30688. https://doi.org/10.1038/srep30688

Wear, S.L., 2016. Missing the boat: Critical threats to coral reefs are neglected at global scale. Marine Policy 74, 153–157. https://doi.org/10.1016/j.marpol.2016.09.009

Wild, C., Hoegh-Guldberg, O., Naumann, M.S., Colombo-Pallotta, M.F., Ateweberhan, M., Fitt, W.K., Iglesias-Prieto, R., Palmer, C., Bythell, J.C., Ortiz, J.-C., Loya, Y., Van Woesik, R., 2011. Climate change impedes scleractinian corals as primary reef ecosystem engineers. Mar. Freshwater Res. 62, 205. https://doi.org/10.1071/MF10254

Woodhead, A.J., Hicks, C.C., Norström, A.V., Williams, G.J., Graham, N.A.J., 2019. Coral reef ecosystem services in the Anthropocene. Functional Ecology 33, 1023–1034. https://doi.org/10.1111/1365-2435.13331

Wooldridge, S.A., 2013. Breakdown of the coral-algae symbiosis: towards formalising a linkage between warm-water bleaching thresholds and the growth rate of the intracellular zooxanthellae. Biogeosciences 10, 1647–1658. https://doi.org/10.5194/bg-10-1647-2013

2. Manuscript

Exposure frequency shapes coral physiology under low oxygen and pH, with limited effects on acute stress resilience

Author: Sophie Littke

Affiliation: University of Algarve, Faro, Portugal

Corresponding author: Sophie Littke, a83071@ualg.pt

Key words: Environmental priming, coral resilience, diel hypoxia and acidification, physiological plasticity, *Agaricia tenuifolia, Siderastrea siderea*

2.1. Abstract

Severe hypoxia, often coupled with low pH, is an emerging threat to coral reefs, yet their combined effects, and the potential for environmental priming to modulate coral responses under such stress, remain understudied. In particular, the frequency and timing of prior sublethal exposure to combined low oxygen and pH are largely unexplored as drivers of coral stress tolerance. We conducted a controlled laboratory experiment to test how the frequency of nightly low dissolved oxygen (DO) and pH exposure shapes physiological responses of two Caribbean coral species, *Agaricia tenuifolia* and *Siderastrea siderea*, during subsequent, acute combined stress. Corals received six (high frequency, HF), three (low frequency, LF), or no (control) priming pulses, each lasting two consecutive nights, over four weeks, mimicking natural diel DO and pH cycles in shallow reefs, followed by 4–7 days of acute stress or ambient conditions. Results revealed contrasting species-specific outcomes. In *A. tenuifolia,* HF priming reduced baseline photosynthetic efficiency by 32% by the end of the priming period, with no further change during acute stress. HF primed *A. tenuifolia* also exhibited a ~42% reduction in symbiont densities, and a nearly tenfold increased risk of tissue loss compared to controls, regardless of acute stress treatment, while biomass and calcification remained unchanged. In contrast, *S. siderea* showed physiological stability across treatments, with LF priming supporting tissue biomass maintenance under acute stress. By the experimental end, biomass declined 28% and 22% in unprimed and HF-primed corals under acute stress*,* respectively, whereas LF primed corals maintained biomass. These findings highlight stress frequency as a critical yet understudied dimension of environmental priming and a direct modulator of baseline coral physiology. HF priming impaired the hypoxia-sensitive *A. tenuifolia*, while LF priming was neutral. The more hypoxia-tolerant *S. siderea* showed subtle LF priming benefits and no HF effects. As climate change and coastal eutrophication intensify diel variability and acute low DO and pH events, understanding frequency-dependent stress responses will improve predictions of reef community trajectories and help identify resilient coral populations.

2.2. Introduction

Tropical coral reefs are increasingly threatened by acute and chronic environmental stressors associated with global climate change and local anthropogenic impacts (Barnard et al., 2021; Hoegh-Guldberg et al., 2017). Among these, ocean warming, ocean acidification (OA), and coastal deoxygenation are particularly harmful to coral physiology. Warming and deoxygenation can severely disrupt coral-algae symbiosis and impair coral metabolism (Hoegh-Guldberg et al., 2017; Hughes et al., 2022; Johnson et al., 2021a), while OA primarily reduces calcification and recruitment (Anthony et al., 2011; Hsiao et al., 2025; Kroeker et al., 2013). All three stressors can reduce physiological performance and, under severe conditions, increase mortality (Hoegh-Guldberg et al., 2017; Johnson et al., 2021a). While the impacts of OA and warming have been extensively studied (e.g., Bove et al., 2020; Hoegh-Guldberg et al., 2017; Hsiao et al., 2025), coastal deoxygenation and its interaction with OA and warming have only recently gained attention as a critical threat to coral reefs (Altieri et al., 2017; Hughes et al., 2022).

OA results from the ocean's absorption of excess atmospheric CO_2 (carbon dioxide), which lowers seawater pH and alters carbonate chemistry, compromising calcifying organisms such as reef-building corals (Orr et al., 2005). Coastal deoxygenation, often driven by warming and nutrient pollution, reduces oxygen solubility and increases biological oxygen demand, leading to the depletion of dissolved oxygen (DO) (Oschlies et al., 2018). Notably, acute hypoxia can be a driver of bleaching in some corals (e.g., Alderdice et al., 2021, 2022; Lucey et al., 2025), challenging the conventional attribution of mass bleaching solely to thermal stress and highlighting the need to integrate the combined roles of hypoxia and OA.

In many shallow reef and lagoon systems, diel fluctuations in DO and pH are common, driven by the balance of daytime photosynthesis and nighttime respiration (Pezner et al., 2023). In photosynthesizing organisms like corals, these fluctuations occur not only at the reef scale but also within their tissues and in the diffusive boundary layers immediately surrounding them (Fusi et al., 2025; Hughes et al., 2020; Shashar et al., 1993), resulting in naturally lower pH and DO at night. While some coral taxa appear adapted to high diel variability (Camp et al., 2017, 2018; Hughes et al., 2022), increasingly frequent and severe hypoxia threatens to push environmental conditions beyond coral adaptive capacity (Johnson et al., 2021a). Globally, 84% of coral reefs already experience at least mild to moderate hypoxia (Pezner et al., 2023). Acute hypoxia events leading to mass bleaching and 70-80% coral mortality have increasingly been reported over the past two decades in regions like Almirante Bay (Altieri et

al., 2017; Johnson et al., 2018), the Gulf of Manmar, India (Raj et al., 2020), and the Flower Garden Banks, USA (Kealoha et al., 2020). These events often recur in the same locations, creating repeated exposure regimes (Deutsch et al., 2024). Similarly, mean surface ocean pH is projected to fall by ~0.04-0.29 units by 2100, depending on the carbon emission scenario (IPCC, 2022). Given that hypoxia and OA predominantly have been shown to act additively on marine taxa (Steckbauer et al., 2020), it is very likely that combined hypoxia-acidification events become not only more frequently, but also increasingly harmful to coral reefs. Susceptibility to these stress events varies substantially among coral species and populations (e.g., Hughes et al., 2020; Johnson et al., 2021b; Lucey et al., 2025, 2024), underscoring the need to understand the mechanisms underlying coral resilience under increasingly variable and extreme DO an pH regimes.

Field evidence suggests that exposure history shapes stress tolerance in corals. In some naturally extreme reef environments, coral populations persist under chronically variable and stressful conditions, exhibiting remarkable stress tolerance (Camp et al., 2019, 2018; Palumbi et al., 2014). Reciprocal transplant experiments (e.g., Kurihara et al., 2021; Lucey et al., 2025; Tanvet et al., 2023) can help distinguish whether trait differences reflect phenotypic plasticity or genetic adaptation, but in practice they often highlight longer-term processes such as local adaptation and natural selection. To specifically resolve short-term acclimation potential, controlled experimental approaches are therefore needed.

One proposed short-term mechanism that could enhance stress tolerance is environmental priming, a process by which prior exposure to mild or sublethal stress improves an organism's capacity to withstand future stress events (Hackerott et al., 2021; Hilker et al., 2016). Priming is well-documented in terrestrial plants (Hilker and Schmülling, 2019) and increasingly studied in marine plants and invertebrates (e.g., Klein et al., 2017; Li et al., 2020; Nguyen et al., 2020). In reef-building corals, however, experimental evidence remains limited and largely focused on single stressors such as thermal stress or OA (see review by Hackerott et al., 2021). Thermal pre-exposure has been shown to improve thermal stress resistance in some coral taxa (e.g., Middlebrook et al., 2008, 2012), and parental exposure to low pH levels alone (Putnam et al., 2020), or in combination with warming (Putnam and Gates, 2015) can shape offspring performance through transgenerational priming. However, priming in the context of hypoxia remains virtually unexplored, even though low DO events are intensifying and recurring in tropical reefs (Pezner et al., 2023). While recent work has begun to clarify how the duration and intensity of low DO exposure influence coral physiology (Mallon et al.,

2025), there is no current evidence of hypoxia priming responses. With priming outcomes depending on many dimensions like exposure duration and intensity (Hackerott et al., 2021), the frequency of stress pre-exposure as a determinant for priming outcome remains largely unaddressed. Thus far, high frequency diel thermal variability has only been shown to enhance thermal tolerance in corals if cumulative exposure does not exceed tolerance thresholds (Safaie et al., 2018). Yet, comparable experiments investigating frequency effects under co-occurring hypoxia and OA are still lacking. Understanding when stress pre-exposure becomes beneficial or detrimental to the coral holobiont is essential to predict coral performance under increasing environmental variability (Hackerott et al., 2021).

To address these knowledge gaps, we tested whether different frequencies of nightly low DO and pH exposure affect coral responses to a subsequent, acute hypoxia-acidification event, using a controlled aquarium experiment that simulated ecologically realistic diel stress cycles. We assessed a comprehensive set of host and symbiont physiological traits in two Caribbean coral species, *Agaricia tenuifolia* (Dana, 1848) and *Siderastrea siderea* (Ellis and Solander, 1786), both abundant on hypoxia-naïve reefs in Almirante Bay, Panama. Understanding species-specific variability in priming capacity and physiological plasticity is essential, as different success of coral taxa under suboptimal conditions can drive shifts in reef community composition (e.g., Lucey et al 2024), reducing habitat complexity and associated ecosystem functions (e.g., Rogers et al., 2015). We hypothesized that repeated exposure to nighttime stress over four weeks, characterized by low DO and pH, would enhance coral tolerance to a subsequent, acute hypoxic-acidification event in a frequency-dependent manner. Specifically, we anticipated that low frequency priming would be more beneficial for the more sensitive *A. tenuifolia,* whereas high frequency priming would be required to elicit a beneficial effect in the more resistant *S. siderea*.

2.3. Material and Methods

Study site, coral collection, and acclimation

The experiment was conducted using corals collected from Punta Caracol reef site (9°22’36’’N 82°18’05’’W) in Almirante Bay, Bocas del Toro, a large semi-enclosed bay on the Caribbean Coast of Panama. This bay exhibits strong spatial and temporal variability in environmental conditions, particularly DO, pH, temperature, and nutrients (Lucey et al., 2020). DO fluctuations in the bay show clear seasonal patterns, with the most severe diel lows typically occurring between September and November (Lucey et al., 2020). Severe, hypoxic events have been recorded within Almirante Bay, notably in 2010 (Altieri et al., 2017) and

2017 (Johnson et al., 2018), leading to drastic coral loss, with live coral cover dropping to ~4% (Altieri et al., 2017). In experimental studies from that region, hypoxic events were defined as reaching levels of DO < 1 mg L^{-1}, with such conditions typically occurring over one to two consecutive nights at inner bay sites (Lucey et al., 2024). In Almirante Bay, the intensity of low DO levels and the occurrence of hypoxic events vary spatially and with depth, with more pronounced diel fluctuations and lower DO minima recorded at inner bay reefs compared to outer bay sites, where the proximity to oceanic inflow creates more stable conditions (Adelson et al., 2022; Lucey et al., 2020).

We collected coral fragments from the comparatively more stable outer bay site of Punta Caracol, which has no documented history of extreme low DO exposure (Lucey et al., 2024). This choice was motivated by previous work showing that corals from hypoxia impacted reefs in Almirante Bay exhibit increased tolerance to subsequent low DO events (Lucey et al., 2025), while conspecifics from more stable sites, such as Punta Caracol, are more susceptible. By using individuals that are naïve to hypoxia, we aimed to test whether tolerance toward low DO and pH could be experimentally induced through laboratory-based environmental priming.

To characterize background reef conditions, high resolution *in-situ* data loggers were deployed at the collection site. These loggers were deployed from September to November 2024 to measure and record temperature, DO, pH, photosynthetically active radiation (PAR), and conductivity levels at regular intervals (See Supplement A for detailed methods; Supplement B, Table S1 for data results).

Coral specimens were collected on 24 September 2024 (Permit: ARB-096-2023, Ministerio de Ambiente), using a hammer and chisel at 4-5.5 m depth. Two species were selected based on their abundance on the hypoxia-naïve collection site: *Siderastrea siderea*, described to be generally more tolerant toward hypoxia and acidification, and *Agaricia tenuifolia*, typically more sensitive towards environmental stress (e.g., Bove et al., 2019; Lucey et al., 2025). To maximize the likelihood of sampling genetically different individuals, six parent colonies per species were sampled at least 10 m apart. Corals were transported submerged in seawater to the Smithsonian Tropical Research Institute (STRI). Each colony was fragmented into six similar-sized ramets using a bandsaw (Gryphon C-40 Diamond Band Saw, Gryphon Corporation, USA) and mounted onto acrylic tiles with coral glue (EcoTech Marine, USA).

Fragments were held indoors at STRI in six 60-liter flowthrough seawater tanks, equipped with a 50µm bubble bead filter, a circulation pump (4W Aquaneat G132, USA), and a heater

for temperature control (Eheim Thermocontrol, 300W, Germany). Water exchange in each tank occurred at a rate of approximately 150 liters per day. Corals were kept under ambient conditions (mean ± SD: Temperature: 29.4 ± 0.4 °C, DO: 6.9 ± 0.3 mg L^{-1}, pH_T: 7.93 ± 0.05, PAR 271 ± 46 µmol photons m^{-2} s^{-1}) for 21 days (until 16 October 2024) to allow healing and acclimation. Illumination was provided by lights (Aqua Illumination Hydra 64HD LED Reef Lights, USA) on a 12:12 hour cycle (5:30-17:30), with one hour sunrise and sunset transitions.

Experimental design

After acclimation, corals underwent a 29-day priming period (16 October 2024 until 14 November 2024), followed by a 4-7 day long acute stress event (15 November 2024 until 20-22 November 2024, Figure 2.1). Two ramets from each parent colony were randomly assigned to each of the three priming frequencies: none (control), low frequency (LF), and high frequency (HF) priming. Treatments were distributed across two replicate tanks, each containing six coral fragments per species. Each fragment was considered a replicate, nested within experimental tank for analyses.

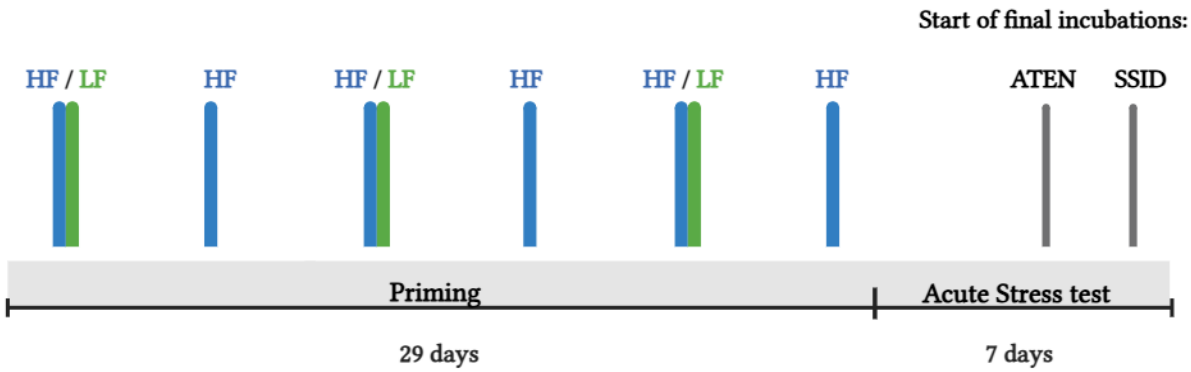

Figure 2.1: Experimental timeline showing priming and acute stress phases. Coral fragments were assigned to one of three priming treatments: high frequency (HF, blue vertical bars), low frequency (LF, green vertical bars), or unmanipulated control (not depicted). HF corals were exposed to a total of six pulses, with three nights between each pulse, while LF corals were exposed to a total of three pulses, with nine nights between each pulse. Each priming pulse was administered over two consecutive nights, with 6 hours each night at target dissolved oxygen and pH levels. Following priming, corals were subjected to a 4–7-day acute stress test, during which they were reassigned to either stress or ambient treatment. During the acute stress test, stress was administered every night. The duration of the acute stress test varied depending on final incubation dates: incubations for *Agaricia tenuifolia* (ATEN) started on day 4 of the acute stress test, while incubations for *Siderastrea siderea* (SSID) started on day 6.

Priming stress pulses mimicked diel low DO and pH cycles observed during hypoxia events in Almirante Bay (Lucey et al., 2025), with target stress conditions applied for six hours over two consecutive nights per pulse, preceded by a 6-hour intermediate step-down and followed by a gradual ramp-up (Figure 2.2). HF corals received six pulses (i.e., one pulse every three

days), while LF corals received every second pulse (three total, one pulse every nine days), with a 3-day recovery period between pulses. Stress conditions during priming pulses (Table 2.1) were sublethal by design, with minimum targets set above extreme field values observed in Almirante Bay during the 2017 hypoxia event (i.e., DO < 1 mg L^{-1}, pH_{NBS} < 7.5, Johnson et al. 2021), to promote physiological plasticity without inducing mortality. DO and pH levels in control tanks were monitored but left unmanipulated to maintain natural diurnal seawater fluctuations. Similarly, treatment tanks were unaltered between priming pulses, during which corals experienced the following daily means ± SD: temperature: 29.3 ± 0.4 °C; DO: 6.77 ± 0.16 mg L^{-1}; pH_T: 7.97 ± 0.04.

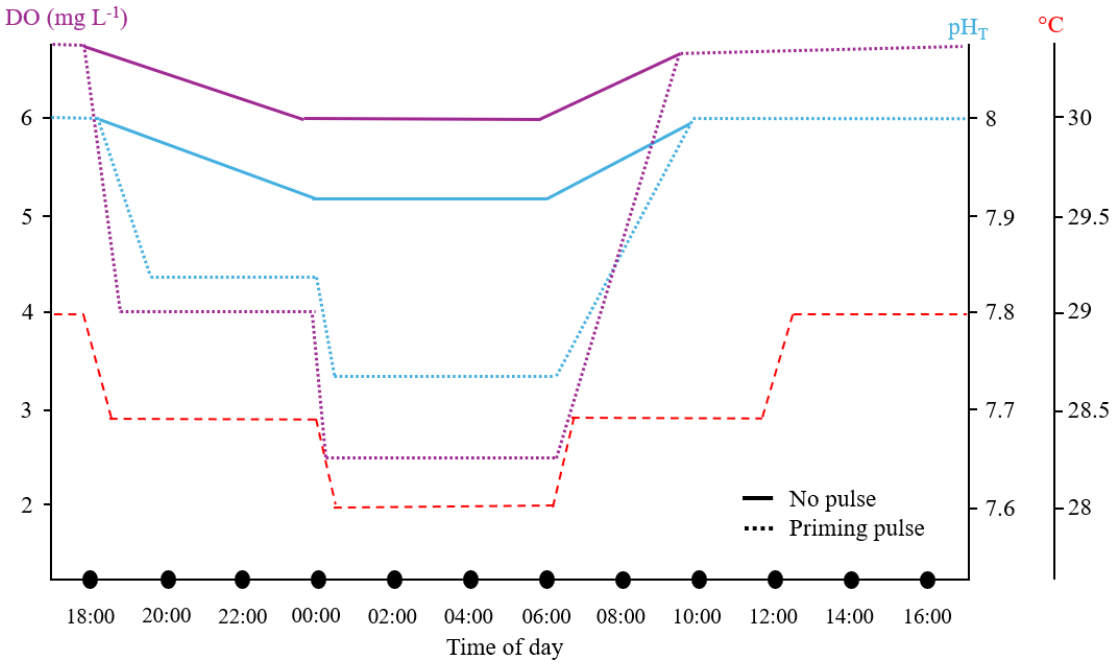

Figure 2.2: Target diel profiles of dissolved oxygen (DO, purple) and total pH (pH_T, blue) over a 24-hour timeframe during the priming period. Solid lines represent baseline (no-pulse or control) conditions, while dashed lines indicate target conditions during priming stress pulses. During pulse nights, DO and pH_T levels were reduced by controlled bubbling of N_2 and CO_2, respectively. No-pulse and control conditions were not manipulated to maintain the natural diurnal variation of incoming seawater. Temperature (red) did not differ among treatment groups and was set to mimic natural variations in Almirante Bay.

Temperature, DO, and pH were monitored and regulated using an Apex Neptune System. Ramp-down of DO and pH was controlled through controlled bubbling of N_2 and CO_2, while ramp-up was achieved by modifying seawater flow-through rates, allowing gradual restoration of ambient conditions. Probes were cleaned daily to ensure data quality. Complementary daily condition checks were performed using a HACH meter (HQ40d, HACH, USA) for temperature, DO, mV, and salinity. Total pH (pH_T) was calculated from the respective mV and temperature measurements (Supplement A). The mV probe was calibrated

every three days using TRIS buffer, purchased from A. Dickson (Scripps), across a temperature range of 24-32 °C. All tanks received the same temperature regime, matching natural diel patterns in Almirante Bay. PAR was maintained at 258 ± 27 μmol photons m^{-2} s^{-1}, and coral fragments were rotated daily within tanks to remove tank positioning effects.

Table 2.1: Tank conditions in each treatment during the diel phases of the priming period. Values represent means ± standard deviations, with the number of manual measurements (HACH meter) in parentheses. These manual checks complemented continuous monitoring by Apex sensors. For unmanipulated controls, values reflect the full priming period, whereas for priming treatments (LF = low frequency, HF = high frequency) only data from active priming pulses were included. LF corals experienced three priming pulses (each spanning two nights), while HF corals experienced six. DO values are compensated for salinity and temperature (Supplement B, Table S2).

		Control	LF	HF
DO (mg L^{-1})	12:00-18:00	7.0 ± 0.2 (34)	6.8 ± 0.2 (6)	7.0 ± 0.1 (10)
	18:00-24:00	6.4 ± 0.1 (28)	4.3 ± 0.1 (14)	4.2 ± 0.1 (24)
	00:00-06:00	6.4 ± 0.4 (4)	2.6 ± 0.1 (2)	2.6 ± 0.1 (4)
	06:00-12:00	6.9 ± 0.2 (14)	6.8 ± 0.1 (6)	6.8 ± 0.2 (10)
pH_T	12:00-18:00	7.98 ± 0.04 (38)	7.91 ± 0.03 (10)	7.92 ± 0.05 (14)
	18:00-24:00	7.97 ± 0.05 (28)	7.86 ± 0.04 (14)	7.85 ± 0.03 (24)
	00:00-06:00	7.94 ± 0.03 (4)	7.75 ± 0.01 (2)	7.75 ± 0.03 (4)
	06:00-12:00	7.96 ± 0.02 (16)	7.95 ± 0.03 (6)	7.96 ± 0.03 (10)
Temperature (°C)	12:00-18:00	29.8 ± 0.4 (38)	29.8 ± 0.4 (10)	29.9 ± 0.4 (14)
	18:00-24:00	29.1 ± 0.5 (28)	29.3 ± 0.5 (14)	29.3 ± 0.5 (24)
	00:00-06:00	28.6 ± 0.1 (4)	29.1 ± 0.0 (2)	29.1 ± 0.1 (4)
	06:00-12:00	29.1 ± 0.5 (16)	29.1 ± 0.5 (6)	29.2 ± 0.5 (10)

After the priming phase, an acute stress test was conducted. Half of all fragments from each priming treatment were randomly reassigned to either ambient or acute stress conditions, with even distribution of parent colonies across tanks. The acute stress test involved nightly low DO and pH exposure over 4-7 nights, simulating an acute hypoxia event in duration (Johnson et al., 2021a; Lucey et al., 2025). Acute stress levels were slightly more severe than in the priming phase (Table 2.2). On the final two nights, after removing all *A. tenuifolia* individuals for final incubations due to clearly visible decline in health, DO stress levels were further intensified for *S. siderea* (targeting ~1.5 mg L^{-1} DO) to increase likelihood of eliciting a measurable physiological response. Since data analyses were performed separately for each species, treatment differences do not affect within species comparison.

For clarity, we refer to “control” corals as those that were not exposed to any priming pulses during the 29-day priming phase. During the subsequent acute stress test, tanks that were left unmanipulated are referred to as “ambient”.

To ensure water chemistry was representative and comparable across tanks, water samples for analysis of total alkalinity (TA, Supplement B, Table S4) were collected at three timepoints: once during acclimation (30 September 2024), and twice during the priming phase (31 October 2024, 08 November 2024). Samples were filtered and preserved with mercuric chloride solution (0.02% of sample volume) for storage at 4°C. Corals were fed brine shrimp nauplii every five days during priming (~ 500 shrimp L^{-1}), and tanks were cleaned after one hour to remove excess food.

Table 2.2: Tank conditions in each treatment during nightly stress pulses of the acute stress test. Values represent means ± standard deviations, with the number of manual measurements (HACH meter) in parentheses. Data are from the first five nights of the stress test, excluding the final two nights during which DO target levels were lowered. DO values are compensated for salinity and temperature (Supplement B, Table S3).

		Ambient	Stress
DO (mg L^{-1})	12:00-18:00	7.0 ± 0.1 (21)	7.0 ± 0.1 (21)
	18:00-24:00	6.5 ± 0.1 (24)	3.6 ± 1.2 (24)
	00:00-06:00	6.3 ± 0.1 (3)	2.2 ± 0.2 (3)
pH_T	12:00-18:00	8.02 ± 0.05 (24)	8.00 ± 0.04 (24)
	18:00-24:00	7.98 ± 0.04 (27)	7.84 ± 0.04 (27)
	00:00-06:00	7.95 ± 0.03 (3)	7.69 ± 0.02 (3)
Temperature (°C)	12:00-18:00	29.0 ± 0.1 (24)	29.0 ± 0.1 (24)
	18:00-24:00	28.6 ± 0.1 (27)	28.5 ± 0.1 (27)
	00:00-06:00	28.2 ± 0.1 (3)	28.0 ± 0.1 (3)

Physiological assessments

To evaluate how priming influenced coral responses to a prolonged hypoxia-acidification event, we assessed a suite of physiological parameters that broadly reflect coral host condition and symbiont function. Survival and tissue cover were visually assessed daily, while photophysiology was monitored on days 0, 9, 19, 29, 33, and 35 using Pulse Amplitude Modulated (PAM) fluorometry to measure F_v/F_m and the Normalized Difference Vegetation Index (NDVI). Symbiont densities, total chlorophyll content (*a* and c_2), tissue biomass, calcification, and critical oxygen tension (P_{crit}) were assessed at the end of the experiment.

Detailed information regarding equipment settings, laboratory procedures, and calculations for some of the physiological parameters can be found in Supplement A.

Tissue cover and survival

Coral health was assessed through visual observations of tissue cover and survival. Tissue cover was recorded as the percentage of visibly healthy tissue remaining on each fragment, while mortality was assumed when no healthy tissue remained, and algal overgrowth was apparent.

Photosynthetic efficiency, NDVI and coral color

Two separate measurements were performed using PAM fluorometry (Diving-PAM-II, Walz, Germany) to assess photophysiology. Specifically, the maximum quantum yield of photosystem II (F_v/F_m) was measured as a proxy for bleaching and photosynthetic performance by the coral's algal symbionts (Symbiodiniaceae) (Warner et al., 1999). Additionally, spectral reflectance at 670 and 750 nm was measured using a spectrometer (Mini-Spec) to calculate the Normalized Difference Vegetation Index (NDVI) following the protocol of Watty et al. (2024), a non-invasive approach to estimate chlorophyll *a* concentrations (e.g., Naugle et al. 2024). Single measurements per coral were conducted for each response parameter during different timepoints throughout the priming period and acute stress test. All measurements were taken in the dark directly within treatment tanks. F_v/F_m measurements were taken at 18:00 to ensure 30-minute dark acclimation. Exact PAM settings, calibration protocols, and calculation details are provided in Supplement A.

Coral tissue coloration was visually assessed within the tanks using the Coral Health Chart (CHC, Coral Watch) on days 0, 10, 21, 29, and 33 as an indicator of bleaching and coral health through variations in pigmentation but was ultimately not statistically analyzed.

Critical oxygen partial pressure

Critical oxygen partial pressure (P_{crit}) was determined via dark closed-chamber oxygen draw-down incubations after the 4–7-day acute stress test to quantify each coral's hypoxia threshold. As it represents the lowest oxygen partial pressure at which metabolic oxygen demand can be maintained before switching to oxyconformity (e.g., Pontes et al., 2023; Seibel, 2011), higher P_{crit} values indicate greater sensitivity to hypoxia. Incubations for all replicates were conducted in temperature-controlled water baths, starting at~100% air saturation (AS) and continuing until oxygen consumption plateaued or DO levels dropped

below 2% AS, typically lasting between 6 and 18 hours. DO and temperature were recorded at 1-minute intervals using optical sensors connected to a multi-channel oxygen meter (Oxy-4 SMA G3, PreSens GmbH, Germany). Blank chambers were included to track background respiration, but no corrections were applied, as P_{crit} calculations rely on the inflection point in oxygen consumption, not on absolute rates. Incubation order followed a consistent priority: ambient fragments before stressed; *A. tenuifolia* before *S. siderea.*

Tissue biomass and calcification

Following incubations at STRI, samples were frozen at -20°C and transported to the University of Amsterdam, where they were stored at -80°C until processing. Coral tissue biomass was then determined using the ash-free dry weight (AFDW) method on ~1x1 cm pieces of coral. The exact surface area was determined from photographs using ImageJ software. Samples were dried at 70°C in a drying oven (ELBANTON, Netherlands) for at least 48 hours until weight was constant, cooled in a desiccator (Glaswerk Wertheim GmbH, Germany), and weighed with an analytical balance (precision = 0.00001 g; ABT 220-5DM, Kern & Sohn GmbH, Germany). They were then ashed at 450°C for 6 hours in a muffle furnace (Carbolite Gero, CWF1100, UK). AFDW was calculated as the difference between dry and ashed weights, with background corrections using blank aluminum pans.

Calcification was assessed as a daily rate of skeletal mass change, calculated from the change in buoyant weight throughout the experiment and normalized to the fragment's surface area. Buoyant weight was recorded at the start of the experiment and again prior to each fragment's respiration incubation using an electronic balance (precision = 0.01 g; Ohaus, SPX222 Scout™ SPX, NJ, USA) to estimate skeletal growth (Jokiel et al., 1978). Prior to weighing, algae (i.e., turf) and debris were gently removed using a soft toothbrush or tweezers. Coral surface area was estimated from 3D models generated in Autodesk ("Autodesk ReCap Photo," 2024) using 360° photo sets captured with a Sony DSC-RX100M7 camera.

Symbiont densities and chlorophyll concentrations

Tissue was removed from ~2 cm^2 of coral skeleton using an airbrush (Master Performance S68, Master Airbrush, USA) with deionized (DI) water (and waterpik for *S. siderea*), and homogenized with a tissue tearer (Biospec, OK, USA). Symbiont densities were counted to a minimum of 100 cells using a Neubauer improved hemacytometer (Sigma Aldrich), with at least six replicate counts per sample. Chlorophyll pigments were extracted in acetone and quantified through absorbance measurements at 630, 663, and 750 nm using a

spectrophotometer (Novaspec Pro, Biochrom, USA) and the equations from Jeffrey and Humphrey (1975).

Data analysis

All statistical analyses were conducted in R version 4.3.1 (R Core Team, 2024). Data processing and visualization were performed using the *tidyverse* suite of packages, including *dplyr* for data manipulation and *ggplot2* for plotting. Analyses were performed separately for each coral species to not obscure treatment effects, as the magnitude of physiological response was expected to differ substantially between species. For each species and physiological variable, the fixed effects in the models were priming treatment (three levels: control, low frequency = LF, high frequency = HF), stress treatment (2 levels: ambient, stress), and their interaction. Experimental day (fixed effect) and Coral ID (random effect) were included in F_v/F_m and NDVI models to account for repeated measurements on the same fragment.

Symbiont densities, total chlorophyll concentrations (sum of chlorophyll *a* and c_2), and tissue biomass were analyzed as endpoint responses measured after the acute stress event. Calcification was analyzed as a rate derived from the change in buoyant weight between the start and end of the experiment, representing net skeletal accretion over the full exposure period. In contrast, F_v/F_m and NDVI were measured repeatedly across multiple timepoints and analyzed for day 0 (baseline), day 29 (end of the priming period), and either day 33 (*A. tenuifolia*) or day 35 (*S. siderea*).

Model structure was informed by significance of random effects, including genotype and tank nested within treatment (priming tank within priming treatment and stress tank within stress treatment), and assessed using the ranova() function in *lmerTest*. When random effects were significant ($p < 0.05$, Supplement B, Tables S5 and S6), we applied linear or generalized linear mixed-effects models (LMMs or GLMMs) using *lme4* or *glmmTMB*. If all random effects were non-significant, simplified linear models (LMs) were fitted with sum contrasts to allow for type III ANOVA (*car*) (e.g., West et al., 2007).

Assumption testing for all models included visual inspection of residual and fitted value plots, Shapiro-Wilk test (*car*) for normality of residuals, and Levene's test (*car*) for homogeneity of variances. Outliers were identified using the *rstatix* package and only removed if they were clear methodological artefacts (Supplement A). Data transformations were applied as needed: biomass was log-transformed to meet model assumptions, while all other physiological

parameters in *S. siderea* were analyzed untransformed. Calcification and F_v/F_m data for *A. tenuifolia* violated model assumptions even after transformation. Therefore, a GLMM with a Gamma distribution and log link (*glmmTMB*) was fitted for calcification. For F_v/F_m in *A. tenuifolia*, a GLMM using a beta distribution, appropriate for proportion-type data bound between 0 and 1, was fit.

Tissue cover and survival analysis were performed using the *survival* and *survminer* packages. For *A. tenuifolia*, we used a Cox proportional hazards model to test for differences in the probability of survival or staying above a threshold of ≥ 75% tissue cover over time. The threshold of 75% tissue cover was chosen based on visual observations throughout the experiment. Due to the rapid onset of tissue sloughing in *A. tenuifolia,* tissue loss > 25% was considered as a sign of stress. The fitting of hazard models for *S. siderea* was not possible due to the absence of mortality or tissue loss events. Kaplan-Meier curves were generated to visualize patterns in tissue cover and survival over time.

Critical oxygen partial pressure, or P_{crit}, was calculated from raw oxygen consumption data (mg L^{-1} h^{-1}) using the segmented regression method (*respR*). To visualize patterns of oxyregulation across treatments and species, oxygen consumption rates were calculated manually by extracting short linear segments (10 min, 10 data points) from oxygen decline curves. These rates were corrected for chamber volume, normalized to coral surface area, and plotted against discrete oxygen concentrations. Linear and Michaelis-Menten models were fitted to each coral's oxygen consumption data to characterize their overall oxyregulatory versus oxyconforming responses.

For all models with significant fixed effects, estimated marginal means and post-hoc pairwise comparisons were calculated (*emmeans*) with Tukey adjustments for multiple testing. Statistical significance was assessed at $\alpha = 0.05$. For visualization, raw means and standard errors were calculated (*dplyr*). Data were visualized by species and treatment combination (*ggplot2*).

For *A. tenuifolia*, two spare fragments (one each from control-ambient and control-stress treatments) were available to compensate for early mortality. One individual in the control-ambient group died prior to the acute stress test and was excluded from endpoint analyses but retained in the survival and tissue cover dataset. As a result, final sample sizes for analyses of endpoint measurements were n = 7 in the control-stress group and n = 6 for all other treatment groups in *A. tenuifolia*. All treatment groups for *S. siderea* had n = 6.

2.4. Results

Tissue cover and survival

In *Agaricia tenuifolia*, priming treatment significantly affected tissue cover (Figure 2.3, left; cox proportional hazards model, p = 0.0003). Fragments exposed to HF priming were nearly ten times more likely to lose tissue to < 75% healthy tissue cover compared to the control (hazard ratio = 9.82, p = 0.0036), whereas LF priming or acute stress exposure had no significant effect (Supplement B, Table S7). Notably, tissue loss in *A. tenuifolia* was typically developed within a single night and usually observed as extensive tissue sloughing during morning checks, suggesting that tissue degradation occurred overnight. In contrast, survival probability (Figure 2.3, right) was not significantly affected by priming or acute stress treatment. In *Siderastrea siderea*, no tissue loss or mortality occurred in any treatment group. Consequently, cox models could not be fitted.

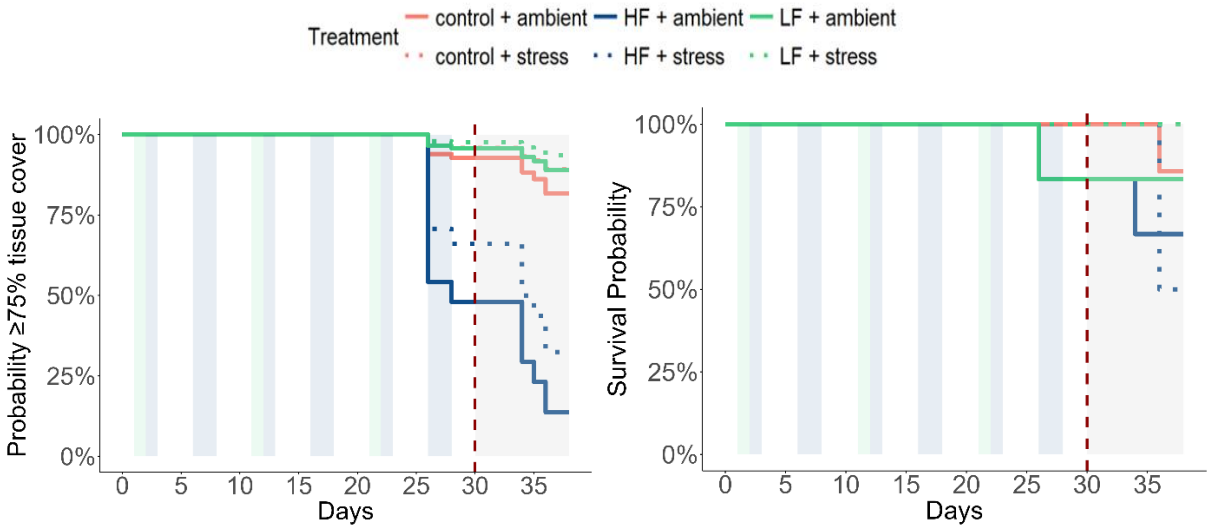

Figure 2.3: Probability of maintaining ≥ 75% tissue cover (left) and survival probability (right) of *Agaricia tenuifolia* fragments during the priming phase and acute stress test. Colors indicate priming treatments (control = orange, high frequency (HF) = blue, low frequency (LF) = green), while line types distinguish subsequent exposure to either ambient (solid) or stress (dotted) conditions during the acute stress test. Shaded rectangles indicate the timing of priming pulse events (HF = faint blue, LF = faint green) and the acute stress test (faint grey). The vertical dashed red line marks the onset of the acute stress test.

Photosynthetic efficiency and NDVI

Maximum quantum yield (F_v/F_m, Figure 2.4, top) in *A. tenuifolia* was significantly affected by priming treatment (ANOVA type III, $p = 0.001$,), day ($p < 0.001$), and their interaction ($p = 0.014$), with no effects of acute stress treatment (Supplement B, Table S9). Photosynthetic efficiency declined across all treatments during the 29-day priming period, with the strongest reduction observed in the HF group. By day 29, F_v/F_m values dropped by 32% in HF primed fragments compared to 17% in both LF primed and control fragments. No further changes occurred between day 29 and day 33. While baseline values on Day 0 did not differ among treatments, HF primed corals exhibited consistently lower F_v/F_m values than control and LF primed corals (mean difference ~11%, $p = 0.004$ for both, Supplement B, Table S12) from day 29 onward, while control and LF were indistinguishable.

In contrast, F_v/F_m in *S. siderea* remained stable throughout the experiment, with no significant effects of priming or acute stress treatment (Supplement B, Table S11) and treatment means consistently ranging between 0.52 and 0.57 across all treatments and timepoints.

NDVI showed significant temporal effects (Figure 2.4, bottom). In *A. tenuifolia,* NDVI dropped by 25% from day 0 to day 29 ($p < 0.0001$, Supplement B, Table S13), regardless of priming exposure, and remained low through day 33. Similarly, *S. siderea* experienced a 16% decline by day 29 ($p < 0.001$, Supplement B, Table S14), which persisted through day 35. However, no significant effects of priming or acute stress were observed in either species (Supplement B, Tables S9 and S11).

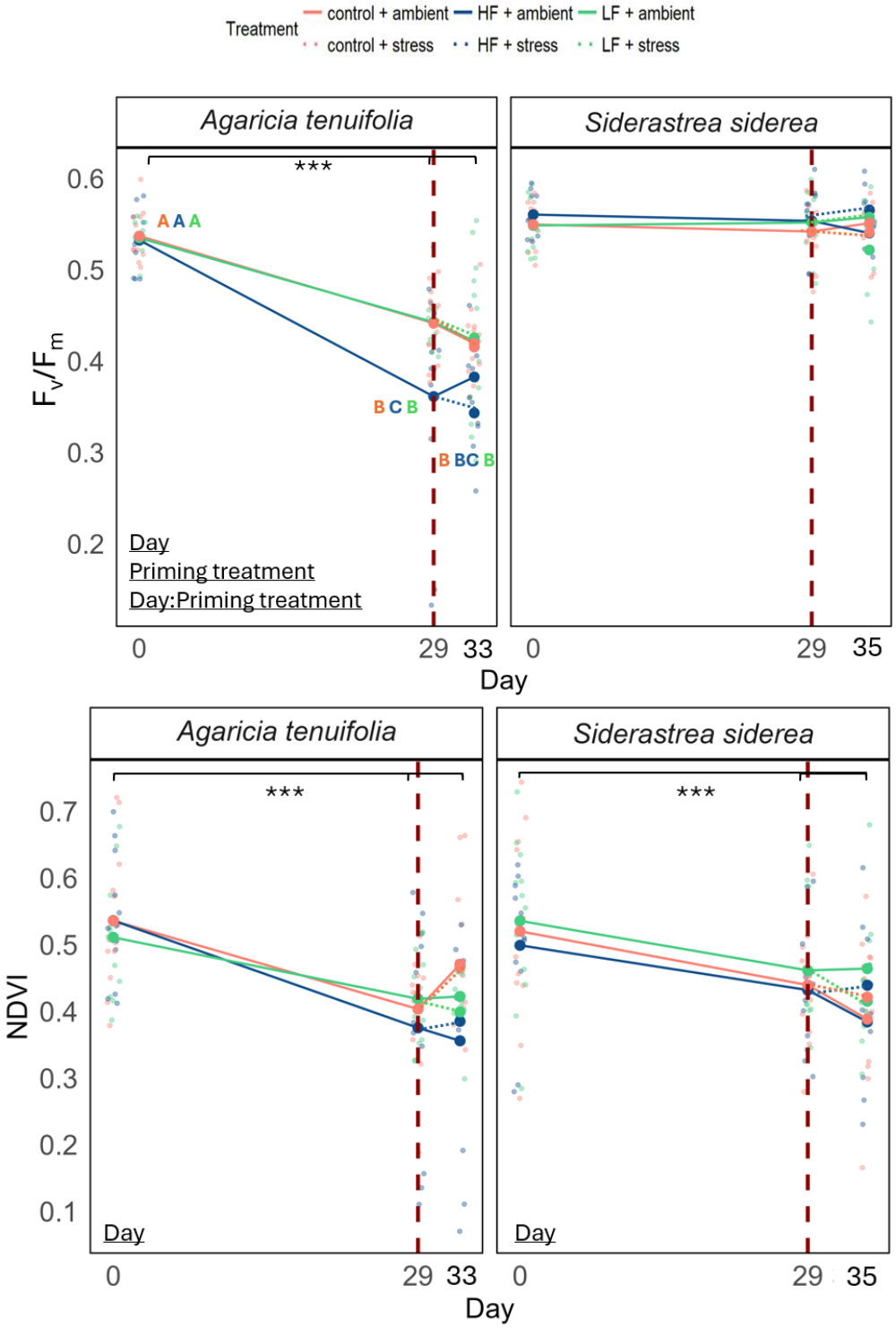

Figure 2.4: Maximum quantum yield of photosystem II (F_v/F_m, top) and Normalized Difference Vegetation Index (NDVI, bottom) over time in *Agaricia tenuifolia* and *Siderastrea siderea*. Colors represent priming treatments (control = orange, high frequency (HF) = blue, low frequency (LF) = green), while line types distinguish exposure to either ambient (solid) or stress (dotted) conditions during the acute stress test. The vertical dashed red line marks the onset of the acute stress test. Points represent mean values based on single measurements per fragment (n = 12-13 during priming, 6-7 per treatment during acute stress test). Significant main effects ($p < 0.05$) from post-hoc analyses are species-specifically displayed underlined, with significant temporal differences marked with asterisks (*$p < 0.05$, **$p < 0.01$, ***$p < 0.001$), while differences among priming treatments are indicated through different letters.

Critical oxygen partial pressure

In *A. tenuifolia*, the MM model, indicative of oxyregulation, provided a better fit in some treatment groups (HF-ambient, LF-stress, and control-stress), though AIC differences between models were occasionally small (ΔAIC = 4-49), limiting confidence in model distinction. In contrast, *S. siderea* exhibited consistent support for the linear model (ΔAIC > 68 in most treatments) suggesting a strong tendency toward oxyconformity, except for one group (control-ambient) showing marginal MM support (ΔAIC ≈ 3).

Across treatments, no clear effects of priming treatment or acute stress exposure were detected on critical oxygen tension (P_{crit}, Figure 2.5) in either species (Supplement B, Tables S8 and S10). Species-mean P_{crit} values across all treatments were comparable (Mean ± SD: *A. tenuifolia:* 2.61 ± 1.32 mg O_2 L^{-1}; *S. siderea*: 2.73 ± 1.23 mg O_2 L^{-1}), although individual fragment estimates varied considerably within each species (*A. tenuifolia:* 0.44-5.96 mg O_2 L^{-1}; *S. siderea*: 0.68-4.45 mg O_2 L^{-1}).

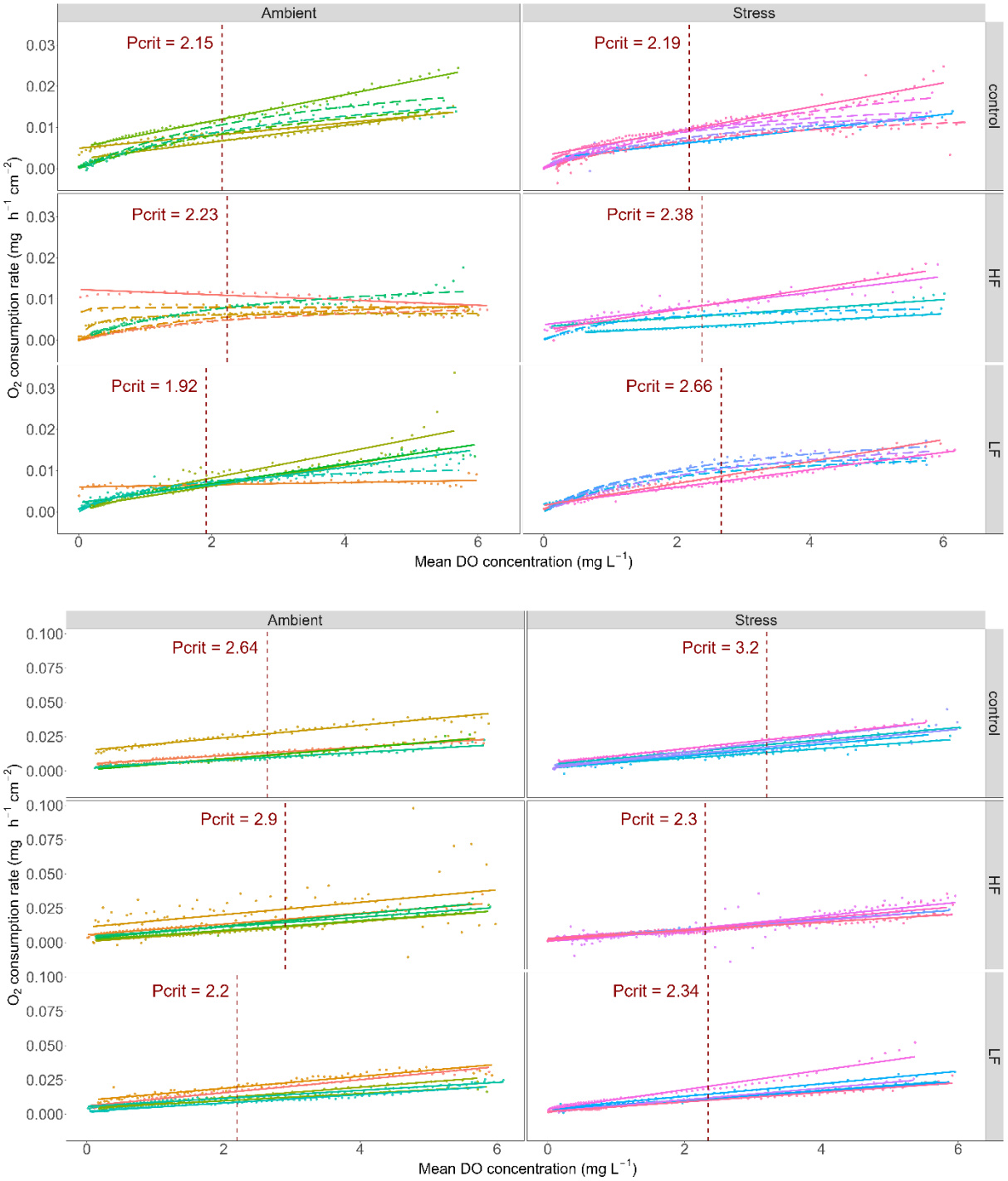

Figure 2.5: Oxygen consumption rates and critical oxygen partial pressure (P_{crit}) estimates in *Agaricia tenuifolia* (top) and *Siderastrea siderea* (bottom) under ambient and stress conditions across priming treatments (HF = high frequency, LF = low frequency, control = unmanipulated). Dashed, dark red vertical lines represent the mean treatment-level P_{crit} value (n = 6-7 per treatment combination) estimated using segmented regression. Solid lines indicate best-fitting linear models (suggesting oxyconformity), while dotted lines indicate best-fitting Michaelis-Menten (MM) models (suggesting oxyregulation). Model fits were selected based on the lowest AIC for each individual fragment.

Biomass and calcification

For *A. tenuifolia*, neither priming nor acute stress exposure affected biomass (Supplement B, Table S8), with treatment means ± SD ranging from 6.0 ± 1.5 mg cm^{-2} in HF-stress fragments to 8.4 ± 1.2 mg cm^{-2} in LF-ambient corals (Figure 2.6, left).

In contrast, *S. siderea* showed significant effects of both priming (ANOVA Type III, p = 0.04) and acute stress (p = 0.001), along with a marginal priming x stress interaction (p = 0.06, Supplement B, Table S10), indicating a more complex response. Under acute stress conditions, biomass was 29% and 21% lower in control (p < 0.001) and HF primed corals (p = 0.05), respectively, compared to LF primed corals. No differences among priming treatments were observed under ambient conditions. Acute stress exposure led to a 28% reduction in biomass in unprimed corals (p = 0.001), and a 22% reduction in HF primed corals (p = 0.01), compared to the respective priming groups not exposed to acute stress, whereas LF primed corals showed no decline (Supplement B, Table S14).

Calcification rates in *A. tenuifolia* and *S. siderea* were not significantly affected by priming, acute stress, or their interaction (Supplement B, Tables S9 and S11).

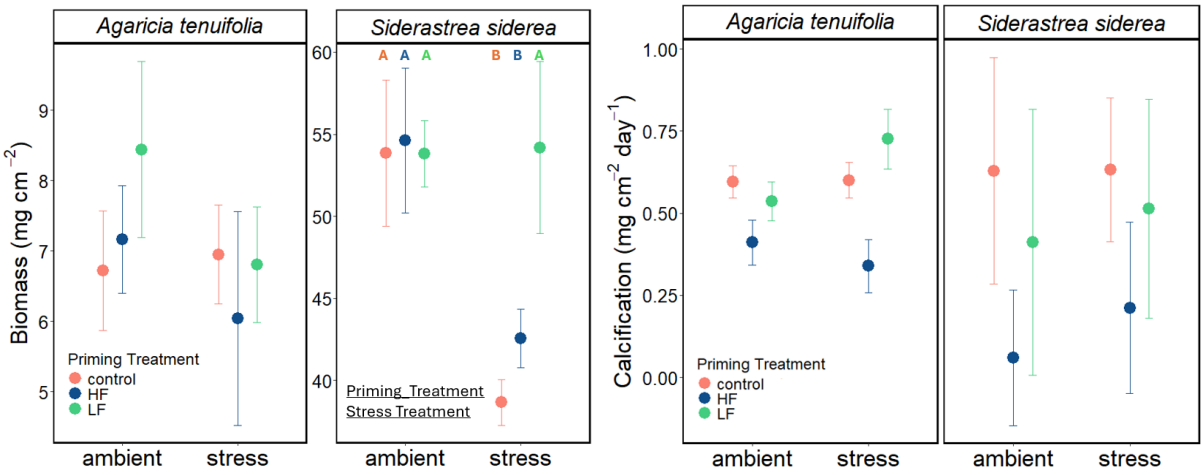

Figure 2.6: Biomass (left) and net calcification rates (right) of *Agaricia tenuifolia* and *Siderastrea siderea* at the end of the experiment. Biomass was assessed as an endpoint measurement, whereas calcification represents a daily rate obtained from changes in buoyant weight. Significant main effects (p < 0.05) from post-hoc analyses are species-specifically displayed underlined, with differences among priming treatment groups indicated through different. Shown is the mean ± standard error (n = 6-7 per treatment combination).

Symbiont densities and total chlorophyll content

Symbiont densities differed markedly between species, with *A. tenuifolia* generally hosting 73% lower symbiont densities than *S. siderea* across all treatments (Figure 2.7). In *A. tenuifolia*, priming treatment significantly affected symbiont densities (ANOVA Type III, p = 0.01, Supplement B, Table S8), with HF primed fragments hosting ~42% and ~50% fewer algal symbionts than control (p = 0.05, Supplement B, Table S13) and LF primed (p = 0.004, Supplement B, Table S13) corals, respectively. *Siderastrea siderea* also showed a significant priming effect (ANOVA Type II, p = 0.05, Supplement B, Table S11), but post hoc comparisons did not reveal significant differences among groups (Supplement B, Table S14).

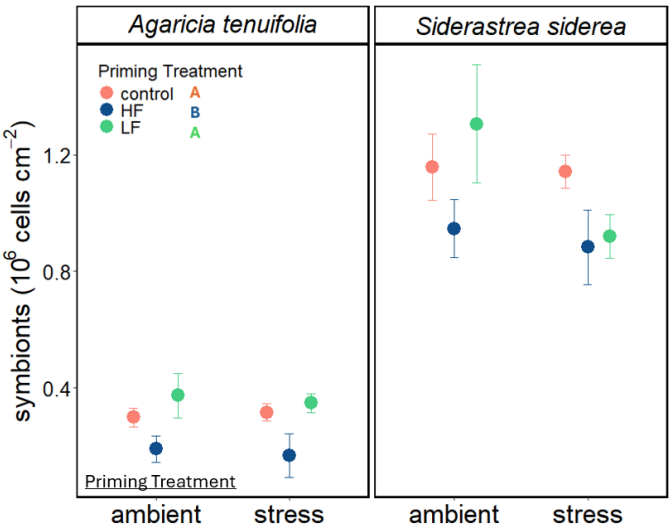

Figure 2.7: Symbiont densities after a 34–37-day long experiment. Significant main effects ($p < 0.05$) from post-hoc analyses are species-specifically displayed underlined, with differences among priming treatment groups indicated through different letters next to the legend. Shown is the mean ± standard error (n = 6-7 per treatment combination).

Total chlorophyll concentrations (chlorophyll *a* and c_2) normalized to coral surface area (Figure 2.8, left) showed no significant treatment effects in either species (Supplement B, Tables S8 and S11). However, when normalized to symbiont density (Figure 2.8, right), *A. tenuifolia* exhibited a significant effect of priming treatment (ANOVA type III, p = 0.04). HF primed corals contained approximately 56% more chlorophyll per cell than control and LF primed fragments, but post-hoc tests did not detect significant pairwise differences (p = 0.06 for both, Supplement B, Table S13). No significant effects were detected in *S. siderea* for either chlorophyll metric (Supplement B, Table S10 and S11).

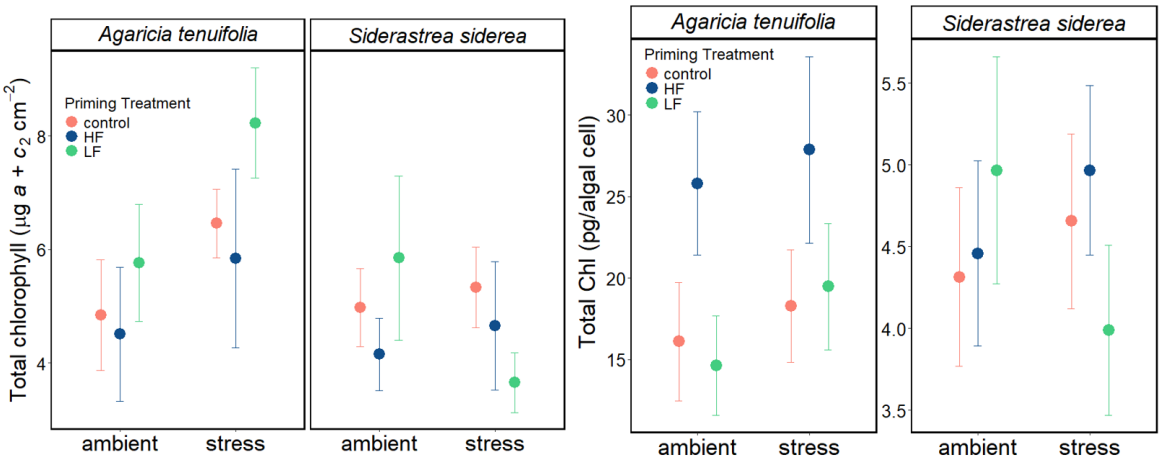

Figure 2.8: Chlorophyll concentrations after a 34–37-day long experiment standardized to surface area (left) and per algal cell (right). Post-hoc analyses did not reveal significant main effects ($p < 0.05$) Shown is the mean ± standard error (n = 6-7 per treatment combination).

2.5. Discussion

By comparing high- and low-frequency (HF and LF) priming regimes across two common Caribbean coral species, *Agaricia tenuifolia* and *Siderastrea siderea,* we aimed to test how repeated low DO and pH stress shapes coral physiology in response to applied acute hypoxia-acidification. We found that while priming frequency modulates baseline coral physiology in a species- and trait-specific manner, carry-over to subsequent acute stress responses was limited, with only one trait in *S. siderea* exhibiting a significant benefit of priming during acute stress.

High frequency exposure acts as a repeated stressor in Agaricia tenuifolia, while low frequency exposure shows subtle potential for priming benefits in Siderastrea siderea

Our results indicate that the outcome of different priming frequencies is likely dependent on species-specific baseline tolerance, each species' recovery capacity, as well as recovery time between priming pulses. Across both species, HF priming showed no potential for beneficial priming, whereas LF priming yielded subtle, trait-limited benefits in *S. siderea*. In *A. tenuifolia*, no interaction between priming treatment and acute stress was detected in any measured parameter. While HF priming caused physiological decline, particularly in photosynthetic parameters, even before the onset of acute stress, LF primed *A. tenuifolia* performed similarly to unprimed controls during acute stress, indicating no clear protective carry-over. In contrast, *S. siderea* maintained overall resistance across most traits regardless of priming or acute stress exposure. Notably, under acute stress, LF priming conferred a subtle

benefit in tissue biomass, whereas HF primed and control (unprimed) corals lost biomass, indicating a narrow temporal window in which priming may enhance resilience.

While a lack of previous hypoxia-acidification priming studies renders comparison to other work difficult, studies on diel thermal variability also reveal divergent outcomes. Safaie et al. (2018) showed that this form of pre-exposure can reduce bleaching susceptibility if cumulative exposure does not exceed tolerance thresholds. However, there is also evidence of unsuccessful priming outcomes, where such variability in the recent past before a thermal stress test reduces coral thermal stress tolerance (Schoepf et al., 2022). These contrasting outcomes reinforce the idea that both the frequency and cumulative intensity of priming pulses determine whether exposure strengthens or weakens performance during subsequent stress. A unifying explanation is the recovery window between pulses. Priming frameworks predict that benefits arise when recovery enables preparatory defenses to persist (e.g., antioxidants, heat shock proteins (HSPs), upregulation of defense genes) and when epigenetic modifications facilitate faster re-activation upon subsequent stress (see review by Hackerott et al., 2021), highlighting the importance of incorporating molecular approaches into future priming experiments. If the initial exposure is too weak or brief, no memory response is detectable, and if it exceeds tolerance, the organism is weakened and potential benefits are lost (Hackerott et al., 2021). Our results fit this framework: LF priming did not impair either species, likely due to the recovery window being long enough (9 days) to prevent cumulative damage, and in case of *S. siderea* even activate subtle preparatory defenses by enabling the maintenance of tissue biomass during acute stress.

Tissue biomass integrates multiple components, including host proteins, lipid stores, and symbiont content, thus serving as a proxy for energetic condition (Grottoli et al., 2004; Rodrigues and Grottoli, 2007). The stability in LF primed *S. siderea* may reflect reduced catabolism of internal reserves (Jacobson et al., 2016). Rather than requiring energy reallocation to mitigate stress-induced damage, these corals may have experienced less physiological strain overall. Alternatively, LF priming may have induced a shift toward metabolic suppression, allowing the coral to downregulate energy-demanding processes while conserving internal resources (Jacobson et al., 2016). In contrast, decreased biomass in HF primed and unprimed corals likely indicates the mobilization of energy reserves to fuel stress responses such as antioxidant activity or cellular repair during the acute stress event. (Grottoli et al., 2004; Rodrigues and Grottoli, 2007; Woods et al., 2022). However, these interpretations

remain speculative, as the underlying pathways cannot be distinguished without molecular analyses.

HF priming did not confer any beneficial or detrimental responses in the more stress-tolerant *S. siderea* but triggered declines in photosynthetic efficiency (F_v/F_m), symbiont density, and tissue cover regardless of acute stress treatment in the more sensitive *A. tenuifolia.* Under hypoxia, corals may shift toward anaerobic metabolism, primarily through fermentation, when aerobic pathways are inhibited by oxygen limitation (Linsmayer et al., 2020; Murphy and Richmond, 2016). This shift is energetically less efficient, producing substantially less ATP and potentially creating energy deficits (Murphy and Richmond, 2016). In *Acropora yongei* fermentation rates spiked at the onset of nightly hypoxia and again at dawn, with sustained activity even during the day when oxygen availability is restored (Linsmayer et al., 2020). Similarly, *Montipora capitata* becomes increasingly reliant on anaerobic metabolism after repeated nightly hypoxia pulses, leading to progressive bleaching and tissue loss after only three to five cycles (Murphy and Richmond, 2016). This pattern of energy limitation may help explain the tissue deterioration and loss of photophysiological integrity seen in HF primed *A. tenuifolia*. Nighttime respiration by symbionts may become a relative burden, potentially triggering expulsion and progressively reducing photosynthate supply. Resulting limited symbiont output likely compounds the inefficiency of anaerobic metabolism under repeated hypoxia, contributing to tissue collapse overnight.

These deleterious effects may be further exacerbated by the stress of repeated reoxygenation. Oxygen reperfusion (Oakley et al., 2014) after hypoxia can increase energetic demand for antioxidant production to counter oxidative damage from bursts of reactive oxygen species (ROS) (Rivera-Ingraham and Lignot, 2017; Teixeira et al., 2013), and trigger lipid peroxidation (Teixeira 2013, Zhang et al. 2023). Rapid reoxygenation may also destabilize the hypoxia inducible factor (HIF) response system, which regulates gene expression and metabolism under low oxygen, potentially causing cellular dysfunction or apoptotic signaling (Alderdice et al., 2022, 2021; Zhang et al., 2023). Activation of caspase-3, an apoptotic marker, has been reported in corals recovering from hypoxia and may be intensified by repeated stress-recovery cycles (Zhang et al., 2023). Consistent with these mechanisms, the overnight tissue sloughing in HF-primed *A. tenuifolia* fragments, which we primarily observed in the mornings following repeated priming pulses, points to a combination of hypoxia-driven energy deficits (Linsmayer et al., 2020; Murphy and Richmond, 2016) and cumulative oxidative stress from deoxygenation-reoxygenation cycles (e.g., Alderdice et al.,

2021; Teixeira et al., 2013) as key contributors to the physiological decline. Notably, in our experimental setup, reoxygenation (termination of nightly N_2 bubbling) coincided with the onset of daylight, a transition we aimed to buffer by allowing DO to gradually rise with water flow and by ramping light intensity over 1 hour. Nonetheless, this combined shift in oxygen availability, while mirroring natural diel cycles, likely exacerbated oxidative stress, which may have amplified the morning tissue-sloughing in HF primed *A. tenuifolia.* Similarly, delayed mortality in *A. tenuifolia* under hypoxic stress followed by full reoxygenation (Lucey et al., 2025), support the notion that hypoxia recovery phases are physiologically challenging, particularly for hypoxia-sensitive species (Lucey et al., 2025; Putnam et al., 2020; Teixeira et al., 2013).

In both species, calcification remained unaffected by priming or acute stress exposure, indicating that hypoxia was the dominant driver of outcomes in our study. While ocean acidification (OA) often depresses coral calcification (e.g., Chan and Connolly, 2013; Kroeker et al., 2013), previous work has also shown that some coral species do not exhibit reduced calcification after month-long OA exposure (Schoepf et al., 2013). This delayed or absent response to OA may be due to the species-specific ability to up-regulate internal pH at relatively low costs (McCulloch et al., 2012), or the utilization of increased CO_2 availability for enhanced algal productivity (Brading et al., 2012) that may support calcification maintenance. However, the latter is unlikely to benefit HF primed *A. tenuifolia*, given the physiological decline in photosynthetic parameters of that group.

Previous studies investigating the role of environmental priming under OA suggest that benefits may require longer timescales or transgenerational exposure. For example, transgenerational preconditioning, in which parental corals were pre-exposed to elevated pCO_2 alone (Putnam et al., 2020) and in combination with warming (Putnam and Gates, 2015), benefited larvae OA tolerance. Similarly, in an OA reciprocal transplant under variable pCO_2 (Brown et al., 2022), corals from naturally variable sites performed better under 8 weeks of variability, while naïve colonies showed limited internal pH buffering and recovery, suggesting that priming benefits may require longer durations. A delayed OA response may explain why calcification remained unchanged across treatment groups in our study, with short-term exposure insufficient to induce measurable effects.

Finally, the recovery window, and consequently priming frequency needed to elicit beneficial outcomes in response to an acute stress event, are likely determined by the timely recovery capacity of each species. In an RTE, *S. siderea* and *A. tenuifolia* from both hypoxia-naïve and

hypoxia-experienced reefs in Almirante Bay, were exposed to a 14-day nightly hypoxia event (6 h night $^{-1}$, DO ~0.3 mg L^{-1}, Lucey et al., 2025). While hypoxia-naïve individuals from both species showed signs of bleaching during the event, *S. siderea* showed photophysiological recovery within 3 days after the event. However, *A. tenuifolia* exhibited continued bleaching and mortality even 14 days after the event, reflecting sustained impairment. The ability of *S. siderea*, to quickly recover from hypoxia stress likely allowed our LF primed corals, with longer intervals between pulses, to regain function and maintain biomass during acute stress, while the window between HF priming pulses (3 days) permitted only partial recovery to prevent cumulative damage, while still catabolizing energy reserves under acute stress. Conversely, the slower recovery capacity of *A. tenuifolia* resulted in neutral effects of LF priming, while HF priming did not allow sufficient recovery, leading to cumulative damage. This underscores the complexity of frequency-dependent environmental priming and the need to consider frequency, intensity, duration, as well as recovery duration and quality as crucial interacting dimensions to predict whether prior exposure enhances or undermines coral resilience.

High baseline tolerance in Siderastrea siderea, contrasted with time-dependent limits in Agaricia tenuifolia

Independent of priming outcomes, our results confirm higher baseline tolerance of *S. siderea* to hypoxia-acidification than *A. tenuifolia.* This aligns with prior work reporting relatively high resilience to warming (e.g., Dawson et al. 2025), acidification (e.g., Radice et al. 2022, Castillo et al 2014), hypoxia (Lucey et al 2025, Mallon et al 2024), and combined stressors such as warming and acidification (Bove et al 2019, 2022) in *S. siderea.* Nevertheless, analyses of skeletal growth bands from coral cores indicate that this species is not immune to environmental change, showing multidecadal growth and density declines under cumulative pressures from local anthropogenic impacts, ocean warming, and OA (Cardoso et al 2025).

By contrast, *A. tenuifolia* displayed time-sensitive tolerance toward combined low DO and pH levels. Control and LF primed corals endured the continuous 4–5-night acute hypoxia-acidification event without marked declines, yet HF primed fragments exhibited physiological deterioration after approximately 5 priming pulses (i.e., 10 nights of cumulative low DO and pH over a 23-day period), indicating a threshold between these exposure durations at the stress amplitudes tested. Other work has identified *A. tenuifolia*'s time-dependent hypoxia threshold as 3-5 consecutive nights of low DO exposure and observed tissue sloughing (Lucey et al., 2024). However, their treatment exposed corals to lower DO levels (0.3-0.5 mg L^{-1})

compared to our treatments (~2.6 mg L^{-1} during priming pulses; ~2.2 mg L^{-1} during nightly acute stress event), highlighting that thresholds are both time- and dose-dependent.

The overall divergence in species-specific tolerance to low DO and pH likely arises from a suite of interacting traits, spanning morphological, trophic, and metabolic characteristics. For example, *S. siderea*'s thick tissue may provide buffering against external fluctuations by creating microenvironmental gradients that foster more diverse microbial communities and distinct tissue-specific gene expression patterns. These features, alongside higher energy reserves and intracellular pH stability, have been linked to greater tolerance toward thermal (e.g., Thornhill et al., 2011) and acidification (Putnam et al., 2016) stress. In contrast, *A. tenuifolia*'s thin tissues transmit environmental change more directly, leaving it immediately exposed to diel low DO and pH stress.

Feeding strategies likely reinforce this divergence. While all corals are mixotrophic, *A. tenufolia* is primarily autotrophic, relying heavily on photosynthates from its Symbiodiniaceae (Seemann et al., 2012), whereas *S. siderea* exhibits higher heterotrophic plasticity and can dynamically shift its diet (Grottoli et al., 2006; Solomon et al., 2025), likely contributing to its persistence in multi-stressor environments (Solomon et al., 2025). Because hypoxia directly impairs photosynthesis and accelerates bleaching (e.g., Johnson et al., 2021a; Long et al., 2024; Lucey et al., 2025; Zhang et al., 2023), *A. tenuifolia*'s reliance on autotrophy likely contributed to its photosynthetic decline, whereas *S. siderea*'s capacity to shift carbon acquisition strategies helped maintain overall physiological stability across multiple traits, despite equal feeding opportunity. Although our feeding regime may not fully replicate natural food availability, the 50µm filtered flow-through seawater still contained suspended particles within the size range corals can capture (e.g., Houlbrèque and Ferrier-Pagès, 2009).

Finally, differences in metabolic regulation appear central to species-specific hypoxia-acidification tolerance. In our experiment, *S. siderea* exhibited oxyconforming respiration across all treatments except the ambient-control group, indicative of metabolic suppression. This is consistent with comparative studies showing *S. siderea* can reduce respiration by up to 83% under hypoxia (Pontes et al., 2023), though it also ranks among the least hypoxia-tolerant species in other work (P_{crit} ~4.5 mg O_2 L^{-1}; Pontes et al., 2023). Although, this value is slightly above the maximum (range: 0.68 – 4.45 mg O_2 L^{-1}) and well above the mean P_{crit} we measured in our present study (2.73 mg O_2 L^{-1}). These differences likely reflect methodological variation (broken stick vs. segmented regression), incubation conditions, and biological variability among fragments. Notably, respiration curves in our analysis often

remained linear, raising questions about the utility of breakpoint-based P_{crit} calculation methods when organisms show oxyconforming or non-linear stress responses. Despite these differences, both studies support *S. siderea*'s capacity for metabolic suppression, while absolute P_{crit} values should be interpreted cautiously across methods and context. Metabolic suppression is characteristic of hypoxia-tolerant animals, allowing ATP demand to be downregulated to match reduced oxygen supply, thereby avoiding energetic collapse. Sensitive species, in contrast, may fail to suppress ATP demand and incur irreversible cellular damage (e.g., Seibel, 2011; Zhang et al., 2023). The deterioration in *A. tenuifolia* under cumulative stress from HF priming may reflect limited capacity for metabolic suppression. While our data cannot directly confirm this, mortality and pronounced photosynthetic decline in that group suggest that energy deficits became unsustainable when photosynthesis was impaired.

Future directions and ecological implications

This study provides a novel experimental assessment of how stress frequency shapes coral physiology under diel hypoxia and acidification. While previous studies explored environmental priming in corals exposed to single or combined stressors (Lucey et al., 2025; Putnam and Gates, 2015), we highlight the importance of recurrence rate as a critical but underexplored dimension of priming. Importantly, frequency interacts with pulse amplitude, duration, and recovery time between pulses, so the thresholds observed here reflect the combined effects of these factors. Given the increasing prevalence of acute hypoxia and acidification on modern reefs, (Altieri et al., 2017; Lucey et al., 2020), this form of variability warrants more attention in climate resilience frameworks. While the acute damage of low DO and pH events is now well recognized (Altieri et al., 2017; Johnson et al., 2018; Kealoha et al., 2020; Raj et al., 2020), we still lack predictive understanding of the timing, intensity, and recurrence patterns that corals can withstand, or that might elicit beneficial acclimatization.

To resolve mechanisms underlying such context-dependent responses, future work should incorporate molecular and metabolic biomarkers, including oxidative stress enzymes, HIF expression, and energy reserve turnover. Investigating symbiont identity may also provide important insights, especially for species like *A. tenuifolia* that rely heavily on autotrophy. Symbiont community composition is well established as a driver of coral thermal tolerance (Berkelmans and Van Oppen, 2006; Turnham et al., 2023), and emerging data on local assemblages in Almirante Bay corals (Aichelman et al., 2025; Linsmayer et al., 2024), provide a basis for future research testing their potential role in hypoxia-acidification

resilience. Additionally, future studies could space the acute stress event further apart from the priming phase to better assess memory effects, including the persistence and decay of priming cues over time, which would help to clarify the temporal limits of environmental memory in corals.

Physiological thresholds are likely species-specific: stress-sensitive species like *A. tenuifolia* may suffer under frequent fluctuations, while tolerant species like *S. siderea* may better integrate prior exposures into their stress response. These patterns carry important conservation implications. If we can identify the traits, thresholds, and exposure histories that promote priming benefits, this knowledge could inform more targeted conservation strategies. Rather than relying solely on broadly stress-tolerant taxa, efforts could include naturally resilient populations that have adapted to fluctuating environments, thereby preserving biodiversity and ecosystem function.

2.6. Acknowledgments
We thank the staff of the Smithsonian Tropical Research Institute (STRI) in Bocas del Toro for their logistical support, assistance at the field station, and the use of their laboratory facilities. We also thank Dr. Rachel Collin for access to the indoor aquarium facility and aquarium equipment. This project was funded through a VIDI grant from the Dutch Research Council (VI.Vidi.203.069, VS) and, in part, a Smithsonian Predoctoral Fellowship (KWJ).

2.7. References

Adelson, A.E., Altieri, A.H., Boza, X., Collin, R., Davis, K.A., Gaul, A., Giddings, S.N., Reed, V., Pawlak, G., 2022. Seasonal hypoxia and temperature inversions in a tropical bay. Limnology & Oceanography 67, 2174–2189. https://doi.org/10.1002/lno.12196

Aichelman, H.E., Benson, B.E., Gomez-Campo, K., Martinez-Rugerio, M.I., Fifer, J.E., Tsang, L., Hughes, A.M., Bove, C.B., Nieves, O.C., Pereslete, A.M., Stanizzi, D., Kriefall, N.G., Baumann, J.H., Rippe, J.P., Gondola, P., Castillo, K.D., Davies, S.W., 2025. Cryptic coral diversity is associated with symbioses, physiology, and response to thermal challenge. Sci. Adv. 11, eadr5237. https://doi.org/10.1126/sciadv.adr5237

Alderdice, R., Perna, G., Cárdenas, A., Hume, B.C.C., Wolf, M., Kühl, M., Pernice, M., Suggett, D.J., Voolstra, C.R., 2022. Deoxygenation lowers the thermal threshold of coral bleaching. Sci Rep 12. https://doi.org/10.1038/s41598-022-22604-3

Alderdice, R., Suggett, D.J., Cárdenas, A., Hughes, D.J., Kühl, M., Pernice, M., Voolstra, C.R., 2021. Divergent expression of hypoxia response systems under deoxygenation in reef-forming corals aligns with bleaching susceptibility. Global Change Biology 27, 312–326. https://doi.org/10.1111/gcb.15436

Altieri, A.H., Harrison, S.B., Seemann, J., Collin, R., Diaz, R.J., Knowlton, N., 2017. Tropical dead zones and mass mortalities on coral reefs. Proc. Natl. Acad. Sci. U.S.A. 114, 3660–3665. https://doi.org/10.1073/pnas.1621517114

Anthony, K.R.N., Maynard, J.A., Diaz-Pulido, G., Mumby, P.J., Marshall, P.A., Cao, L., Hoegh-Guldberg, O., 2011. Ocean acidification and warming will lower coral reef resilience: CO2 AND CORAL REEF RESILIENCE. Global Change Biology 17, 1798–1808. https://doi.org/10.1111/j.1365-2486.2010.02364.x

Barnard, P.L., Dugan, J.E., Page, H.M., Wood, N.J., Hart, J.A.F., Cayan, D.R., Erikson, L.H., Hubbard, D.M., Myers, M.R., Melack, J.M., Iacobellis, S.F., 2021. Multiple climate change-driven tipping points for coastal systems. Sci Rep 11, 15560. https://doi.org/10.1038/s41598-021-94942-7

Berkelmans, R., Van Oppen, M.J.H., 2006. The role of zooxanthellae in the thermal tolerance of corals: a 'nugget of hope' for coral reefs in an era of climate change. Proc. R. Soc. B. 273, 2305–2312. https://doi.org/10.1098/rspb.2006.3567

Bove, C.B., Davies, S.W., Ries, J.B., Umbanhowar, J., Thomasson, B.C., Farquhar, E.B., McCoppin, J.A., Castillo, K.D., 2022. Global change differentially modulates Caribbean coral physiology. PLoS ONE 17, e0273897. https://doi.org/10.1371/journal.pone.0273897

Bove, C.B., Ries, J.B., Davies, S.W., Westfield, I.T., Umbanhowar, J., Castillo, K.D., 2019. Common Caribbean corals exhibit highly variable responses to future acidification and warming. Proc. R. Soc. B. 286, 20182840. https://doi.org/10.1098/rspb.2018.2840

Bove, C.B., Umbanhowar, J., Castillo, K.D., 2020. Meta-Analysis Reveals Reduced Coral Calcification Under Projected Ocean Warming but Not Under Acidification Across the Caribbean Sea. Front. Mar. Sci. 7, 127. https://doi.org/10.3389/fmars.2020.00127

Brading, P., Warner, M.E., Davey, P., Smith, D.J., Achterberg, E.P., Suggett, D.J., 2012. Differential effects of ocean acidification on growth and photosynthesis among phylotypes of *Symbiodinium* (Dinophyceae). Limnology & Oceanography 57, 1255–1255. https://doi.org/10.4319/lo.2012.57.4.1255

Brown, K.T., Mello-Athayde, M.A., Sampayo, E.M., Chai, A., Dove, S., Barott, K.L., 2022. Environmental memory gained from exposure to extreme pCO_2 variability promotes coral cellular acid–base homeostasis. Proc. R. Soc. B. 289, 20220941. https://doi.org/10.1098/rspb.2022.0941

Camp, E., Edmondson, J., Doheny, A., Rumney, J., Grima, A., Huete, A., Suggett, D., 2019. Mangrove lagoons of the Great Barrier Reef support coral populations persisting under extreme environmental conditions. Mar. Ecol. Prog. Ser. 625, 1–14. https://doi.org/10.3354/meps13073

Camp, E.F., Nitschke, M.R., Rodolfo-Metalpa, R., Houlbreque, F., Gardner, S.G., Smith, D.J., Zampighi, M., Suggett, D.J., 2017. Reef-building corals thrive within hot-acidified and deoxygenated waters. Sci Rep 7, 2434. https://doi.org/10.1038/s41598-017-02383-y

Camp, E.F., Schoepf, V., Mumby, P.J., Hardtke, L.A., Rodolfo-Metalpa, R., Smith, D.J., Suggett, D.J., 2018. The Future of Coral Reefs Subject to Rapid Climate Change: Lessons from Natural Extreme Environments. Front. Mar. Sci. 5, 4. https://doi.org/10.3389/fmars.2018.00004

Cardoso, G.O., Kersting, D.K., Brachert, T.C., Heiss, G.A., Leinfelder, R., Maréchal, J.-P., D'Olivo, J.P., 2025. Emerging skeletal growth responses of Siderastrea siderea corals to multidecadal anthropogenic impacts in Martinique, Caribbean Sea. Sci Rep 15, 23127. https://doi.org/10.1038/s41598-025-08709-5

Castillo, K.D., Ries, J.B., Bruno, J.F., Westfield, I.T., 2014. The reef-building coral *Siderastrea siderea* exhibits parabolic responses to ocean acidification and warming. Proc. R. Soc. B. 281, 20141856. https://doi.org/10.1098/rspb.2014.1856

Chan, N.C.S., Connolly, S.R., 2013. Sensitivity of coral calcification to ocean acidification: a meta-analysis. Global Change Biology 19, 282–290. https://doi.org/10.1111/gcb.12011

Dana, J.D., 1848. Zoophytes. Printed by C. Sherman, Philadelphia,. https://doi.org/10.5962/bhl.title.70845

Dawson, D.D., Craig, N., Klepac, C.N., Lippert, M., Cornwell, B., Castillo, W., Quigley, C., Palumbi, S.R., 2025. From stress to survival: identifying heat-resistant corals in Belize for conservation and restoration. https://doi.org/10.1101/2025.08.17.670758

DelValls, T.A., Dickson, A.G., 1998. The pH of buffers based on 2-amino-2-hydroxymethyl-1,3-propanediol ('tris') in synthetic sea water. Deep Sea Research Part I: Oceanographic Research Papers 45, 1541–1554. https://doi.org/10.1016/s0967-0637(98)00019-3

Deutsch, C.J., Self-Sullivan, C., Mignucci-Giannoni, A., 2008. Trichechus manatus. The IUCN Red List of Threatened Species 2008. https://doi.org/10.2305/IUCN.UK.2008.RLTS.T22103A9356917.en

Ellis, J., Solander, D.C., 1786. The natural history of many curious and uncommon zoophytes : collected from various parts of the globe /. Printed for Benjamin White and Son ... and Peter Elmsly ..., London : https://doi.org/10.5962/bhl.title.64985

Fusi, M., Stephenson, F., Navarrete, S.A., Tapia, F.J., Largier, J.L., Marasco, R., Rueger, T., MacDonald, C., Daffonchio, D., Fernandez, M., Wieters, E.A., Booth, J., Daghio, M., Sugden, H., Scaife, K., Evans, D.M., Moore, P., Baldanzi, S., 2025. The ecology of the oxyscape in coastal ecosystems. Trends in Ecology & Evolution S0169534725001636. https://doi.org/10.1016/j.tree.2025.06.008

Grottoli, A.G., Rodrigues, L.J., Juarez, C., 2004. Lipids and stable carbon isotopes in two species of Hawaiian corals, Porites compressa and Montipora verrucosa, following a bleaching event. Marine Biology 145. https://doi.org/10.1007/s00227-004-1337-3

Hackerott, S., Martell, H.A., Eirin-Lopez, J.M., 2021. Coral environmental memory: causes, mechanisms, and consequences for future reefs. Trends in Ecology & Evolution 36, 1011–1023. https://doi.org/10.1016/j.tree.2021.06.014

Hilker, M., Schmülling, T., 2019. Stress priming, memory, and signalling in plants. Plant Cell & Environment 42, 753–761. https://doi.org/10.1111/pce.13526

Hilker, M., Schwachtje, J., Baier, M., Balazadeh, S., Bäurle, I., Geiselhardt, S., Hincha, D.K., Kunze, R., Mueller-Roeber, B., Rillig, M.C., Rolff, J., Romeis, T., Schmülling, T.,

Steppuhn, A., Van Dongen, J., Whitcomb, S.J., Wurst, S., Zuther, E., Kopka, J., 2016. Priming and memory of stress responses in organisms lacking a nervous system. Biological Reviews 91, 1118–1133. https://doi.org/10.1111/brv.12215
Hoegh-Guldberg, O., Poloczanska, E.S., Skirving, W., Dove, S., 2017. Coral Reef Ecosystems under Climate Change and Ocean Acidification. Front. Mar. Sci. 4, 158. https://doi.org/10.3389/fmars.2017.00158
Houlbrèque, F., Ferrier-Pagès, C., 2009. Heterotrophy in Tropical Scleractinian Corals. Biological Reviews 84, 1–17. https://doi.org/10.1111/j.1469-185X.2008.00058.x
Hsiao, S.-C., Wu, H.-L., Fu, H.-S., Chen, W.-B., 2025. Accelerated Ocean acidification (1985–2022) threatens tropical coral reefs and highlights biogeochemical refugia for marine conservation. Journal of Sea Research 207, 102612. https://doi.org/10.1016/j.seares.2025.102612
Hughes, D.J., Alderdice, R., Cooney, C., Kühl, M., Pernice, M., Voolstra, C.R., Suggett, D.J., 2020. Coral reef survival under accelerating ocean deoxygenation. Nat. Clim. Chang. 10, 296–307. https://doi.org/10.1038/s41558-020-0737-9
Hughes, D.J., Alexander, J., Cobbs, G., Kühl, M., Cooney, C., Pernice, M., Varkey, D., Voolstra, C.R., Suggett, D.J., 2022. Widespread oxyregulation in tropical corals under hypoxia. Marine Pollution Bulletin 179, 113722. https://doi.org/10.1016/j.marpolbul.2022.113722
IPCC, 2022. The Ocean and Cryosphere in a Changing Climate: Special Report of the Intergovernmental Panel on Climate Change, 1st ed. Cambridge University Press. https://doi.org/10.1017/9781009157964
Jacobson, L.M., Edmunds, P.J., Muller, E.B., Nisbet, R.M., 2016. The implications of reduced metabolic rate in a resource-limited coral. Journal of Experimental Biology. https://doi.org/10.1242/jeb.136044
Jeffrey, S.W., Humphrey, G.F., 1975. New spectrophotometric equations for determining chlorophylls a, b, c1 and c2 in higher plants, algae and natural phytoplankton. Biochemie und Physiologie der Pflanzen 167, 191–194. https://doi.org/10.1016/S0015-3796(17)30778-3
Johnson, M.D., Rodriguez, L.M., Altieri, A.H., 2018. Shallow-water hypoxia and mass mortality on a Caribbean coral reef. bms 94, 143–144. https://doi.org/10.5343/bms.2017.1163
Johnson, M.D., Scott, J.J., Leray, M., Lucey, N., Bravo, L.M.R., Wied, W.L., Altieri, A.H., 2021a. Rapid ecosystem-scale consequences of acute deoxygenation on a Caribbean coral reef. Nat Commun 12, 4522. https://doi.org/10.1038/s41467-021-24777-3
Johnson, M.D., Swaminathan, S.D., Nixon, E.N., Paul, V.J., Altieri, A.H., 2021b. Differential susceptibility of reef-building corals to deoxygenation reveals remarkable hypoxia tolerance. Sci Rep 11, 23168. https://doi.org/10.1038/s41598-021-01078-9
Kealoha, A.K., Doyle, S.M., Shamberger, K.E.F., Sylvan, J.B., Hetland, R.D., DiMarco, S.F., 2020. Localized hypoxia may have caused coral reef mortality at the Flower Garden Banks. Coral Reefs 39, 119–132. https://doi.org/10.1007/s00338-019-01883-9
Klein, S.G., Pitt, K.A., Carroll, A.R., 2017. Pre-exposure to simultaneous, but not individual, climate change stressors limits acclimation capacity of Irukandji jellyfish polyps to predicted climate scenarios. Coral Reefs 36, 987–1000. https://doi.org/10.1007/s00338-017-1590-9
Kroeker, K.J., Kordas, R.L., Crim, R., Hendriks, I.E., Ramajo, L., Singh, G.S., Duarte, C.M., Gattuso, J., 2013. Impacts of ocean acidification on marine organisms: quantifying sensitivities and interaction with warming. Global Change Biology 19, 1884–1896. https://doi.org/10.1111/gcb.12179
Kurihara, H., Watanabe, A., Tsugi, A., Mimura, I., Hongo, C., Kawai, T., Reimer, J.D., Kimoto, K., Gouezo, M., Golbuu, Y., 2021. Potential local adaptation of corals at

acidified and warmed Nikko Bay, Palau. Sci Rep 11. https://doi.org/10.1038/s41598-021-90614-8
Li, H., Huang, X., Zhan, A., 2020. Stress Memory of Recurrent Environmental Challenges in Marine Invasive Species: Ciona robusta as a Case Study. Front. Physiol. 11, 94. https://doi.org/10.3389/fphys.2020.00094
Linsmayer, L.B., Deheyn, D.D., Tomanek, L., Tresguerres, M., 2020. Dynamic regulation of coral energy metabolism throughout the diel cycle. Sci Rep 10, 19881. https://doi.org/10.1038/s41598-020-76828-2
Linsmayer, L.B., Noel, S.K., Leray, M., Wangpraseurt, D., Hassibi, C., Kline, D.I., Tresguerres, M., 2024. Effects of bleaching on oxygen dynamics and energy metabolism of two Caribbean coral species. Science of The Total Environment 919, 170753. https://doi.org/10.1016/j.scitotenv.2024.170753
Long, Y., Sinutok, S., Buapet, P., Yucharoen, M., 2024. Unraveling the physiological responses of morphologically distinct corals to low oxygen. PeerJ 12, e18095. https://doi.org/10.7717/peerj.18095
Lucey, N., César-Ávila, C., Eckert, A., Veintimilla, P., Collin, R., 2025. Locally Adapted Coral Species Withstand a 2-Week Hypoxic Event. Oceans 6, 5. https://doi.org/10.3390/oceans6010005
Lucey, N., Haskett, E., Collin, R., 2020. Multi-stressor Extremes Found on a Tropical Coral Reef Impair Performance. Front. Mar. Sci. 7, 588764. https://doi.org/10.3389/fmars.2020.588764
Lucey, N.M., César-Ávila, C., Eckert, A., Rajagopalan, A., Brister, W.C., Kline, E., Altieri, A.H., Deutsch, C.A., Collin, R., 2024. Coral Community Composition Linked to Hypoxia Exposure. Global Change Biology 30. https://doi.org/10.1111/gcb.17545
Mallon, J.E., Altieri, A.H., Cyronak, T., Melendez-Declet, C.V., Paul, V.J., Johnson, M.D., 2025. Sublethal changes to coral metabolism in response to deoxygenation. Journal of Experimental Biology 228, JEB249638. https://doi.org/10.1242/jeb.249638
McCulloch, M., Falter, J., Trotter, J., Montagna, P., 2012. Coral resilience to ocean acidification and global warming through pH up-regulation. Nature Clim Change 2, 623–627. https://doi.org/10.1038/nclimate1473
Middlebrook, R., Anthony, K.R.N., Hoegh-Guldberg, O., Dove, S., 2012. Thermal priming affects symbiont photosynthesis but does not alter bleaching susceptibility in Acropora millepora. Journal of Experimental Marine Biology and Ecology 432–433, 64–72. https://doi.org/10.1016/j.jembe.2012.07.005
Middlebrook, R., Hoegh-Guldberg, O., Leggat, W., 2008. The effect of thermal history on the susceptibility of reef-building corals to thermal stress. Journal of Experimental Biology 211, 1050–1056. https://doi.org/10.1242/jeb.013284
Murphy, J.W.A., Richmond, R.H., 2016. Changes to coral health and metabolic activity under oxygen deprivation. PeerJ 4, e1956. https://doi.org/10.7717/peerj.1956
Naugle, M., Denis, H., Mocellin, V., Laffy, P., Popovic, I., Bay, L., Howells, E., 2024. Environmental, host, and symbiont drivers of heat tolerance in a species complex of reef-building corals. https://doi.org/10.1101/2024.01.31.575130
Nguyen, H.M., Kim, M., Ralph, P.J., Marín-Guirao, L., Pernice, M., Procaccini, G., 2020. Stress Memory in Seagrasses: First Insight Into the Effects of Thermal Priming and the Role of Epigenetic Modifications. Front. Plant Sci. 11, 494. https://doi.org/10.3389/fpls.2020.00494
Oakley, C.A., Hopkinson, B.M., Schmidt, G.W., 2014. Mitochondrial terminal alternative oxidase and its enhancement by thermal stress in the coral symbiont Symbiodinium. Coral Reefs 33, 543–552. https://doi.org/10.1007/s00338-014-1147-0
Orr, J.C., Fabry, V.J., Aumont, O., Bopp, L., Doney, S.C., Feely, R.A., Gnanadesikan, A., Gruber, N., Ishida, A., Joos, F., Key, R.M., Lindsay, K., Maier-Reimer, E., Matear, R.,

Monfray, P., Mouchet, A., Najjar, R.G., Plattner, G.-K., Rodgers, K.B., Sabine, C.L., Sarmiento, J.L., Schlitzer, R., Slater, R.D., Totterdell, I.J., Weirig, M.-F., Yamanaka, Y., Yool, A., 2005. Anthropogenic ocean acidification over the twenty-first century and its impact on calcifying organisms. Nature 437, 681–686. https://doi.org/10.1038/nature04095

Oschlies, A., Brandt, P., Stramma, L., Schmidtko, S., 2018. Drivers and mechanisms of ocean deoxygenation. Nature Geosci 11, 467–473. https://doi.org/10.1038/s41561-018-0152-2

Palumbi, S.R., Barshis, D.J., Traylor-Knowles, N., Bay, R.A., 2014. Mechanisms of reef coral resistance to future climate change. Science 344, 895–898. https://doi.org/10.1126/science.1251336

Pezner, A.K., Courtney, T.A., Barkley, H.C., Chou, W.-C., Chu, H.-C., Clements, S.M., Cyronak, T., DeGrandpre, M.D., Kekuewa, S.A.H., Kline, D.I., Liang, Y.-B., Martz, T.R., Mitarai, S., Page, H.N., Rintoul, M.S., Smith, J.E., Soong, K., Takeshita, Y., Tresguerres, M., Wei, Y., Yates, K.K., Andersson, A.J., 2023. Increasing hypoxia on global coral reefs under ocean warming. Nat. Clim. Chang. 13, 403–409. https://doi.org/10.1038/s41558-023-01619-2

Pontes, E., Langdon, C., Al-Horani, F.A., 2023. Caribbean scleractinian corals exhibit highly variable tolerances to acute hypoxia. Front. Mar. Sci. 10, 1120262. https://doi.org/10.3389/fmars.2023.1120262

Putnam, H.M., Davidson, J.M., Gates, R.D., 2016. Ocean acidification influences host DNA methylation and phenotypic plasticity in environmentally susceptible corals. Evolutionary Applications 9, 1165–1178. https://doi.org/10.1111/eva.12408

Putnam, H.M., Gates, R.D., 2015. Preconditioning in the reef-building coral *Pocillopora damicornis* and the potential for trans-generational acclimatization in coral larvae under future climate change conditions. Journal of Experimental Biology 218, 2365–2372. https://doi.org/10.1242/jeb.123018

Putnam, H.M., Ritson-Williams, R., Cruz, J.A., Davidson, J.M., Gates, R.D., 2020. Environmentally-induced parental or developmental conditioning influences coral offspring ecological performance. Sci Rep 10, 13664. https://doi.org/10.1038/s41598-020-70605-x

Radice, V.Z., Martinez, A., Paytan, A., Potts, D.C., Barshis, D.J., 2024. Complex dynamics of coral gene expression responses to low pH across species. Molecular Ecology 33, e17186. https://doi.org/10.1111/mec.17186

Raj, K.D., Mathews, G., Obura, D.O., Laju, R.L., Bharath, M.S., Kumar, P.D., Arasamuthu, A., Kumar, T.K.A., Edward, J.K.P., 2020. Low oxygen levels caused by Noctiluca scintillans bloom kills corals in Gulf of Mannar, India. Sci Rep 10, 22133. https://doi.org/10.1038/s41598-020-79152-x

Rivera-Ingraham, G.A., Lignot, J.-H., 2017. Osmoregulation, bioenergetics and oxidative stress in coastal marine invertebrates: raising the questions for future research. Journal of Experimental Biology 220, 1749–1760. https://doi.org/10.1242/jeb.135624

Rodrigues, L.J., Grottoli, A.G., 2007. Energy reserves and metabolism as indicators of coral recovery from bleaching. Limnology & Oceanography 52, 1874–1882. https://doi.org/10.4319/lo.2007.52.5.1874

Rogers, A., Harborne, A.R., Brown, C.J., Bozec, Y., Castro, C., Chollett, I., Hock, K., Knowland, C.A., Marshell, A., Ortiz, J.C., Razak, T., Roff, G., Samper-Villarreal, J., Saunders, M.I., Wolff, N.H., Mumby, P.J., 2015. Anticipative management for coral reef ecosystem services in the 21st century. Global Change Biology 21, 504–514. https://doi.org/10.1111/gcb.12725

Safaie, A., Silbiger, N.J., McClanahan, T.R., Pawlak, G., Barshis, D.J., Hench, J.L., Rogers, J.S., Williams, G.J., Davis, K.A., 2018. High frequency temperature variability

reduces the risk of coral bleaching. Nat Commun 9, 1671. https://doi.org/10.1038/s41467-018-04074-2
Schoepf, V., Grottoli, A.G., Warner, M.E., Cai, W.-J., Melman, T.F., Hoadley, K.D., Pettay, D.T., Hu, X., Li, Q., Xu, H., Wang, Y., Matsui, Y., Baumann, J.H., 2013. Coral Energy Reserves and Calcification in a High-CO2 World at Two Temperatures. PLoS ONE 8, e75049. https://doi.org/10.1371/journal.pone.0075049
Schoepf, V., Sanderson, H., Larcombe, E., 2022. Coral heat tolerance under variable temperatures: Effects of different variability regimes and past environmental history vs. current exposure. Limnology & Oceanography 67, 404–418. https://doi.org/10.1002/lno.12000
Seemann, J., Carballo-Bolaños, R., Berry, K., González, C.T., Richter, C., Leinfelder, R.R., 2012. Importance of heterotrophic adaptations of corals to maintain energy reserves. Proceedings of the 12th International Coral Reef Symposium, Cairns, Australia 19A, 9–13.
Seibel, B.A., 2011. Critical oxygen levels and metabolic suppression in oceanic oxygen minimum zones. Journal of Experimental Biology 214, 326–336. https://doi.org/10.1242/jeb.049171
Shashar, N., Cohen, Y., Loya, Y., 1993. Extreme Diel Fluctuations of Oxygen in Diffusive Boundary Layers Surrounding Stony Corals. The Biological Bulletin 185, 455–461. https://doi.org/10.2307/1542485
Solomon, S.L., De Goeij, J.M., Croasdale, E.M., Schoepf, V., 2025. Seasonality modulates coral trophic plasticity in an extreme, multi-stressor environment. Limnology & Oceanography 70, 1466–1480. https://doi.org/10.1002/lno.70046
Steckbauer, A., Klein, S.G., Duarte, C.M., 2020. Additive impacts of deoxygenation and acidification threaten marine biota. Global Change Biology 26, 5602–5612. https://doi.org/10.1111/gcb.15252
Tanvet, C., Camp, E.F., Sutton, J., Houlbrèque, F., Thouzeau, G., Rodolfo-Metalpa, R., 2023. Corals adapted to extreme and fluctuating seawater pH increase calcification rates and have unique symbiont communities. Ecology and Evolution 13. https://doi.org/10.1002/ece3.10099
Teixeira, T., Diniz, M., Calado, R., Rosa, R., 2013. Coral physiological adaptations to air exposure: Heat shock and oxidative stress responses in Veretillum cynomorium. Journal of Experimental Marine Biology and Ecology 439, 35–41. https://doi.org/10.1016/j.jembe.2012.10.010
Thornhill, D.J., Rotjan, R.D., Todd, B.D., Chilcoat, G.C., Iglesias-Prieto, R., Kemp, D.W., LaJeunesse, T.C., Reynolds, J.M., Schmidt, G.W., Shannon, T., Warner, M.E., Fitt, W.K., 2011. A Connection between Colony Biomass and Death in Caribbean Reef-Building Corals. PLoS ONE 6, e29535. https://doi.org/10.1371/journal.pone.0029535
Turnham, K.E., Aschaffenburg, M.D., Pettay, D.T., Paz-García, D.A., Reyes-Bonilla, H., Pinzón, J., Timmins, E., Smith, R.T., McGinley, M.P., Warner, M.E., LaJeunesse, T.C., 2023. High physiological function for corals with thermally tolerant, host-adapted symbionts. Proc. R. Soc. B. 290. https://doi.org/10.1098/rspb.2023.1021
Warner, M.E., Fitt, W.K., Schmidt, G.W., 1999. Damage to photosystem II in symbiotic dinoflagellates: A determinant of coral bleaching. Proc. Natl. Acad. Sci. U.S.A. 96, 8007–8012. https://doi.org/10.1073/pnas.96.14.8007
Watty, K., Schoepf, V., Van Der Zande, R., 2024. Measuring coral reflectance and calculating NDVI as a proxy for chlorophyll a with the DIVING-PAM-II v1. https://doi.org/10.17504/protocols.io.rm7vzjqd5lx1/v1
West, B.T., Welch, K.B., Gałecki, A.T., 2007. Linear mixed models: a practical guide using statistical software. Chapman & Hall/CRC, Boca Raton, Fla.

Woods, H.A., Moran, A.L., Atkinson, D., Audzijonyte, A., Berenbrink, M., Borges, F.O., Burnett, K.G., Burnett, L.E., Coates, C.J., Collin, R., Costa-Paiva, E.M., Duncan, M.I., Ern, R., Laetz, E.M.J., Levin, L.A., Lindmark, M., Lucey, N.M., McCormick, L.R., Pierson, J.J., Rosa, R., Roman, M.R., Sampaio, E., Schulte, P.M., Sperling, E.A., Walczyńska, A., Verberk, W.C.E.P., 2022. Integrative Approaches to Understanding Organismal Responses to Aquatic Deoxygenation. The Biological Bulletin 243, 85–103. https://doi.org/10.1086/722899

Zhang, K., Wu, Z., Liu, Z., Tang, J., Cai, W., An, M., Zhou, Z., 2023. Acute hypoxia induces reduction of algal symbiont density and suppression of energy metabolism in the scleractinian coral Pocillopora damicornis. Marine Pollution Bulletin 191, 114897. https://doi.org/10.1016/j.marpolbul.2023.114897

2.8. Supplementary Materials

Supplement A. Supplementary Text

Methods

Environmental data collection

High resolution *in-situ* data loggers were deployed at Punta Caracol coral collection site at two depths (~3 m and 10 m). These loggers were used to measure and record temperature (ENVloggers T7.3, ElectricBlue, Australia), dissolved oxygen (MiniDOT, PME, USA), pH (AquapHOx, PyroScience GmbH, Germany), photosynthetically active radiation (PAR, Odyssey Xtreem, Odyssey, New Zealand), and conductivity (Odyssey, New Zealand) levels at 10-minute intervals. All loggers were attached to a cement block, with PAR loggers oriented upward and conductivity sensors at least 10 cm distant from any other parts of the block.

All environmental sensors were calibrated or verified prior to deployment. DO loggers were submerged in solutions representing 0% and 100% saturation to confirm accurate readings. Field calibration adjustments were applied based on manufacturer recommendations. pH sensors were pre-calibrated using buffer solutions at pH 2 and 11, and post-deployment drift was corrected using a pH 2 reference in accordance with manufacturer recommendations. PAR sensors were calibrated against a miniPAR reference sensor (Odyssey, Dataflow Systems, New Zealand) before field use. To confirm post-deployment accuracy, all PAR loggers and the miniPAR reference sensor were deployed together at 3 m for one week to compare readings. Conductivity sensors were placed in a shared seawater system for at least 24 hours to verify consistent calibration. Loggers were cleaned regularly to minimize fouling. Cleaning occurred on 18, 24, and 27 September, and 24 and 31 October 2024.

PAM measurements

F_v/F_m measurements were taken using a miniature fiberoptic probe following a 30-minute dark acclimation. PAM settings were: gain = 2, damp = 2, saturation intensity = 4, saturation width = 0.8, measuring light intensity = 11, and frequency 3. Gain was increased if F_0 readings were below 300.

NDVI was calculated from reflectance measurements taken at wavelength of 670 nm and 750 nm, using a spectrometer (Mini-Spec) equipped with a reflectance probe. Prior to each set of measurements, the instrument was calibrated using a white reflectance standard. From the obtained spectral data, the NDVI was calculated as:

$$NDVI = (R_{750}-R_{670})/(R_{750}+R_{670}) \quad (1)$$

Where R_{750} and R_{670} represent reflectance at 750 nm and 670 nm, respectively.

Critical oxygen partial pressure

Incubations were conducted in airtight acrylic chambers (350 mL or 550 mL), filled with water from each coral's respective holding tank to maintain acclimatized conditions. Coral fragments were positioned on platforms above magnetic stir bars to ensure continuous water mixing. Chambers were placed on magnetic stir plates (Thermo Scientific, USA) and partially submerged in a temperature-controlled water bath maintained at ~28°C with circulation flow. All oxygen sensors were calibrated prior to the incubations using 100% oxygen saturated seawater from aeration for 15 min and 0% saturated sodium sulfite solution.

Coral fragments and tiles were gently cleaned of algae and dark-acclimated for 30 minutes. To determine oxygen consumption rates of each fragment, the volume of water in each chamber was measured to account for displacement by the coral and tile. Blank chambers (no coral) were included in most incubation rounds to assess background respiration in the seawater. However, blank corrections were not applied in the calculation of oxygen consumption rates.

Incubations were conducted in a prioritized order: ambient *A. tenuifolia* fragments were incubated first, beginning on day 33 of the experiment, followed by stress-treated *A. tenuifolia*. Incubations of *S. siderea* fragments began on day 35, following the same order of ambient first, followed by stress treatment.

Symbiont densities and chlorophyll content

Coral fragments were frozen at -20 °C immediately following respiration incubations, shipped to Amsterdam, and stored at -80 °C for subsequent laboratory analysis at the University of Amsterdam. Tissue was removed from ~2 cm^2 of coral skeleton using an airbrush (Master Performance S68, Master Airbrush, USA) with deionized (DI) water. For *S. siderea*, a waterpik was used in addition to the airbrush to ensure complete tissue removal. In case of partial tissue loss, aliquots were prepared from the intact and visibly healthy portions of the coral tissue.

The resulting slurry was homogenized with a tissue tearer (Biospec, OK, USA) for at least one minute and centrifuged for 10 minutes at 4000 rpm. The supernatant was discarded, and the pellet was washed by resuspension in 2 mL DI and centrifuged again. The final pellet resuspension was done in 5 mL DI water.

Symbiont densities were counted using a Neubauer improved hemacytometer (Sigma Aldrich) with an aliquot load of 15 µL per chamber. A minimum of 100 symbiont cells were counted across consistent fields (maximum 9 fields á 0.1 µL) for each replicate count of a coral sample. Six replicate counts were conducted per sample and increased to a maximum of ten if the coefficient of variation exceeded 10 %. Replicate counts were averaged and standardized to surface area.

Chlorophyll was extracted from aliquots kept on ice and in darkness to prevent degradation. Samples were centrifuged for 10 min at 400 rpm, and the supernatant was discarded. The algal pellet was resuspended in 100 % acetone and stored for 24 hours at -20°C for complete chlorophyll extraction. After extraction, absorbance was measured at 630 nm, 663 nm, and 750 nm using a spectrophotometer (Novaspec Pro, Biochrom, USA), with the 750 nm reading used to correct for turbidity and background scattering. Chlorophyll concentrations were calculated using the following equations (Jeffrey and Humphrey, 1975):

$$Chl_a\ (\mu g\ mL^{-1}) = 11.43\ (E_{663}) - 0.64\ (E_{630}) \quad (2)$$

$$Chl_{c2}\ (\mu g\ mL^{-1}) = 27.09\ (E_{630}) - 3.63\ (E_{663}) \quad (3)$$

Outliers

Several data points were excluded from analyses after outlier analysis due to clear biological or technical artefacts. For all chlorophyll-related metrics, fragments W48 and W55 were removed as they contained no algal symbionts. Additionally, fragments W4, W56, and K4 (W marks *A. tenuifolia*, K marks *S. siderea*) were excluded from both chlorophyll datasets due to visible algal overgrowth, leading to an unquantifiable amount of turf algae in the slurry, which compromised sample integrity. For biomass, fragment W38 was removed as one side lacked tissue and was heavily overgrown with algae, likely influencing biomass measurements. Finally for calcification, W56 was excluded due to the absence of a final buoyant weight measurement caused by early mortality.

Calculation of total pH (pH_T) from mV and temperature.

pH on the total scale (pH_T) was calculated from millivolt (mV) and temperature (°C) readings recorded in each tank using a HACH mV probe. The probe was calibrated approximately every 3 days using certified TRIS buffer, and the linear regression of mV versus temperature from the TRIS calibration closest in time to the tank measurement was applied. Calibrations were performed over a temperature range of approximately 24-32 °C to match the tank conditions during the experiment.

pH_T of TRIS buffer was calculated for each temperature with an assumed salinity of 35 using the equation of (DelValls and Dickson, 1998). Final pH_T values were used to calculate offset between target pH_T and Apex probe readings, allowing for accurate calibration of experimental pH treatments. All calculations were performed in R using the *seacarb* package.

For each tank, pH_T was estimated using the following equation:

$$pH_T = pH_{Tris}(T) + \frac{(E_{Tris} - E_{Tank})}{(\ln_{10} \times R \times T/F)} \quad (4)$$

where:

E_{tris} is the electrode potential (in volts) predicted for the tank temperature from the TRIS calibration regression

E_{tank} is the electrode potential (in volts) measured in the tank

R is the gas constant (8.31451 J mol^{-1} K^{-1})

T is the tank temperature in kelvin

F is the Faraday constant (96485.309 C mol^{-1}).

Supplement B. Tables

Table S1: Environmental conditions at Punta Caracol. Mean ± SD, minimum, and maximum values of dissolved oxygen (DO), pH, temperature, salinity, and photosynthetically active radiation (PAR) measured at ~3 m and ~10 m depth between September and November 2024 at the coral collection site, Punta Caracol, Almirante Bay, Panama.

Depth	Parameter	Mean	±	SD	Min	Max
3 m	DO (mg L^{-1})	5.84	±	1.10	1.53	14.18
	pH	7.87	±	0.06	7.64	8.03
	Temperature (°C)	30.63	±	0.46	29.30	32.10
	Salinity (‰)	31.65	±	1.67	24.21	33.51
	PAR (µmol photons m^{-2} s^{-1})	130.01	±	214.93	0.00	1076.84
10 m	DO (mg L^{-1})	5.56	±	0.99	2.67	14.12
	pH	7.89	±	0.05	7.73	8.24
	Temperature (°C)	30.66	±	0.24	29.90	31.30
	Salinity (‰)	30.77	±	1.21	23.15	32.50
	PAR (µmol photons m^{-2} s^{-1})	34.79	±	58.66	0.00	339.79

Table S2: Salinity correction table for the priming period. Correction factors used to adjust discrete dissolved oxygen (DO) measurements (mg L^{-1}) obtained with a HACH HQ40D meter to account for the effect of temperature and salinity on oxygen solubility in seawater. Each correction factor corresponds to a specific combination of temperature (°C) and salinity (‰) and was applied by multiplying the raw DO readings.

Temp.	Salinity (‰)														
(°C)	33.4	33.5	33.6	33.7	33.8	33.9	34.0	34.1	34.2	34.3	34.4	34.5	34.6	34.7	34.8
28.5	0.8308	0.8304	0.8299	0.8294	0.8290	0.8285	0.8280	0.8276	0.8271	0.8267	0.8262	0.8258	0.8253	0.8248	0.8244
28.6	0.8309	0.8305	0.8300	0.8295	0.8291	0.8286	0.8282	0.8277	0.8272	0.8268	0.8263	0.8259	0.8254	0.8249	0.8245
28.7	0.8310	0.8306	0.8301	0.8296	0.8292	0.8287	0.8283	0.8278	0.8273	0.8269	0.8264	0.8260	0.8255	0.8251	0.8246
28.8	0.8311	0.8307	0.8302	0.8297	0.8293	0.8288	0.8284	0.8279	0.8275	0.8270	0.8265	0.8261	0.8256	0.8252	0.8247
28.9	0.8312	0.8308	0.8303	0.8299	0.8294	0.8289	0.8285	0.8280	0.8276	0.8271	0.8266	0.8262	0.8257	0.8253	0.8248
29.0	0.8313	0.8309	0.8304	0.8300	0.8295	0.8290	0.8286	0.8281	0.8277	0.8272	0.8267	0.8263	0.8258	0.8254	0.8249
29.1	0.8314	0.8310	0.8305	0.8301	0.8296	0.8291	0.8287	0.8282	0.8278	0.8273	0.8269	0.8264	0.8259	0.8255	0.8250
29.2	0.8315	0.8311	0.8306	0.8302	0.8297	0.8292	0.8288	0.8283	0.8279	0.8274	0.8270	0.8265	0.8260	0.8256	0.8251
29.3	0.8316	0.8312	0.8307	0.8303	0.8298	0.8294	0.8289	0.8284	0.8280	0.8275	0.8271	0.8266	0.8262	0.8257	0.8252
29.4	0.8317	0.8313	0.8308	0.8304	0.8299	0.8295	0.8290	0.8285	0.8281	0.8276	0.8272	0.8267	0.8263	0.8258	0.8253
29.5	0.8319	0.8314	0.8309	0.8305	0.8300	0.8296	0.8291	0.8286	0.8282	0.8277	0.8273	0.8268	0.8264	0.8259	0.8255
29.6	0.8320	0.8315	0.8310	0.8306	0.8301	0.8297	0.8292	0.8288	0.8283	0.8278	0.8274	0.8269	0.8265	0.8260	0.8256
29.7	0.8321	0.8316	0.8311	0.8307	0.8302	0.8298	0.8293	0.8289	0.8284	0.8279	0.8275	0.8270	0.8266	0.8261	0.8257
29.8	0.8322	0.8317	0.8312	0.8308	0.8303	0.8299	0.8294	0.8290	0.8285	0.8280	0.8276	0.8271	0.8267	0.8262	0.8258
29.9	0.8323	0.8318	0.8313	0.8309	0.8304	0.8300	0.8295	0.8291	0.8286	0.8282	0.8277	0.8272	0.8268	0.8263	0.8259
30.0	0.8324	0.8319	0.8314	0.8310	0.8305	0.8301	0.8296	0.8292	0.8287	0.8283	0.8278	0.8273	0.8269	0.8264	0.8260

Table S3: Salinity correction table for the acute stress test. Correction factors used to adjust discrete dissolved oxygen (DO) measurements (mg L^{-1}) obtained with a HACH HQ40D meter to account for the effect of temperature and salinity on oxygen solubility in seawater. Each correction factor corresponds to a specific combination of temperature (°C) and salinity (‰) and was applied by multiplying the raw DO readings.

Temp.	Salinity (‰)		
(°C)	30.9	31.0	31.1
28.0	0.8419	0.8415	0.8410
28.1	0.8420	0.8416	0.8411
28.2	0.8421	0.8417	0.8412
28.3	0.8422	0.8418	0.8413
28.4	0.8423	0.8419	0.8414
28.5	0.8424	0.8420	0.8415
28.6	0.8425	0.8420	0.8416
28.7	0.8426	0.8421	0.8417
28.8	0.8427	0.8422	0.8418
28.9	0.8428	0.8423	0.8419
29.0	0.8429	0.8424	0.8420
29.1	0.8430	0.8425	0.8421

Table S4: Mean (± SD) carbonate chemistry parameters measured from single spot water samples per tank during the acclimation and priming periods of the experiment**.** Parameters include partial pressure of CO_2 (pCO_2), dissolved inorganic carbon (DIC), total alkalinity (TA), and aragonite saturation state ($\Omega_{Aragonite}$). Numbers in parantheses indicate the number of replicate tanks sampled (n) for each treatment and period.

		pCO_2 (µatm)	DIC (mol kg^{-1})	TA (µmol kg^{-1})	$\Omega_{Aragonite}$
Acclimation 30 Sep 2024	(2)	571 ± 50	1.92E-03 ± 1.55E-06	2135 ± 18	2.65 ± 0.22
Priming 31 Oct 2024	Control (2)	455 ± 1	1.96E-03 ± 4.71E-06	2253 ± 5	3.50 ± 0.01
	LF (2)	454 ± 37	1.95E-03 ± 1.85E-05	2248 ± 3	3.49 ± 0.15
	HF (2)	438 ± 11	1.96E-03 ± 1.43E-05	2265 ± 11	3.61 ± 0.03
Priming 15 Nov 2024	Ambient (3)	474 ± 12	1.91E-03 ± 2.45E-06	2173 ± 2	3.11 ± 0.03
	Stress (3)	471 ± 37	1.89E-03 ± 1.16E-05	2160 ± 5	3.10 ± 0.14

Table S5: Results of random effect testing using restricted likelihood ratio tests (RANOVA) for *Agaricia tenuifolia*. Random factors tested included tank nested within priming and stress treatments, genotype, and coral ID (to account for repeated measurements). Parameters assessed were maximum quantum yield of PSII (F_v/F_m), normalized difference vegetation index (NDVI), critical oxygen tension (P_{crit}), tissue biomass, calcification, symbiont density, and chlorophyll content (per area and per cell). For each random effect, the number of parameters (npar), log-likelihood (logLik), Akaike Information Criterion (AIC), likelihood ratio test statistic (LRT), degrees of freedom (df), and p-value are reported. Significance levels are indicated for p-values (*p < 0.05, **p < 0.01, ***p < 0.001). Non-significant random effects indicated that simplified linear models could be used for subsequent analyses.

Parameter	Random factor	npar	logLik	AIC	LRT	df	P-value (sig. level)
F_v/F_m	Tank in Priming	22	119.88	-195.75	0.20861	1	0.6479
	Tank in Stress	22	119.98	-195.96	0	1	1
	Genotype	22	119.65	-195.31	0.65289	1	0.4191
	Coral ID	22	118.76	-193.52	2.44485	1	0.1179
NDVI	Tank in Priming	22	58.912	-73.824	1.16737	1	0.2799
	Tank in Stress	22	59.496	-74.991	0	1	1
	Genotype	22	59.496	-74.991	0	1	1
	Coral ID	22	59.473	-74.946	0.04534	1	0.8314
P_{crit} mg L^{-1} O_2	Tank in Priming	9	-55.391	128.78	1.98338	1	0.159
	Tank in Stress	9	-54.848	127.69	0.89712	1	0.3436
	Genotype	9	-54.399	126.8	0	1	1
Tissue biomass mg cm^{-2}	Tank in Priming	9	-74.922	167.84	0.06569	1	0.7977
	Tank in Stress	9	-74.89	167.78	0	1	1
	Genotype	9	-74.906	167.81	0.03263	1	0.8567
Calcification mg cm^{-2} day^{-1}	Tank in Priming	9	5.64	6.7201	0.00518	1	0.9426
	Tank in Stress	9	5.6426	6.7149	0	1	1
	Genotype	9	5.6398	6.7204	0.00551	1	0.9408
Symbiont density cells cm^{-2}	Tank in Priming	9	14.292	-10.584	1.09667	1	0.295
	Tank in Stress	9	14.84	-11.681	0	1	0.9999
	Genotype	9	14.799	-11.598	0.08267	1	0.7737
Chlorophyll cm^{-2}	Tank in Priming	9	-68.65	155.3	1.1581	1	0.2819
	Tank in Stress	9	-68.071	154.14	0	1	1
	Genotype	9	-68.071	154.14	0	1	1
Chlorophyll pg $cell^{-1}$	Tank in Priming	9	-107.55	233.1	3.6495	1	0.05609
	Tank in Stress	9	-105.72	229.25	0	1	1
	Genotype	9	-105.75	229.45	0.0421	1	0.83751

Table S6: Results of random effect testing using restricted likelihood ratio tests (RANOVA) for *Siderastrea siderea*. Random factors tested included tank nested within priming and stress treatments, genotype, and coral ID (to account for repeated measurements). Parameters assessed were maximum quantum yield (F_v/F_m), normalized difference vegetation index (NDVI), critical oxygen tension (P_{crit}), tissue biomass, calcification, symbiont density, and chlorophyll content (per area and per cell). For each random effect, the number of parameters (npar), log-likelihood (logLik), Akaike Information Criterion (AIC), likelihood ratio test statistic (LRT), degrees of freedom (df), and p-value are reported. Significance levels are indicated for p-values (*p < 0.05, **p < 0.01, ***p < 0.001). Random effects that were non-significant supported the use of simplified linear models in subsequent analyses.

Parameter	Random factor	npar	logLik	AIC	LRT	df	P-value (sig. level)
F_v/F_m	Tank in Priming	22	216.2	-388.4	0	1	1
	Tank in Stress	22	216.2	-388.4	0	1	1
	Genotype	22	200.53	-357.05	31.3499	1	2.155e-08 (***)
	Coral ID	22	213.48	-382.96	5.4387	1	0.0197 (*)
NDVI	Tank in Priming	22	72.878	-101.76	0	1	0.999829
	Tank in Stress	22	72.86	-101.72	0.0354	1	0.8507343
	Genotype	22	67.004	-90.009	11.7472	1	0.0006094 (***)
	Coral ID	22	70.585	-97.17	4.5857	1	0.0322391
P_{crit} mg L^{-1} O_2	Tank in Priming	9	-50.384	118.77	0.33413	1	0.5632
	Tank in Stress	9	-50.395	118.79	0.3546	1	0.5515
	Genotype	9	-50.217	118.44	0	1	1
Tissue biomass mg cm^{-2}	Tank in Priming	9	-112.88	243.75	0.34246	1	0.5584
	Tank in Stress	9	-112.71	243.41	0	1	1
	Genotype	9	-112.71	243.41	0	1	1
Calcification mg cm^{-2} day^{-1}	Tank in Priming	9	-34.803	87.606	0	1	0.999997
	Tank in Stress	9	-34.803	87.606	0	1	1
	Genotype	9	-39.025	96.05	8.4438	1	0.003663 (**)
Symbiont density cells cm^{-2}	Tank in Priming	9	-9.458	36.916	0	1	1
	Tank in Stress	9	-9.7072	37.414	0.4985	1	0.48016
	Genotype	9	-11.617	41.233	4.3173	1	0.03773 (*)
Chlorophyll cm^{-2}	Tank in Priming	9	-66.153	150.31	0.3926	1	0.53093
	Tank in Stress	9	-65.957	149.91	0	1	1
	Genotype	9	-68.051	154.1	4.1892	1	0.04068 (*)
Chlorophyll pg $cell^{-1}$	Tank in Priming	9	-53.888	125.78	0.19844	1	0.656
	Tank in Stress	9	-53.789	125.58	0	1	0.9999
	Genotype	9	-55.132	128.26	2.6874	1	0.1011

Table S7. Results of Cox proportional hazard models testing the effects of priming treatment (high-frequency, HF; low-frequency, LF) and acute stress exposure on *Agaricia tenuifolia*. Two endpoints were evaluated: probability of tissue cover declining to ≤ 75% and probability of survival. Model outputs include regression coefficients (coef), hazard ratios (exp(coef)), standard error (se(coef)), z statistic, and p-values. Significance levels are indicated for p-values (*p < 0.05, **p < 0.01, ***p < 0.001).

Parameter	Effect	coef	exp (coef)	se (coef)	z	p-value (sig. level)
Tissue cover probability ≤ 75%	Priming_TreatmentHF	2.2846	9.8214	0.7856	2.908	0.00364 (**)
	Priming_TreatmentLF	-0.5517	0.5759	1.2248	-0.45	0.65238
	Stress_Treatmentstress	-0.5692	0.566	0.5803	-0.98	0.32666
Survival probability	Priming_TreatmentHF	1.9566	7.0749	1.0967	1.784	0.0755
	Priming_TreatmentLF	0.2186	1.2443	1.4144	0.155	0.8772
	Stress_Treatmentstress	-0.4169	0.6591	0.765	-0.55	0.5857

Table S8. Results of linear models (LM) testing the effects of priming treatment, stress treatment, and their interaction on physiological parameters of *Agaricia tenuifolia*. LM were applied because no random effects were statistically significant or required to account for repeated measures. Parameters tested included critical oxygen threshold (Pcrit, mg L^{-1} O_2), tissue biomass (mg cm^{-2}), symbiont density (cells cm^{-2}), chlorophyll concentration per area (cm^{-2}), and chlorophyll concentration per symbiont cell (pg $cell^{-1}$). Significance levels are indicated for p-values (*p < 0.05, **p < 0.01, ***p < 0.001).

Parameter	Effect	Sum sq	df	F-value	p-value (sig. level)
P_{crit} mg L^{-1} O_2	Priming_Treatment	0.1382	2	0.04062	0.9602
	Stress_Treatment	0.8805	1	0.5178	0.4772
	Priming_Treatment:Stress_Treatment	0.9041	2	0.2658	0.7683
Tissue biomass mg cm^{-2}	Priming_Treatment	0.1497	2	0.7092	0.5001
	Stress_Treatment	0.1493	1	1.414	0.2437
	Priming_Treatment:Stress_Treatment	0.1433	2	0.6785	0.515
Symbiont density cells cm^{-2}	Priming_Treatment	0.209	2	6.379	0.004784 (**)
	Stress_Treatment	0.001052	1	0.06423	0.8016
	Priming_Treatment:Stress_Treatment	0.003504	2	0.107	0.8989
Chlorophyll cm^{-2}	Priming_Treatment	17.74	2	1.625	0.2149
	Stress_Treatment	18.91	1	3.464	0.07324
	Priming_Treatment:Stress_Treatment	4.474	2	0.4098	0.6677
Chlorophyll pg $cell^{-1}$	Priming_Treatment	644.5	2	3.668	0.03484 (*)
	Stress_Treatment	75.42	1	0.8584	0.3621
	Priming_Treatment:Stress_Treatment	14.09	2	0.08019	0.9231

Table S9. Results of generalized linear mixed models (GLMM) and linear mixed-effects models (lmer) testing the effects of priming treatment, stress treatment, day, and their interactions on physiological parameters of *Agaricia tenuifolia*. A GLMM with a Gamma distribution and log link (glmmTMB) was fitted for calcification rates (mg cm^{-2} day^{-1}). For F_v/F_m, a GLMM with a Beta distribution, appropriate for proportional data bounded between 0 and 1, was used. For NDVI, a linear mixed-effects model (lmer) was applied with coral ID included as a random factor to account for repeated measures across days. Significance levels are indicated for p-values (*p < 0.05, **p < 0.01, ***p < 0.001).

Parameter	Effect	Chisq	df	p-value (sig. level)
F_v/F_m	Priming_Treatment	13.51	2	0.001162 (**)
	Stress_Treatment	0.1236	1	0.7251
	Day	155.9	2	1.387e-34 (***)
	Priming_Treatment:Stress_Treatment	0.5123	2	0.774
	Priming_Treatment:Day	12.55	4	0.01368 (*)
	Stress_Treatment:Day	0.8016	2	0.6698
	Priming_Treatment:Stress_Treatment:Day	1.466	4	0.8327
NDVI	Priming_Treatment	2.497	2	0.2869
	Stress_Treatment	0.07223	1	0.7881
	Day	32.94	2	7.021e-08 (***)
	Priming_Treatment:Stress_Treatment	0.09034	2	0.9558
	Priming_Treatment:Day	4.109	4	0.3914
	Stress_Treatment:Day	0.8059	2	0.6683
	Priming_Treatment:Stress_Treatment:Day	5.121	4	0.2751
Calcification mg cm^{-2} day^{-1}	Priming_Treatment	5.101	2	0.07804
	Stress_Treatment	0.002424	1	0.9607
	Priming_Treatment:Stress_Treatment	4.416	2	0.1099

Table S10. Results of linear models (LM) testing the effects of priming treatment, stress treatment, and their interaction on physiological parameters of *Siderastrea siderea*. LM were applied because no random effects were statistically significant or required to account for repeated measures. Parameters tested included critical oxygen threshold (P_{crit}, mg L^{-1} O_2), tissue biomass (mg cm^{-2}), and chlorophyll concentration per symbiont cell (pg $cell^{-1}$). Significance levels are indicated for p-values (*p < 0.05, **p < 0.01, ***p < 0.001).

Parameter	Effect	Sum sq	df	F-value	p-value (sig. level)
P_{crit} mg L^{-1} O_2	Priming_Treatment	2.536	2	0.9228	0.8917
	Stress_Treatment	0.01156	1	0.008415	0.9262
	Priming_Treatment:Stress_Treatment	2.084	2	0.7583	0.3723
Tissue biomass mg cm^{-2}	Priming_Treatment	0.173	2	3.544	0.04154 (*)
	Stress_Treatment	0.3185	1	13.05	0.001094 (**)
	Priming_Treatment:Stress_Treatment	0.1542	2	3.159	0.05686
Chlorophyll pg $cell^{-1}$	Priming_Treatment	0.4194	2	0.1151	0.4084
	Stress_Treatment	0.0159	1	0.008726	0.9275
	Priming_Treatment:Stress_Treatment	3.727	2	1.022	0.4772

Table S11. Results of linear mixed-effects models (lmer) testing the effects of priming treatment, stress treatment, day, and their interactions on physiological parameters of *Siderastrea siderea*. Lmer models were applied to account for significant random factors or repeated measurements. Parameters tested included F_v/F_m, NDVI, calcification rates (mg cm^{-2} day^{-1}), symbiont density (cells cm^{-2}), and chlorophyll concentration per area (cm^{-2}). Significance levels are indicated for p-values (*p < 0.05, **p < 0.01, ***p < 0.001).

Parameter	Effect	Chisq	df	p-value (sig. level)
F_v/F_m	Priming_Treatment	4.547	2	0.103
	Stress_Treatment	0.000318	1	0.9858
	Day	3.714	2	0.1561
	Priming_Treatment:Stress_Treatment	0.5828	2	0.7472
	Priming_Treatment:Day	4.237	4	0.3748
	Stress_Treatment:Day	5.681	2	0.05839
	Priming_Treatment:Stress_Treatment:Day	5.185	4	0.2688
NDVI	Priming_Treatment	1.623	2	0.4443
	Stress_Treatment	0.6608	1	0.4163
	Day	34.07	2	3.99E-8 (***)
	Priming_Treatment:Stress_Treatment	2.157	2	0.3401
	Priming_Treatment:Day	0.4404	4	0.979
	Stress_Treatment:Day	2.186	2	0.33524
	Priming_Treatment:Stress_Treatment:Day	2.425	4	0.6582
Calcification mg cm^{-2} day^{-1}	Priming_Treatment	4.832	2	0.08928
	Stress_Treatment	0.2095	1	0.6471
	Priming_Treatment:Stress_Treatment	0.348	2	0.8403
Symbiont density cells cm^{-2}	Priming_Treatment	6.099	2	0.04739 (*)
	Stress_Treatment	3.399	1	0.06522
	Priming_Treatment:Stress_Treatment	1.607	2	0.4478
Chlorophyll cm^{-2}	Priming_Treatment	1.137	2	0.5663
	Stress_Treatment	0.8368	1	0.3603
	Priming_Treatment:Stress_Treatment	1.793	2	0.4079

Table S12. Post hoc pairwise comparisons for statistically significant main effects for F_v/F_m in *Agaricia tenuifolia*. Results are based on a GLMM with Beta distribution with "Day" and "Priming treatment" as significant main effects. Shown are estimated odds ratios between treatment and time levels, standard errors (SE), degrees of freedom (df), z-ratios, and corresponding p-values. Significance levels are indicated for p-values (*p < 0.05, **p < 0.01, ***p < 0.001).

Parameter	contrast				odds ratio	SE	df	z.ratio	p-value (sig. level)
F_v/F_m	Day0	control	/ Day29	control	1.461	0.1168	Inf	4.744	0.0001 (***)
	Day0	control	/ Day33	control	1.608	0.129	Inf	5.923	<.0001 (***)
	Day0	control	/ Day0	HF	1.018	0.0935	Inf	0.194	1
	Day0	control	/ Day29	HF	2.123	0.1978	Inf	8.081	<.0001 (***)
	Day0	control	/ Day33	HF	2.035	0.1897	Inf	7.621	<.0001 (***)
	Day0	control	/ Day0	LF	1.008	0.0926	Inf	0.092	1
	Day0	control	/ Day29	LF	1.458	0.1341	Inf	4.103	0.0013 (**)
	Day0	control	/ Day33	LF	1.584	0.1457	Inf	4.999	<.0001 (***)
	Day29	control	/ Day33	control	1.101	0.0897	Inf	1.176	0.9616
	Day29	control	/ Day0	HF	0.697	0.0652	Inf	-3.86	0.0036 (**)
	Day29	control	/ Day29	HF	1.453	0.1379	Inf	3.939	0.0027 (**)
	Day29	control	/ Day33	HF	1.393	0.1323	Inf	3.487	0.0144 (*)
	Day29	control	/ Day0	LF	0.69	0.0646	Inf	-3.96	0.0024 (**)
	Day29	control	/ Day29	LF	0.998	0.0936	Inf	-0.02	1
	Day29	control	/ Day33	LF	1.084	0.1016	Inf	0.861	0.9948
	Day33	control	/ Day0	HF	0.633	0.0594	Inf	-4.87	<.0001 (***)
	Day33	control	/ Day29	HF	1.32	0.1256	Inf	2.921	0.0836
	Day33	control	/ Day33	HF	1.265	0.1205	Inf	2.472	0.2454
	Day33	control	/ Day0	LF	0.627	0.0588	Inf	-4.97	<.0001 (***)
	Day33	control	/ Day29	LF	0.907	0.0852	Inf	-1.04	0.9821
	Day33	control	/ Day33	LF	0.985	0.0926	Inf	-0.16	1
	Day0	HF	/ Day29	HF	2.086	0.1786	Inf	8.583	<.0001 (***)
	Day0	HF	/ Day33	HF	1.999	0.1713	Inf	8.082	<.0001 (***)
	Day0	HF	/ Day0	LF	0.991	0.0945	Inf	-0.1	1
	Day0	HF	/ Day29	LF	1.433	0.1368	Inf	3.765	0.0052 (**)
	Day0	HF	/ Day33	LF	1.556	0.1486	Inf	4.628	0.0001 (***)
	Day29	HF	/ Day33	HF	0.958	0.0835	Inf	-0.49	0.9999
	Day29	HF	/ Day0	LF	0.475	0.0459	Inf	-7.71	<.0001 (***)
	Day29	HF	/ Day29	LF	0.687	0.0665	Inf	-3.88	0.0033 (**)
	Day29	HF	/ Day33	LF	0.746	0.0722	Inf	-3.03	0.0621
	Day33	HF	/ Day0	LF	0.496	0.0479	Inf	-7.26	<.0001 (***)
	Day33	HF	/ Day29	LF	0.717	0.0694	Inf	-3.44	0.0169 (*)
	Day33	HF	/ Day33	LF	0.778	0.0754	Inf	-2.59	0.1915
	Day0	LF	/ Day29	LF	1.446	0.1219	Inf	4.378	0.0004 (***)
	Day0	LF	/ Day33	LF	1.571	0.1324	Inf	5.355	<.0001 (***)
	Day29	LF	/ Day33	LF	1.086	0.0917	Inf	0.977	0.988

Table S13. Post hoc pairwise comparisons for *Agaricia tenuifolia* for statistically significant main effects. Results are based on linear mixed-effects models (lmer) for NDVI and, and a linear model (LM) for symbiont density and chlorophyll per cell. Significant main effects were "Day" for NDVI, and "Priming treatment" for symbiont densities and chlorophyll per cell. Shown are estimated contrasts between treatment or time levels, standard errors (SE), degrees of freedom (df), t-ratios, and corresponding p-values. Significance levels are indicated for p-values (*p < 0.05, **p < 0.01, ***p < 0.001).

Parameter	contrast	estimate	SE	df	t.ratio	p-value (sig. level)
NDVI	Day0 -Day29	0.1288	0.0244	62.9	5.287	<.0001 (***)
	Day0 - Day33	0.1109	0.0244	62.9	4.553	0.0001 (***)
	Day29 - Day33	-0.0179	0.0245	62.4	-0.731	0.7462
Symbiont density cells cm^{-2}	control - HF	0.1281	0.0513	31	2.496	0.0463 (*)
	control - LF	-0.0532	0.0513	31	-1.037	0.5595
	HF - LF	-0.1813	0.0522	31	-3.47	0.0043 (**)
Chlorophyll pg $cell^{-1}$	control - HF	-9.645	4.08	28	-2.361	0.0636
	control - LF	0.135	3.85	28	0.035	0.9993
	HF - LF	9.78	4.06	28	2.41	0.0575

Table S14. Post hoc pairwise comparisons for *Siderastrea siderea* for statistically significant main effects. Results are based on linear mixed-effects models (lmer) for NDVI and symbiont density, and a linear model (LM) for tissue biomass. Significant main effects were "Day" for NDVI, "Priming treatment" and "Stress treatment" for tissue biomass, and "Priming treatment" for symbiont densities. Shown are estimated contrasts between treatment or time levels, standard errors (SE), degrees of freedom (df), t-ratios, and corresponding p-values. Significance levels are indicated for p-values (*p < 0.05, **p < 0.01, ***p < 0.001).

Parameter	contrast	estimate	SE	df	t.ratio	p-value (sig. level)
NDVI	Day0 -Day29	0.074	0.0177	60	4.176	0.0003 (***)
	Day0 - Day33	0.0996	0.0177	60	5.62	<.0001 (***)
	Day29 - Day33	0.0256	0.0177	60	1.444	0.3251
Tissue biomass mg cm^{-2}	control ambient / HF ambient	0.985	0.0889	30	-0.166	1
	control ambient / LF ambient	0.988	0.0891	30	-0.135	1
	control ambient / control stress	1.374	0.1239	30	3.522	0.0159 (*)
	control ambient / HF stress	1.25	0.1127	30	2.471	0.165
	control ambient / LF stress	0.997	0.0899	30	-0.037	1
	HF ambient / LF ambient	1.003	0.0905	30	0.031	1
	HF ambient / control stress	1.395	0.1258	30	3.688	0.0105 (*)
	HF ambient / HF stress	1.269	0.1144	30	2.637	0.1193
	HF ambient / LF stress	1.012	0.0913	30	0.129	1
	LF ambient / control stress	1.391	0.1254	30	3.657	0.0113 (*)
	LF ambient / HF stress	1.265	0.1141	30	2.606	0.127
	LF ambient / LF stress	1.009	0.091	30	0.098	1
	control stress / HF stress	0.91	0.082	30	-1.051	0.8964
	control stress / LF stress	0.725	0.0654	30	-3.559	0.0145 (*)
	HF stress / LF stress	0.798	0.0719	30	-2.508	0.1538
Symbiont density cells cm^{-2}	control - HF	0.236	0.103	25	2.298	0.0746
	control - LF	0.0375	0.103	25	0.365	0.9293
	HF - LF	-0.1985	0.103	25	-1.932	0.1505